

5-2010

## Protein-Protein Interactions That Regulate Neurotransmitter Release from Retinal Ribbon Synapses

(Leigh) Beth T. Latham

Follow this and additional works at: [https://digitalcommons.library.tmc.edu/utgsbs\\_dissertations](https://digitalcommons.library.tmc.edu/utgsbs_dissertations)

 Part of the [Molecular and Cellular Neuroscience Commons](#)

---

### Recommended Citation

Latham, (Leigh) Beth T., "Protein-Protein Interactions That Regulate Neurotransmitter Release from Retinal Ribbon Synapses" (2010). *The University of Texas MD Anderson Cancer Center UTHealth Graduate School of Biomedical Sciences Dissertations and Theses (Open Access)*. 29.  
[https://digitalcommons.library.tmc.edu/utgsbs\\_dissertations/29](https://digitalcommons.library.tmc.edu/utgsbs_dissertations/29)

This Dissertation (PhD) is brought to you for free and open access by the The University of Texas MD Anderson Cancer Center UTHealth Graduate School of Biomedical Sciences at DigitalCommons@TMC. It has been accepted for inclusion in The University of Texas MD Anderson Cancer Center UTHealth Graduate School of Biomedical Sciences Dissertations and Theses (Open Access) by an authorized administrator of DigitalCommons@TMC. For more information, please contact [digitalcommons@library.tmc.edu](mailto:digitalcommons@library.tmc.edu).

## **Chapter 1: Background and Significance**



## **Chemical Synapses in the Nervous System**

Nerve cells communicate through synaptic transmission at a specialized site referred to as the synapse. Chemical transmission is the most common form of synaptic transmission in the nervous system. A chemical synapse consists of a presynaptic nerve terminal in close proximity to a postsynaptic neuron. The major steps in chemical synaptic transmission are: 1) activation of presynaptic voltage-gated calcium channels during depolarization of the presynaptic plasma membrane, 2) movement of calcium through the activated channels into the presynaptic nerve terminal, 3) exocytosis of neurotransmitter-filled synaptic vesicles from the nerve terminal, 4) diffusion of neurotransmitter across the synaptic cleft, and 5) binding of neurotransmitter to receptors on the postsynaptic cell, resulting in activation of postsynaptic signaling cascades (refer to Figure 1).

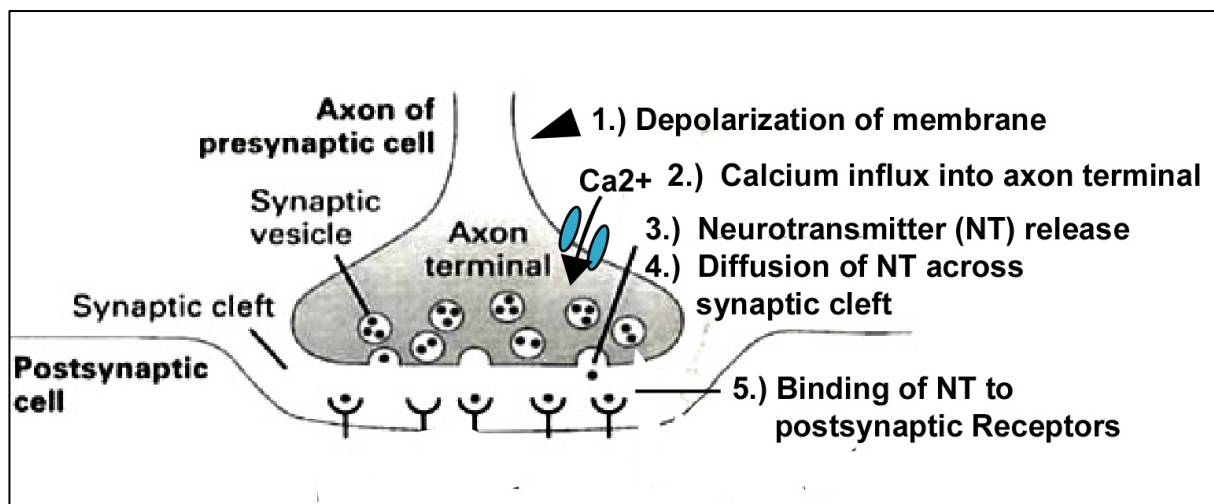


**Figure 1. Illustration of Synaptic Transmission at a Chemical Synapse**

Synaptic vesicle exocytosis is an important step in chemical neurotransmission. Knowledge of the biochemical mechanisms underlying synaptic vesicle exocytosis has increased substantially over the years. However, most studies have focused on elucidating the protein-protein interactions that regulate vesicle release from one type of chemical synapse in

the nervous system, the "conventional" synapse (reviewed in (Rizo and Rosenmund, 2008). Relatively little is known about the molecular mechanisms that underlie vesicle release from the retinal ribbon synapse, another type of chemical synapse in the nervous system. In order to truly understand how synaptic vesicle exocytosis works, it is important to elucidate the protein-protein interactions involved in synaptic vesicle release from all types of chemical synapses. As such, the focus of this study was to elucidate the composition and functional properties of the synaptic vesicle exocytotic machinery of ribbon synapses of the vertebrate retina.

### **Vertebrate Retina: An Overview**

The first step in vision is the projection of visual images onto the retina, a transparent sheet of nervous tissue in the back of the eye. The vertebrate retina is a multi-layered structure with five major classes of neurons. The retinal neurons are the photoreceptors, horizontal cells, bipolar cells, amacrine cells, and ganglion cells. The manner in which these cells are organized within the retina gives rise to distinct layers referred to as the outer nuclear layer, outer plexiform layer, inner nuclear layer, inner plexiform layer, and the ganglion cell layer. The outer nuclear is composed of photoreceptor cell bodies. The outer plexiform layer is where photoreceptors make synaptic contacts with bipolar and horizontal cells. The inner nuclear layer consists of the amacrine and bipolar cell bodies. The inner plexiform layer is where bipolar cells, amacrine cells and ganglion cells make synaptic contacts. The ganglion cell layer is comprised of ganglion cell bodies and amacrine cell bodies (Figure 2).

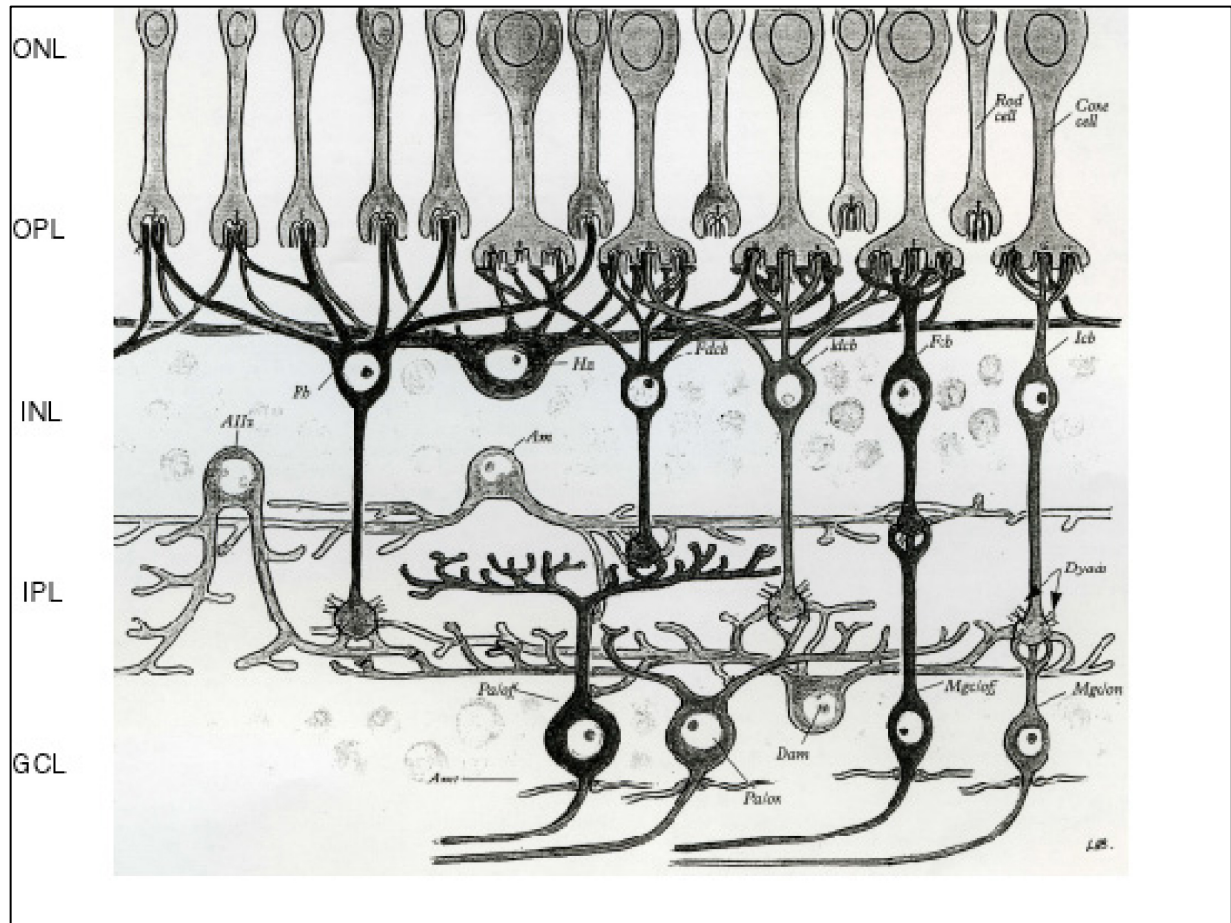


**Figure 2. Organization of the Vertebrate Retina**

ONL=outer nuclear layer; OPL=outer plexiform layer; INL=inner nuclear layer; IPL=inner plexiform layer; GCL=ganglion cell layer. Figure modified from ref.28 with permission of Elsevier (copyright 1971).

The direction of information flow in the vertebrate retina can be described as follows: (1) photoreceptors detect photons of light and convert light signals into a neural signal that is transmitted to the horizontal and bipolar cells, (2) the bipolar cells pass on the neural signal they receive from photoreceptors to amacrine and retinal ganglion cells in the inner retina, (3) upon receipt of the neural signal from the bipolar cells, ganglion cells send an electrical signal to the brain via the optic nerve. This chain of events allows vertebrates to see the world (Rodieck, 1998). The focus of this project is the molecular basis of neurotransmitter release

from synapses of photoreceptors and bipolar cells. As such, the photoreceptors and bipolar cells will be the only retinal neurons discussed from this point on.

### **Photoreceptors and Bipolar Cells: A Brief Description**

Photoreceptors are the primary sensory receptors of the retina. The vertebrate retina contains two types of photoreceptors: rods and cones (refer to figure 3). Rods signal variations in light intensity in dim light, whereas cones signal changes in light intensity in the brighter conditions of daylight. Although rods and cones are designed to operate at different light levels, these two types of cells work in the same general manner. Briefly, when a photoreceptor captures a photon of light, a biochemical cascade within its outer segment is initiated which leads to hyperpolarization of the outer

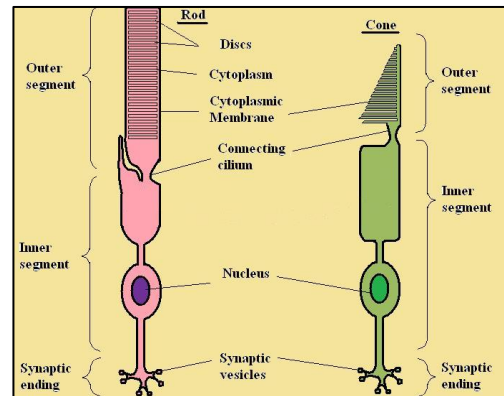


**Figure 3. Photoreceptors in Vertebrate Retina.**

segment membrane. The hyperpolarization spreads to the synaptic terminal membrane which triggers the closure of presynaptic voltage-gated calcium channels. The closing of the calcium channels reduces the amount of calcium within the synaptic terminal. This, in turn, leads to a decrease in the rate of neurotransmitter release at the synaptic terminal.

The rate at which a photoreceptor absorbs photons determines the degree to which it is hyperpolarized. The more photons absorbed, the greater the level of hyperpolarization. Thus, neurotransmitter release from photoreceptors is graded and is maximal in the dark and minimal in bright light (Rodieck, 1998).

### **Bipolar Cells**

Bipolar cells transfer information from the photoreceptors to the ganglion cells (Figure 4). Mammalian bipolar cells receive their inputs from either rods or cones, but not both. A mammalian bipolar cell is thus designated as a rod bipolar or cone bipolar cell depending upon which type of photoreceptor it receives input from. In contrast to mammalian bipolar cells,

some bipolar cells in fish receive input from both rods and cones. One example is the Mb1 bipolar cell in the goldfish (Sherry et al., 1993).

Bipolar cells are classified as either on or off-type, based on how they respond to glutamate released by the photoreceptors. On-bipolar cells are hyperpolarized by glutamate, whereas off-bipolar cells are depolarized by glutamate. Thus, an on-bipolar cell is active (depolarized) when the photoreceptors that synapse on it are in light and an off-bipolar cell is active when the photoreceptors that synapse on it are in the dark.

Bipolar cells typically do not generate  $\text{Na}^+$ -action potentials. Instead, they respond to the release of glutamate from photoreceptors with graded changes in membrane potential.

Thus, bipolar cells use graded potentials to transmit information to amacrine and retinal ganglion cell in the inner retina (Rodieck, 1998).

Why do photoreceptors and bipolar cells use graded potentials to transmit information instead of  $\text{Na}^+$ -action potentials? With graded signaling, photoreceptors and bipolar cells can vary their synaptic output continuously, and thus transfer more information to their postsynaptic partners (Parsons and Sterling, 2003).

### **Synapses of Photoreceptors and Bipolar Cells in the Retina**

Photoreceptors and bipolar cells release neurotransmitter at specialized chemical synapses called ribbon synapses. Of note, ribbon synapses are not exclusive to photoreceptors and bipolar cells. This synapse type is also found in cochlear and vestibular hair cells and in pinealocytes. In general, ribbon synapses are present in neurons that use graded potentials to transmit information (Parsons and Sterling, 2003; Sterling and Matthew, 2004). This study focused on the ribbon synapses in the retina because photoreceptors and bipolar cells are relatively easy to access and the hair cell synaptic vesicle fusion machinery has been characterized already (Gil -Loyzaga et al., 1988; Saffieddine et al., 1997; Safieddine et al., 1999; Roux et al., 2006).



**Figure 4. Golgi-Stained Rod Bipolar Cell from reference 85.**

The active zones of retinal ribbon synapses are marked by a proteinaceous structure termed the synaptic ribbon, which lies perpendicular to the plasma membrane and to which a large number of synaptic vesicles are tethered (examples: turtle cone  $\approx 700$  vesicles/active zone; goldfish Mb1 bipolar cell  $\approx 110$  vesicles/ribbon) (Figure 5). The tethered synaptic vesicles are believed to be fusion competent and comprise the readily releasable pool of vesicles. In addition to the ribbon-associated pool of vesicles, a large cytoplasmic pool of vesicles is also present in ribbon synapses. It is thought the cytoplasmic pool of vesicles might be involved in the replenishment of the releasable vesicle pool (Lenzi et al., 2001; Sterling and Matthews, 2005; Heidelberger et al., 2005).

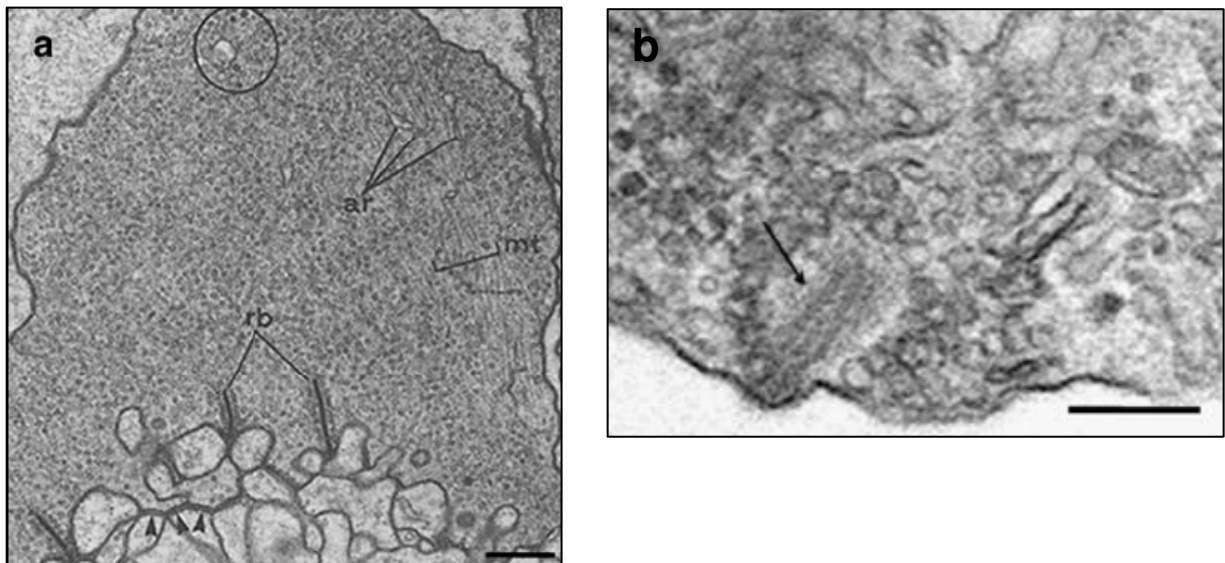


**Figure 5. Vertebrate Retinal Ribbon Synapses**

A. Electron micrograph of a dark-adapted, turtle cone presynaptic terminal. rb = synaptic ribbon, ar = agranular reticulum, mt = microtubules. Scale bar = 0.5  $\mu\text{m}$ . Figure from ref. 58, with kind permission from The Rockefeller University Press (Copyright 1978) B. Electron micrograph shows a goldfish bipolar cell ribbon-style synapse. Arrow denotes synaptic ribbon. Scale bar = 0.15  $\mu\text{m}$ . Figure from reference 83, with kind permission from Springer Science + Business Media (Copyright 2009).

The physiology of the retinal ribbon synapse differs from the physiology of the “conventional” chemical synapse found in the majority of nerve cells. A retinal ribbon synapse is capable of releasing neurotransmitter tonically (sustained) in response to graded changes in membrane potential or phasically (transient) in response to a large change in membrane

potential. Conversely, neurotransmitter is typically released from conventional synapses in a phasic burst in response to an action potential (Heidelberger et al., 1994; Jackman et al., 2009).

The ability of photoreceptors and bipolar cells to accurately encode changes in light intensity is largely due to the versatile release properties of their synapses. Why, in regard to neurotransmitter release, are retinal ribbon synapses more versatile than conventional synapses? Because synaptic vesicle exocytosis is a controlled process regulated by a series of protein-protein interactions, it has been proposed that the presynaptic proteins present in retinal ribbon synapses are different from those present in conventional synapses. Several groups have undertaken the task of analyzing the presynaptic proteins in conventional and retinal ribbon synapses and their results show that although the presynaptic proteins in the two synapse types are largely similar, there are a few molecular differences (Brandstätter et al., 1996; Morgans et al., 1996; von Kriegstein et al., 1999; Sherry et al., 2003; Reim et al., 2005; Sherry et al., 2006). One molecular difference of particular interest is that the composition of the protein complex which mediates the docking/fusion of synaptic vesicles with the presynaptic plasma membrane differs between the two synapse types. This complex, referred to as the SNARE (soluble N-ethylmaleimide-sensitive factor attachment receptor) complex, is described in the next section.

### **SNARE complex: Structure and Function**

SNAREs are small proteins (18-42 kDa) that participate in membrane trafficking in eukaryotic cells. These proteins are localized to the membranes of transport vesicles, subcellular compartments, and the cytoplasmic side of the plasma membrane. SNAREs are classified according to the membrane on which they primarily reside. Vesicle membrane SNAREs are referred to as v-SNAREs, while target membrane SNAREs are referred to as t-SNAREs. All members of the SNARE family contain a segment of 60-70 conserved amino acid residues in their membrane-proximal regions, referred to as the SNARE motif or SNARE binding domain. The SNARE proteins interact with one another through their SNARE binding

domains to form SNARE complexes (Sutton et al., 1998). The SNARE complex that has been studied most extensively is the synaptic SNARE complex found in conventional synapses. This complex is composed of synaptobrevin/VAMP2, SNAP-25, and syntaxin 1A/B. Synaptobrevin/VAMP2 is an integral membrane protein located on synaptic vesicles. It is anchored by its C-terminal transmembrane domain to the vesicle membrane. The N-terminal domain of synaptobrevin/VAMP2, which contains the SNARE binding domain, faces the cytoplasm. SNAP-25 is covalently attached to the cytoplasmic side of the presynaptic plasma membrane by palmitoylation. It is composed of an N-terminal domain and a C-terminal domain that are attached to one another by a cysteine-rich linker region. The N and C-terminal domains both have SNARE binding domains. Syntaxin 1A/B is an integral membrane protein that is attached to the presynaptic plasma membrane via its C-terminal transmembrane domain. The cytoplasmic domain of syntaxin is composed of an unfolded NH2-terminal domain followed by a bundle of three alpha helices (Habc), a linker domain, and the SNARE binding domain (aka H3 domain) (Figure 6).

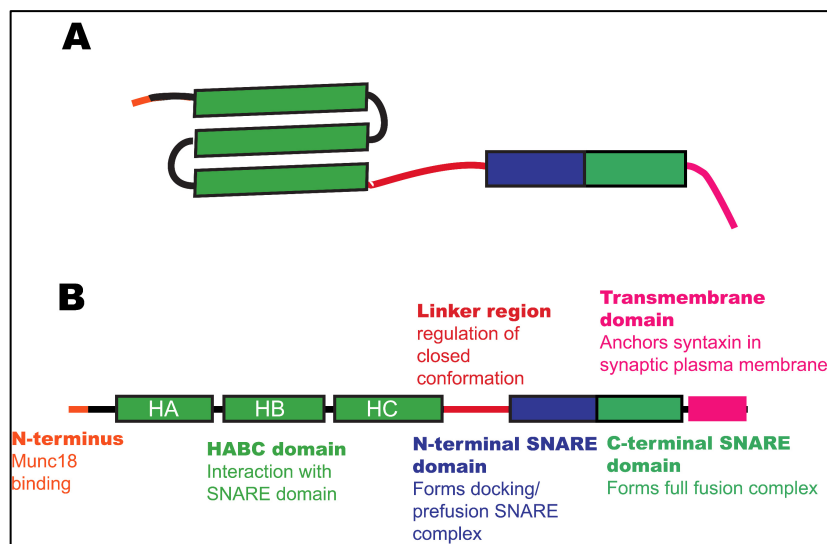


**Figure 6. Structure of Syntaxin 1A/B**

A. Open conformation of syntaxin 1A/B protein. B. Domain structure of syntaxin 1A/B protein.



In conventional synapses, the SNARE complex mediates the docking of synaptic vesicles to the presynaptic plasma membrane. It is believed the synaptic SNARE complex assembles in the following manner: (1) either prior to or during docking of a synaptic vesicle with the presynaptic plasma membrane, syntaxin 1A/B and SNAP-25 interact to form what is referred to as the t-SNARE complex, which has a high-affinity binding site for synaptobrevin/VAMP2 (Söllner, 1993; Pevsner, 1994), (2) when a synaptic vesicle is in close enough proximity to the presynaptic plasma membrane, the N-terminal portion of the SNARE motifs of SNAP-25, syntaxin 1A/B, and synaptobrevin/VAMP2 begin to interact, (3) as docking proceeds, the SNARE motifs zipper together in the N to C-terminal direction to form a parallel, four-helix core complex with SNAP-25 contributing two helices and synaptobrevin/VAMP2 and syntaxin 1A/B contributing one helix each (Sutton et. al., 1998; Toonan and Verhage, 2003) (Figure 7). Formation of the helical complex docks the synaptic vesicle at the release site.

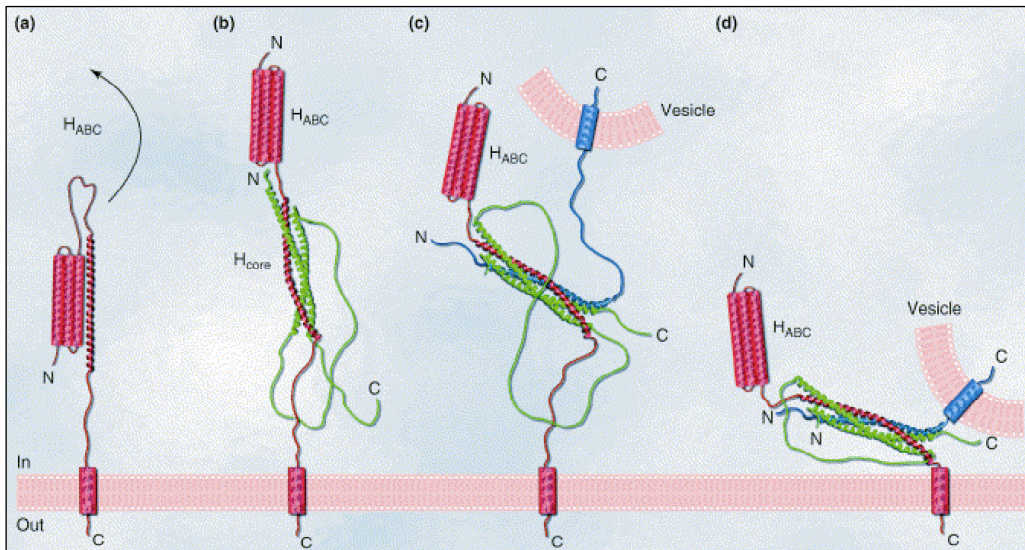


**Figure 7. Assembly of SNARE Complex**

a. The N-terminal H<sub>ABC</sub> domain of syntaxin 1A/B interacts with the SNARE (H3) domain to fold into a closed conformation. b. The SNARE binding domains of syntaxin 1A and SNAP-25 interact to form what is referred to as the t-SNARE complex. The t-SNARE complex has a high-affinity binding site for synaptobrevin/VAMP2. c,d The SNARE motifs zipper together in the N to C-terminal direction to form a parallel, four-helix core complex. Blue, synaptobrevin/VAMP2; Green, SNAP-25; Pink, syntaxin 1A/B. Figure from reference 73, with kind permission from Elsevier (Copyright 2009).

In regard to fusion of synaptic vesicles with the presynaptic plasma membrane, it has been demonstrated *in vitro* that in the absence of any additional cofactors, the synaptic SNARE complex is capable of mediating the fusion of membrane bilayers. The synaptic SNARE complex is thus considered to be the minimal “core machinery” that catalyzes fusion of synaptic vesicle membranes with the presynaptic plasma membrane (Weber et al., 1998).

### **SNARE Complex in Retinal Ribbon Synapses**

The SNARE complexes in conventional and retinal ribbon synapses differ in that syntaxin 1A/B is not a constituent of the retinal ribbon synapse SNARE complex. Past studies have shown the syntaxin isoform present in the retinal ribbon synapse SNARE complex is syntaxin 3 (Brandstätter et al., 1996; Morgans et al., 1996). Four syntaxin 3 isoforms have been found in mice that are generated by differential splicing of the syntaxin 3 gene: syntaxin 3A, B, C, and D. Syntaxin 3A and 3B have identical N-terminal regions, but differ in the C-terminal portion of the SNARE domain and the transmembrane domain. Syntaxin 3C is identical to syntaxin 3B, except for a short stretch of amino acids in its N-terminus. Syntaxin 3D is a truncated protein that lacks a SNARE domain and transmembrane domain; therefore, is not likely to be a SNARE protein (refer to Figure 8 on next page) (Ibaraki et al., 1995).

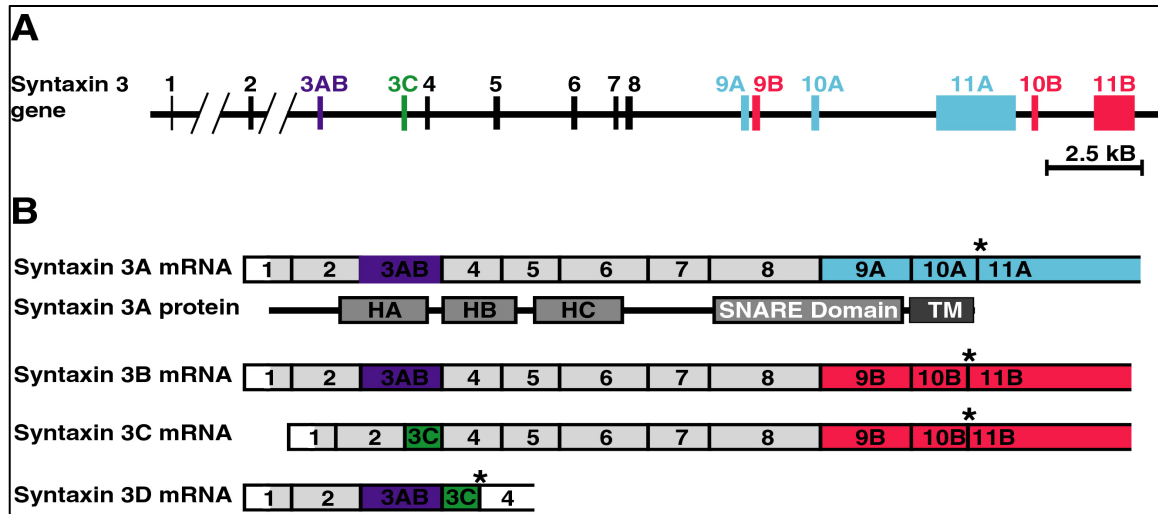


**Figure 8. Syntaxin 3 Isoforms are Generated By Differential Splicing of the Syntaxin 3 Gene**

A. Mouse syntaxin 3 gene. Differentially spliced exons are depicted in different colors that correspond to the differentially spliced mRNA transcripts depicted in B: exon 3AB, purple; exon 3C, green; exons 9A, 10A, 11A, light blue; exons 9B, 10B, 11B, red. B. Structure of the mRNAs of the different isoforms of syntaxin 3. Stop codons at the end of the translated regions are marked by an asterisk. Domain structure of the syntaxin 3A protein is shown beneath the syntaxin 3A mRNA transcript. different domains of the protein are marked: HA, HB, HC domains (HA, HB, HC), SNARE domain, and transmembrane domain (TM). Figure is modified from reference 10 with kind permission from Elsevier.

The previous studies that showed syntaxin 3 as the syntaxin isoform in retinal ribbon synapses did not distinguish which syntaxin 3 isoform is present in the photoreceptor and bipolar cell SNARE complex ( Brandstätter et al., 1996; Morgans et al., 1996). Using Reverse Transcriptase-PCR (RT-PCR) and *in situ* hybridization, our lab has shown that syntaxin 3B is the syntaxin 3 isoform present in the retina. In support of a role for syntaxin 3B in neurotransmitter release, data from a reconstituted liposome fusion assay shows syntaxin 3B can form a complex with SNAP-25 and synaptobrevin/VAMP2 and mediate fusion of membrane bilayers *in vitro* (Curtis et al., 2008). Given that the SNARE core complex has been shown to be essential for neurotransmitter release in conventional synapses, the main goal of this project was to elucidate how syntaxin 3B interacts with other synaptic proteins to regulate neurotransmitter release from retinal ribbon synapses.

### **Presynaptic Proteins in Conventional and Retinal Ribbon Synapses**

The molecular differences between retinal ribbon and conventional synapses are not limited to the SNARE complex. The table below summarizes the molecular differences between these two synapse types that have been found to date.

**Table 1. Presynaptic Proteins Involved in Synaptic Vesicle Exocytosis in Retinal Ribbon and Conventional Synapses.**

<b>Presynaptic Protein</b>	<b>Isoform found in ribbon synapses of the rodent retina</b>	<b>Isoform found in conventional synapses</b>	<b>Presumed biological function</b>
Syntaxin	<b>Syntaxin 3B</b> , (Curtis et al., 2008)	Syntaxin 1A and 1B	Part of SNARE complex
SNAP-25	SNAP-25 (Brandstätter et al., 1996)	SNAP-25	Part of SNARE complex
Synaptobrevin/VAMP	Synaptobrevin 2/VAMP 2 (Ullrich and Südhof, 1994)	Synaptobrevin 2/VAMP 2	Part of SNARE complex
Complexin	<b>Complexin 3 and 4</b> (Reim et al., 2005)	Complexin 1,2 and 3	Binds to SNARE complex, regulator of exocytosis
Synaptotagmin	Synaptotagmin 1 (Fox and Sanes, 2007)	Synaptotagmin 1 and 2	Low affinity Ca <sup>2+</sup> sensor for synaptic vesicle exocytosis
Munc18/N-sec 1	Present but exact isoform unknown (Ullrich and Südhof, 1994)	Munc18-1	Binds to syntaxins and SNARE complex, regulator of exocytosis
Munc13	<b>Absent (Schmitz et al., 2001)</b>	Munc13-1	Regulator of exocytosis
Calcium Channels	<b>L type, (Cav1.3 and Cav1.4) (Mansergh et al., 2005; Xiao et al., 2007)</b>	N, P/Q, R type	Mediates Ca <sup>2+</sup> entry into synaptic terminal
Synapsins	<b>Absent (Mandell et al., 1990)</b>	Synapsin 1,2 and 3	Regulates reserve pool of synaptic vesicles

The proteins listed above are thought to be the main components of the synaptic vesicle exocytotic fusion machinery (reviewed in (Rizo and Rosenmund, 2008)). As shown in Table 1,

the composition of the synaptic vesicle exocytotic fusion machinery differs between retinal ribbon and conventional synapses. Although the interactions between the proteins which make up synaptic vesicle exocytotic fusion machinery in retinal ribbon synapses have not been well-characterized, a hypothetical model of synaptic vesicle exocytosis in retinal ribbon synapses is shown on the next page in Figure 9. The model assumes that syntaxin 3B has the same basic functional properties as syntaxin 1A/B. In addition, it is assumed that the complexin isoforms do not differ from each other in how they regulate the SNARE complex. To test the model shown in Figure 9, I used molecular and biochemical techniques to characterize the interactions between syntaxin 3B and the other constituents of the synaptic vesicle exocytotic fusion machinery in retinal ribbon synapses.

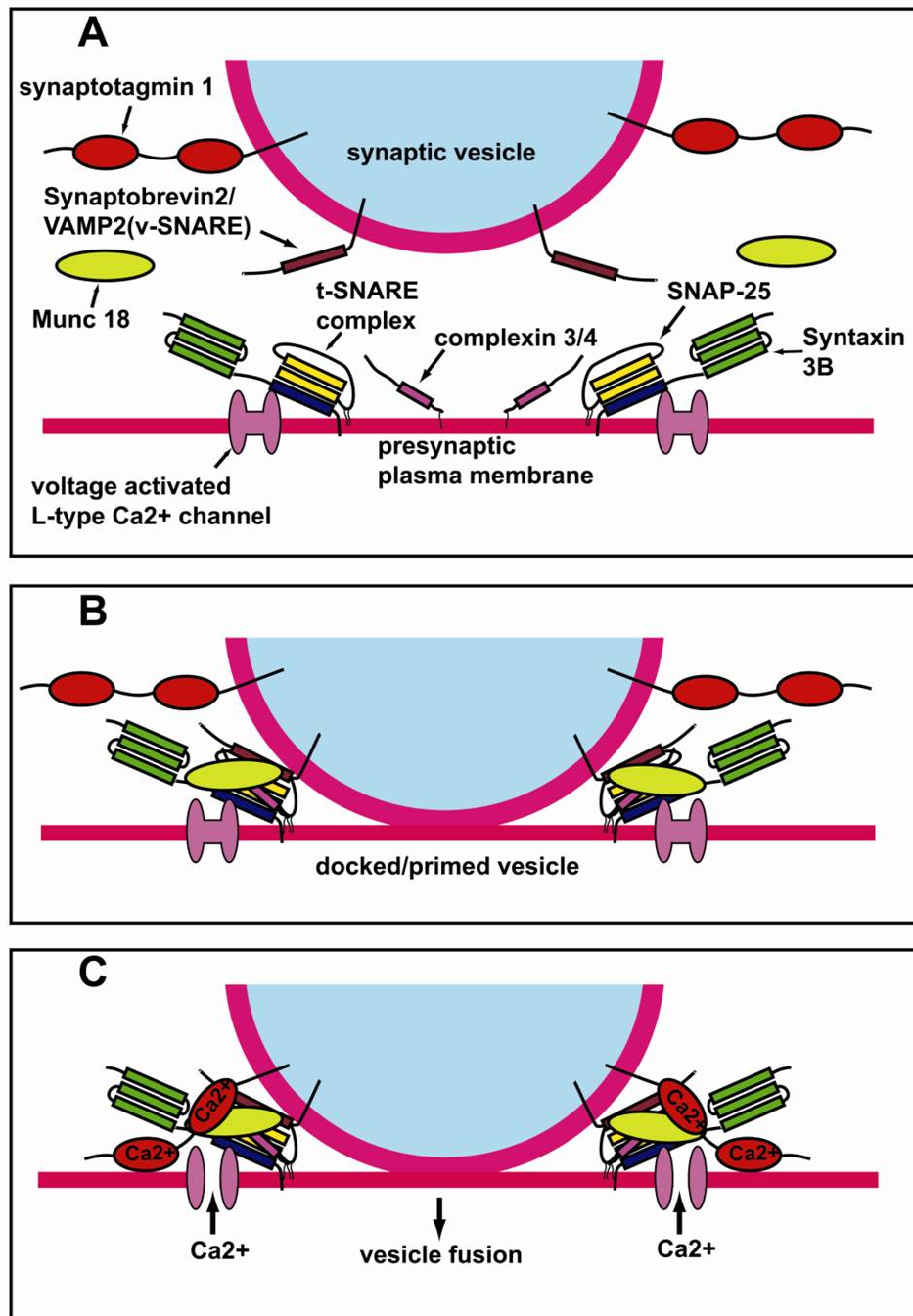


### **Figure 9. Model of Synaptic Vesicle Exocytosis in Retinal Ribbon Synapses**

A. t-SNARE complex is formed between SNAP-25 and syntaxin 3B. B. SNARE complex is formed between the t-SNARE complex and the v-SNARE synaptobrevin 2/VAMP 2. This complex physically docks the synaptic vesicle at the plasma membrane. Munc18/N-sec1 and complexins 3 or 4 then bind to the SNARE complex to stabilize it. C. Depolarization of the membrane opens voltage-gated L-type calcium channels. The L-type calcium channels are kept in proximity of the t-SNARE complex by binding to syntaxin 3B. This results in the vesicles being exposed to a high concentration of calcium upon activation of the channels. The calcium ions near the vesicle bind to the two C2 domains of the synaptic vesicle protein, synaptotagmin 1. Synaptotagmin 1 then binds to the plasma membrane and the SNARE complex and triggers fast synaptic vesicle exocytosis.

## **Chapter 2: Interaction Between Syntaxin 3B and Presynaptic Proteins from Mammalian Retina**

2.1 Characterization of the interaction between Syntaxin 3B and SNAP-25.

2.2 Syntaxin 3B and Ca<sub>v</sub>1.4 channel.

2.3 Proteomics to identify syntaxin 3B interacting proteins.

## **Material and Methods**

### **Antibodies**

SNAP-25 Ab: The monoclonal SNAP25 antibody (CL71.1) (Synaptic Systems) was raised against full-length recombinant rat SNAP25B His6 fusion protein. It recognizes an epitope between positions amino acid 20 and 40 that is conserved between the splice forms SNAP25A and -B from rat and mouse (information from manufacturer). L-type channel Ab: Rabbit antiserum was generated against a N-terminal peptide (CSESEVGKDTTPEPSPANGT) derived from the  $\alpha 1$  subunit of the mouse  $\text{Ca}_v1.4$  channel and purified using the same peptide as described in Janz and Südhof (Neuroscience, 1999). Spectrin  $\alpha$ II ( $\alpha$  Fodrin [D8B7]) Ab: Clone D8B7 was developed against the  $\alpha$ II spectrin SH3 domain (non-erythroid spectrin) (information from Abcam).

### **GST- Pulldown**

Glutathione S-transferase (GST) fusion proteins were expressed in *Escherichia coli* BL21 cells and purified with glutathione-sepharose beads. Frozen mouse retinas (Pel-Freez) were homogenized in buffer A consisting of 20 mM HEPES-NaOH, pH 7.4, 0.2 mM phenylmethylsulfonyl fluoride (PMSF), 2  $\mu\text{g}/\text{ml}$  aprotinin, 2  $\mu\text{g}/\text{ml}$  pepstatin, and 2  $\mu\text{g}/\text{ml}$  leupeptin. After homogenization, the Bradford Protein Assay (Pierce) was used to check the protein concentration of the homogenate. Once the homogenate protein concentration was determined, an equal amount of buffer B (20 mM HEPES-NaOH, pH 7.4, 0.2 M NaCl, 2% Triton X-100) was added to the homogenate, and the sample was incubated at 4°C with rotation for 30 minutes. The homogenate was then centrifuged for 1 hour at 20,000 rpm at 4°C in a JA-20 rotor and the supernatant used for binding experiments. The protein concentration of the supernatant was adjusted by dilution to 0.1 mg/ml. Binding reactions were performed with 150  $\mu\text{M}$  CaCl<sub>2</sub> or 2 mM EGTA. Glutathione-Sepharose beads were added to a MicroBio-Spin Chromatography Column (Bio-Rad) and one milliliter of the extract was mixed with the glutathione sepharose beads. The reactions were then incubated overnight at 4°C, with rotation. After overnight incubation, the glutathione-sepharose beads were washed 4X with



cold wash buffer (20 mM HEPES-NaOH, pH 7.4, 0.1 M NaCl, 1% Triton X-100 with either 150  $\mu$ M CaCl<sub>2</sub> or 2 mM EGTA). Proteins were eluted from the beads by adding SDS reducing sample buffer, and the samples were analyzed by SDS-PAGE and Western blotting.

### **Plasmid Construction**

A mouse EST clone (accession No. BC024844, IMAGE clone No. 5357204) coding for full-length syntaxin 3B was used as a template to generate syntaxin 3B expression constructs by PCR. The syntaxin 3B GST fusion construct (pGST-synt.3B) was generated by cloning a BamHI/ EcoRI fragment which encoded the cytoplasmic domain of syntaxin 3B (residues 2–264) into the pGEX-KG expression vector. The syntaxin 3B GST fusion construct (pGST-synt.3B SNARE domain) was generated by cloning a BamHI/ EcoRI fragment which encoded the syntaxin 3B SNARE domain into the pGEX-KG expression vector. The syntaxin 1 GST fusion construct containing the cytoplasmic domain without the transmembrane domain (residues 4–267) has been described by Pevsner et al. (1994a). All constructs were verified by direct sequencing.

### **Chemical Cross-linking**

Lyophilized Protein A-Sepharose beads (0.25g ) were weighed out, resuspended in 1X PBS, and washed 3X with 1X PBS. After the washes, the beads were resuspended in 1ml 1X PBS. One ml of diluted antiserum, preimmune serum, or rabbit serum was mixed with the Protein A-Sepharose beads. The sample was rotated at room temperature for 20 min. After the 20 min. incubation, the sample was spun down and the soup removed. The beads were washed 2X with 1X PBS and transferred to Micro-BioSpin Chromatography Column (Biorad). The beads were then washed again with 1X PBS (5X). Two vials (4mg) of DSS ((Disuccinimidyl suberate, (Pierce, Product # 21658) was dissolved in 500ul DMSO. The dissolved DSS was transferred to a new tube and 1 ml of 1X PBS was added to the DSS. The solution was pipetted onto the Protein A-Sepharose beads on the column. The column was rotated for 1 hr. at room temperature. After the 1hr. incubation, the column was placed in a test tube, and the beads were washed with 5 ml of 1X PBS. One mL of 1M Tris-HCl, pH 7.5 was added to the column.

The column was rotated for 10 minutes. After the 10 min. incubation, the 1M Tris-HCl, pH 7.5 solution was drained from the column and 1 ml of 50mM Glycine pH 2.8 was pipetted onto the column. The column was inverted several times. Afterwards, the glycine solution was drained from the column and the beads were washed with 1 ml of 50mM Glycine pH 2.8. After the glycine wash, the beads were washed 3X with 1X PBS and used for immunoprecipitation experiments.

### **Transfection of HEK293 cells**

Day 1: untransfected HEK 293 cells in DMEM, 10% FCS w/o antibiotics were plated onto 10 cm tissue culture plates and incubated at 37 Celsius in a CO<sub>2</sub> incubator overnight. Day 2: expression vectors (pcDNA-  $\alpha 2\delta$ (3ug), pcDNA- $\beta 2A$  (3 ug), pcDNA- $\alpha 1.4$  (3 ug), pCMV-Synt. 3B (3 ug),) were diluted in Opti-Mem I medium. The diluted DNA was then mixed with Lipofectamine 2000 diluted in Opti-Mem I and incubated for 20 min. at room temp. After the 20 min. incubation, the Lipofectamine/DNA mixture was added to the untransfected HEK cells from Day 1. The culture plates were incubated at 37 Celsius in a CO<sub>2</sub> incubator for 6 hours at which time the medium was changed. The plates were then incubated at 37 Celsius in a CO<sub>2</sub> incubator for 48 hours. For a negative control, untransfected HEK 293 cells were incubated alongside the transfected HEK 293 cells.

### **Immunoprecipitation with HEK 293 Cell Extract**

Untransfected and transfected HEK cells were removed from tissue culture plates by scraping with a rubber policeman. Cells were centrifuged at 500-700 rpm for 10 min. The soups were removed and the pellets were weighed. The weight of the pellet (mg) x 5 = volume of lysis buffer (20 mM HEPES-NaOH, pH 7.4, Complete Mini Tablet (Roche)) added to each pellet. The pellets in lysis buffer were homogenized with the TissueMiser (Fisher Scientific). After homogenization, 1 volume of Buffer B (20 mM HEPES-NaOH, pH 7.4, 0.2 M NaCl, 2% Triton X-100) was added to the homogenates and the samples were incubated at 4°C with rotation for 45 minutes. The samples were then centrifuged at 4000 RPM for 30 min. After centrifugation, aliquots of the supernatants (extracts) were removed and saved for analysis by

Western blotting. One milliliter of the untransfected or transfected cell extract was then incubated with either Syntaxin 3 antiserum antibodies cross-linked to Protein A-Sepharose beads (100  $\mu$ l) or rabbit serum antibodies cross-linked to Protein A-Sepharose beads (100  $\mu$ l). The samples were incubated for 1 hr. at room temperature with rotation. After the 1 hr. incubation, the beads were washed 4X with cold wash buffer (20 mM HEPES-NaOH, pH 7.4, 0.1 M NaCl, 1% Triton X-100). Proteins were eluted from the beads by adding 2X SDS reducing sample buffer and analyzed by SDS-PAGE and Western blotting.

#### **Immunoprecipitation with Mouse Retina Extract**

Ten frozen mouse retinas (PelFreez) were homogenized in 570  $\mu$ l of Buffer A (20mM HEPES, pH 7.4, 0.2 mM PMSF, 2  $\mu$ g/ml aprotinin, 2  $\mu$ g/ml pepstatin, 2  $\mu$ g/ml leupeptin) with the TissueMiser (Fisher Scientific). After homogenization, 570  $\mu$ l of Buffer B (20 mM HEPES, pH 7.4, 0.2 M NaCl, 2% TX-100) was added and the sample was incubated at 4 degrees Celsius for 30 min. with rotation. After rotation, the sample was centrifuged at 13,000 rpm in a microcentrifuge at 4 degrees Celsius for 30 min. The supernatant (350  $\mu$ l) was mixed with 100  $\mu$ l of syntaxin 3 Ab cross-linked to Protein A-Sepharose beads. For a negative control, the supernatant was also mixed with preimmune serum Abs cross-linked to Protein A-Sepharose beads. The samples were rotated for 4 hours at 4 degrees Celsius. The beads were then washed 4X with Wash Buffer ( 20 mM HEPES, pH 7.4, 0.1 M NaCl , 1% TX-100). This was followed by four washes with 50 mM glycine, pH 2.8 (100 $\mu$ l/wash). Each glycine wash was collected and neutralized with 10  $\mu$ l of 1M Tris-HCl, pH 8.0. The beads were then washed 2X with 20 mM HEPES-NaOH, 2% SDS (100 $\mu$ l/wash). After these washes, 2X SDS Sample Buffer was added to the beads, the glycine washes, and the 20 mM HEPES-NaOH, 2% SDS washes. The samples were then analyzed by Western blotting.

#### **Immunoprecipitation with Bovine Retina Extract**

Ten frozen bovine retinas (PelFreez) were homogenized in 18.6 mL of Buffer A (20mM HEPES pH 7.4, Complete Mini Tablets (Roche)) with the TissueMiser (Fisher Scientific). After homogenization, an equal volume of Buffer B (20 mM HEPES, pH 7.4, 0.2 M NaCl, 2% TX-

100) was added and the sample was incubated at 4 degrees Celsius for 30 min. with rotation. The sample was then centrifuged at 4000 rpm for 20 min. (Sorvall RT Plus). After centrifugation, the supernatant (37.2 mL) was mixed with 1 mL of Syntaxin 3 antiserum antibodies cross-linked to Protein A-Sepharose beads. The sample was then rotated for 45 min. at room temperature. After the 45 min. incubation, the sample was spun down and the beads were transferred to a Poly-Prep Chromatography Column (Bio-Rad). The beads were then washed 4X with Wash Buffer (20 mM HEPES, pH 7.4, 0.1 M NaCl, 1% TX-100). This was followed by four washes with 50 mM Glycine, pH 2.8 (500ul/wash). Each glycine wash was collected and neutralized with 100 µl of 1M Tris-HCl, pH 8.0. The neutralized washes were pooled together and mixed with beads that had rabbit serum IgG antibodies crosslinked to them (600 µl). The sample was incubated overnight at 4 degrees Celsius with rotation. The next day, fractions of the flow-thru were collected (each fraction = 500 µl flow-thru). The beads were washed three times with 1X PBS (200µl/wash). The washes were also collected in fractions. The Bradford Protein Assay (Pierce) was used to determine the amount of protein in each fraction. The fractions with a significant amount of protein were pooled together. The pooled sample was then concentrated twice with Centricon Ultracel YM-3. Aliquots of the concentrated samples were analyzed by coomassie dye, silver staining, and western blotting. Protein bands visible on the coomassie stained gels were cut out and analyzed by mass spectrometry.

### **Western Blot**

Blots were preblocked for 1 hr in TBST containing 5% goat serum and 5% nonfat milk (blocking milk). The blots were then incubated with the primary antibody (SNAP-25 CL71.1 1:10,000 (Synaptic Systems), Syntaxin 3 Ab 1:1000, L-type Calcium channel ( $\alpha_1F$ ) Ab 1:2000, or Spectrin  $\alpha$  II Ab 1:1000 (Abcam)) in blocking milk for 1 hr at room temperature. The blots were then washed three times with 1X TBST (10 min./wash). The secondary antibody in blocking milk (HRP Goat anti-rabbit 1:5000 (Zymed) or HRP Goat anti-mouse 1:2000) was then incubated with the blot for 1 hr. at room temp. After incubation with the secondary

antibody, the blots were washed as described above. The blots were then developed using SuperSignal West Pico Chemiluminescent Substrate (Pierce) or ECL Plus Western Blotting Detection System (Amersham).

## **2.1 Characterization of the Interaction between Syntaxin 3B and SNAP-25.**

As mentioned in the Introduction, in conventional synapses, syntaxin 1A/B and SNAP-25 interact to form what is referred to as the t-SNARE complex. Formation of this complex is thought to be an important step in the assembly of the SNARE complex at conventional synapses (Söllner, 1993; Pevsner, 1994). In Curtis et al., 2008, the interaction between mouse syntaxin 3B and SNAP-25 was examined using a GST-Pulldown Assay (refer to Figure 10).

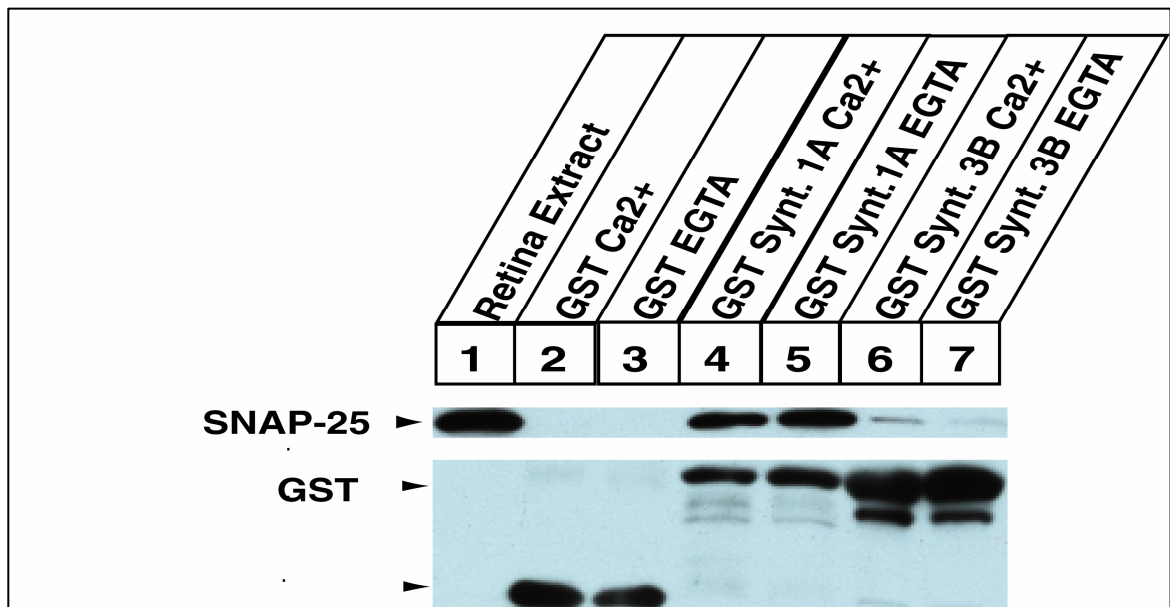


**Figure 10. SNAP-25 Binds Weakly to Syntaxin 3B**

Lane 1: Mouse retina extract without calcium or EGTA. Lanes 2 and 3: For a negative control, GST attached to glutathione sepharose beads was subjected to the same conditions as the GST-fusion proteins. Lanes 4-7: Mouse retina extract with either 150  $\mu$ M calcium or 2 mM EGTA was incubated with the indicated GST-fusion proteins (GST-syntaxin 1A and GST-syntaxin 3B). Reprinted from reference 10 with kind permission from Elsevier.

As shown in Figure 10, the results of the pull-down showed that syntaxin 3B can bind to SNAP-25; however, SNAP-25 binding with syntaxin 3B is much weaker than with syntaxin 1A. Why does SNAP-25 have a lower affinity for syntaxin 3B? One explanation for this difference in affinity is syntaxin 3B might reside more in the closed state than syntaxin 1A. Syntaxin 1A has been shown to exist in both an open and a closed state. In the closed state, the N-terminus of syntaxin 1A folds over onto the SNARE binding domain blocking its interaction with

SNAP-25 (Dulubova et al., 1999). Interestingly, the N-terminal region is where the amino acid sequence of syntaxin 3B differs the most from the amino acid sequence of syntaxin 1A (refer to Figure 11).

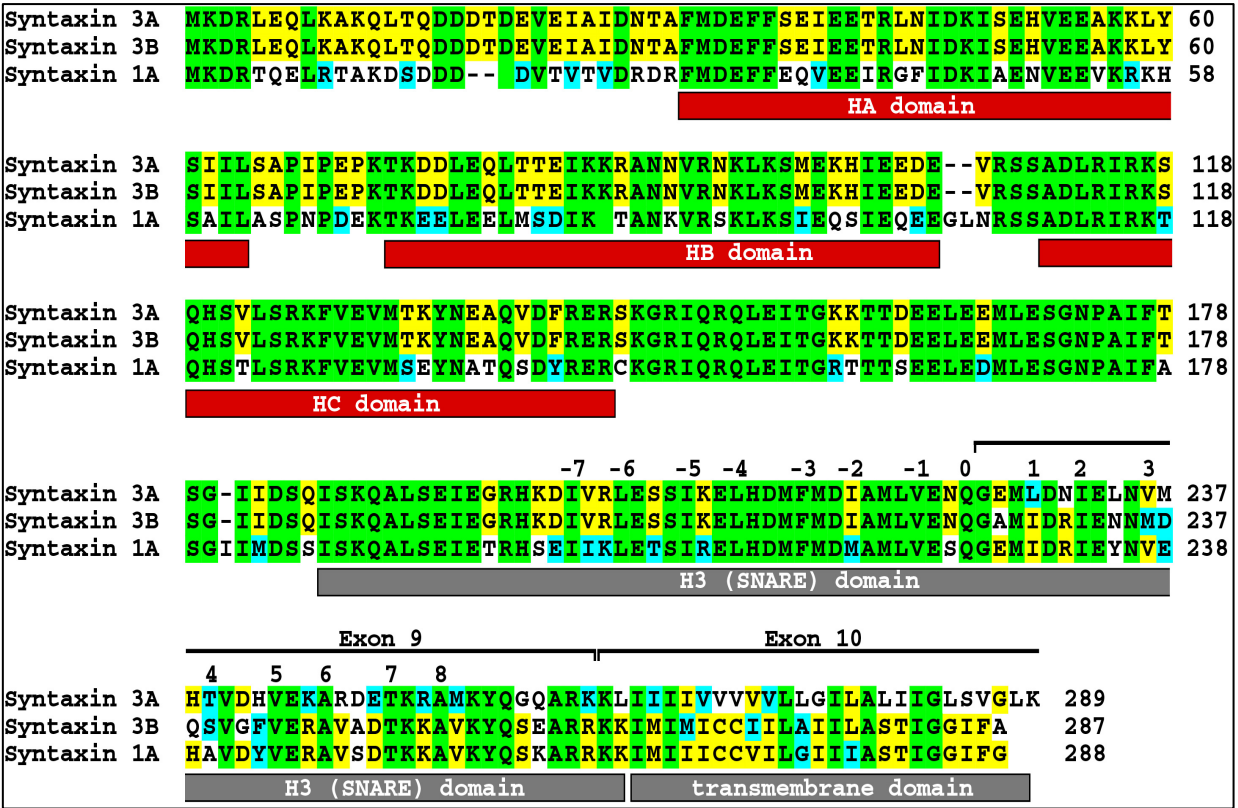


**Figure 11. Sequence Alignment of Mouse Syntaxin Isoforms**

The amino acid sequences of syntaxin 1A, syntaxin 3B and syntaxin 3A have been aligned to assess homology between the syntaxin isoforms. Sequences are identified on the left and residues numbered on the right. Amino acid residues conserved between all three syntaxin isoforms are labeled with green background. Residues conserved between two of the syntaxin isoforms are labeled with yellow background. Conservative exchange residues are labeled with blue background. The N-terminal domain of the syntaxins is a three-helix bundle comprised of helix A (HA), helix B (HB), and helix C (HC). The SNARE domain is one helix (H3). Figure is modified from reference 10 with kind permission from Elsevier.

To test whether the N-terminal domain of syntaxin 3B is responsible for the weak interaction between syntaxin 3B and SNAP-25 *in vitro*, a recombinant protein consisting of Glutathione-S-Transferase (GST) fused to the SNARE domain of syntaxin 3B was generated and used in a GST Pulldown Assay. The GST fusion protein was immobilized on glutathione beads and incubated with mouse retina extract. SNAP-25 bound to the syntaxin 3B SNARE

domain was detected by immunoblotting. Results of the pulldowns are shown in the figure below.

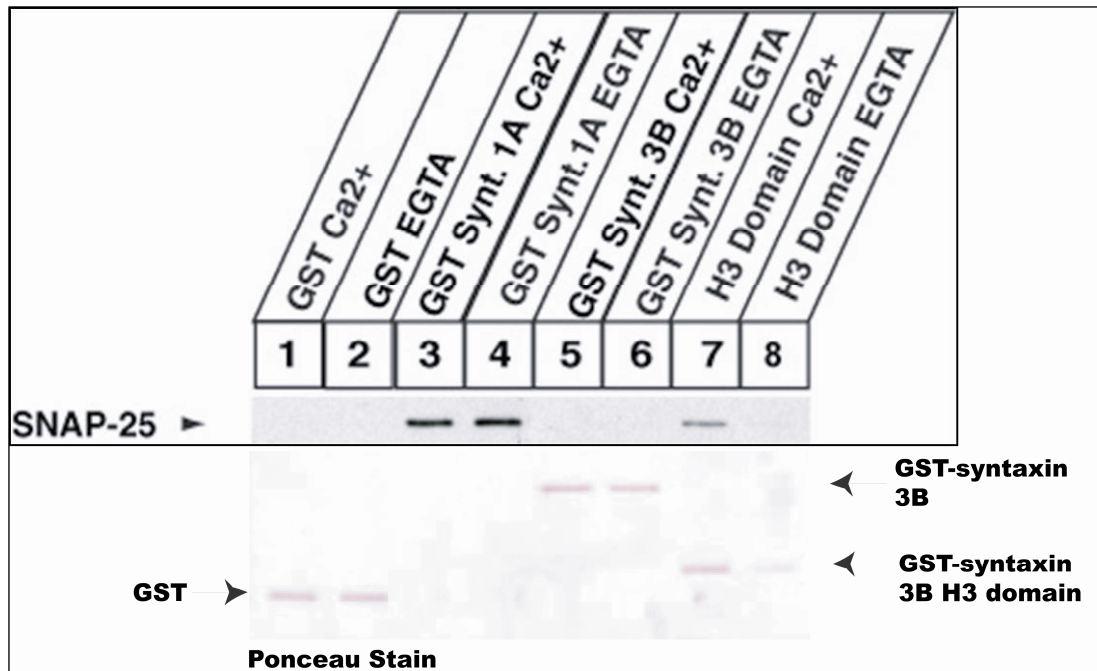


**Figure 12. Removal of Syntaxin 3B's N-terminal Domain Increases Binding between Syntaxin 3B and SNAP-25.**

Lanes 1-2: For a negative control, Glutathione-S-Transferase (GST) bound to glutathione sepharose beads was incubated with retina extract that had either 150  $\mu$ M calcium or 2 mM EGTA added to it. Lanes 3-8: Retina extract with either 150  $\mu$ M calcium or 2 mM EGTA was incubated with the indicated GST-fusion proteins (GST-syntaxin 1A, GST-syntaxin 3B, H3 domain). The H3 domain protein was syntaxin 3B minus its N-terminal domain. The nitrocellulose membrane was stained with Ponceau to check that the amount of GST fusion protein in each pulldown was comparable (results below SNAP-25 blot). Blot shown is from one experiment. Other members of the Janz lab repeated this experiment and obtained similar results.

As shown in Figure 12, when the N-terminal domain of syntaxin 3B is removed, more SNAP-25 binds to syntaxin 3B, (compare lane 5 with lane 7). Although the increase in binding appears to be  $\text{Ca}^{2+}$ - dependent, this must be interpreted with caution as the Ponceau stain indicates there are differences in the amount of protein on the blot (compare lanes 7 & 8). The binding of SNAP-25 to GST-fusion proteins is specific as no binding was observed with GST (Lanes 1 & 2). The results of the GST Pulldown support the idea that the N-terminus of



syntaxin 3B plays a role in the weak binding between syntaxin 3B and SNAP-25 that was observed previously in Curtis et al., 2008.

## **2.2 Syntaxin 3B and Ca<sub>v</sub>1.4 channel**

Vesicular neurotransmitter release requires an increase in intracellular calcium within the nerve terminal of a neuron. The calcium channels which support release at conventional synapses are N-type (Ca<sub>v</sub>2.2), P/Q-type (Ca<sub>v</sub>2.1), R-type (Ca<sub>v</sub>2.3) and L-type (Ca<sub>v</sub>1.2 and Ca<sub>v</sub>1.3) (Tippens et al., 2008). Neurotransmitter release from bipolar cells is mainly supported by the Ca<sub>v</sub>1.3 L-type channel, whereas release from photoreceptors is supported by Ca<sub>v</sub>1.3 and Ca<sub>v</sub>1.4 L-type channels (Heidelberger and Matthews, 1992; Morgans, 2001; LoGiudice et al., 2005).

The rapid fusion of synaptic vesicles with the presynaptic plasma membrane upon activation of presynaptic voltage-gated calcium channels suggests the secretory machinery (i.e., SNARE complex and associated proteins) and the calcium channels must be physically and functionally coupled (reviewed in Atlas, 2001). Consistent with this idea, syntaxin 1A/B can interact with and modulate several of the presynaptic calcium channels which support neurotransmitter release from conventional synapses (Sheng et al., 1994; Wiser et al., 1996). One calcium channel modulated by syntaxin 1A is the L-type calcium channel (Ca<sub>v</sub>1.2). Several studies have shown two cysteine residues (C271, C272) in the transmembrane domain of syntaxin 1A play a major role in the modulation of Ca<sub>v</sub>1.2 channel kinetics (Arien et al., 2003; Cohen et al., 2007). Interestingly, C271 and C272 are conserved in syntaxin 3B. This suggests syntaxin 3B may be capable of interacting with and regulating Ca<sub>v</sub>1.2 and/or calcium channels similar to Ca<sub>v</sub>1.2 such as Ca<sub>v</sub>1.3 and Ca<sub>v</sub>1.4.

To date, it is unknown whether syntaxin 3B can bind to and modulate the kinetics of Ca<sub>v</sub>1.3 and Ca<sub>v</sub>1.4. To address whether syntaxin 3B can interact with the Ca<sub>v</sub>1.4 channel, my lab generated a polyclonal antibody against a peptide sequence within the alpha 1F subunit ( $\alpha_{1F}$ ) of the Ca<sub>v</sub>1.4 channel. To confirm the antibody can recognize the Ca<sub>v</sub>1.4 channel and assess whether recombinant syntaxin 3B and Ca<sub>v</sub>1.4 can form a complex, HEK 293 cells

were transfected with cDNAs that encoded syntaxin 3B and the  $\alpha_{1F}$ ,  $\beta_{2A}$ ,  $\alpha_{2\delta}$  subunits of the  $\text{Ca}_v1.4$  channel. Extract from the transfected cells was probed on a Western blot with the  $\text{Ca}_v1.4$  antibody. The results are shown in Figure 13.

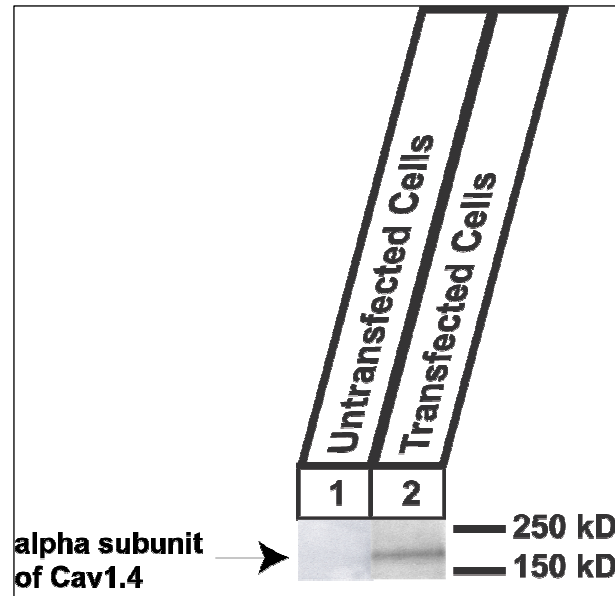


**Figure 13. Verification  $\text{Ca}_v1.4$  Antibody Recognizes Alpha 1F Subunit in Extract**

Lane 1: Total protein extract from untransfected HEK 293 cells. Lane 2: Total protein extract from HEK 293 cells transfected with  $\text{Ca}_v1.4$  channel subunits and syntaxin 3B (blot with syntaxin 3 antibody not shown). A prominent band at  $\sim 230$  kD, the predicted molecular weight of  $\alpha_{1F}$ , is detected in extract from transfected cells. Blot shown is representative of three experiments.

As shown in Figure 13, the  $\text{Ca}_v1.4$  channel antibody generated by my lab can detect the  $\alpha_{1F}$  subunit in extract from HEK 293 cells transfected with the  $\text{Ca}_v1.4$  channel. Extract from untransfected and transfected HEK 293 cells (shown in Figure 13), was used for immunoprecipitation experiments with a syntaxin 3 antibody. Unfortunately, the results of these experiments were inconclusive because the syntaxin 3 antibody reacted with recombinant syntaxin 3B and unidentified HEK 293 cell proteins (data not shown). In spite of this, the data shown in Figure 13 indicates the  $\text{Ca}_v1.4$  channel antibody can be used to analyze whether the  $\text{Ca}_v1.4$  channel is a binding partner of syntaxin 3B.

Immunoprecipitation (IP) experiments with mouse retina extract and syntaxin 3 antiserum were performed to determine if native syntaxin 3B can interact with native  $\text{Ca}_v1.4$ . As shown in the figure below, the syntaxin 3 antiserum immunoprecipitated syntaxin 3B from mouse retina extract (Figure 14, Lane 1). Syntaxin 3 antiserum is comprised of antibodies specific for mouse syntaxin 3 and antibodies that were present in the host rabbit prior to it being injected with the syntaxin 3 antigen. To ensure syntaxin 3B was immunoprecipitated by the syntaxin 3-specific antibodies and not other IgG antibodies present in the antiserum, an immunoprecipitation was performed with preimmune serum (Figure 14, Lane 2). The lack of syntaxin 3B in the preimmune serum precipitate indicates the syntaxin 3 antibody specifically immunoprecipitated syntaxin 3B from the retina extract. As shown in Lane 1, the  $\text{Ca}_v1.4$  channel co-immunoprecipitated with syntaxin 3B. The  $\text{Ca}_v1.4$  channel was not present in the preimmune serum immunoprecipitate which verified the channel was immunoprecipitated only when the syntaxin 3 antibody was present (Lane 2). Since the syntaxin 3 antibody recognizes syntaxin 3B and not the  $\text{Ca}_v1.4$  channel, the data shown in Figure 14 indicate syntaxin 3B and the  $\text{Ca}_v1.4$  channel were immunoprecipitated from the mouse retina extract as a complex.

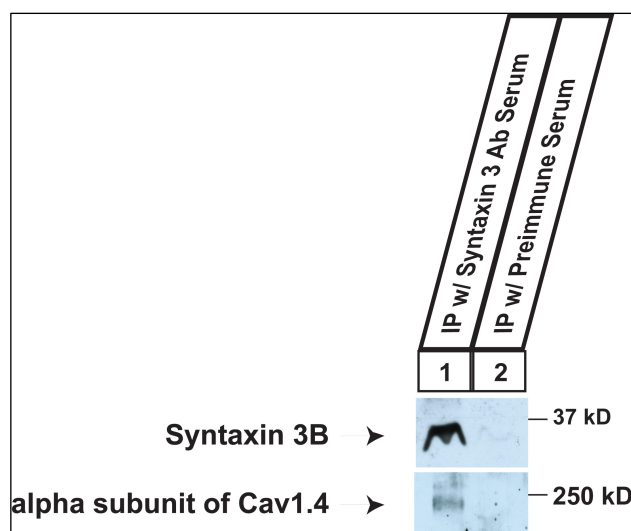


**Figure 14. Syntaxin 3B and the  $\text{Ca}_v1.4$  Channel Interact**

Syntaxin 3 antiserum antibodies coupled to Protein A-Sepharose beads was used to immunoprecipitate syntaxin 3B from mouse retina extract. Precipitates were analyzed by Western blotting using syntaxin 3 and alpha 1F-specific antibodies. IPs were repeated four times.

### **2.3 Proteomics to Identify Syntaxin 3B Interacting Proteins**

Mass spectrometry was used to confirm Ca<sub>v</sub>1.4 is a binding partner of syntaxin 3B and identify other proteins that interact with syntaxin 3B. For these experiments, syntaxin 3 antiserum antibodies chemically cross-linked to Protein A-Sepharose beads were incubated with bovine retina extract for a period of time. The beads were then washed several times to remove material that had bound non-specifically to the beads. The immunoprecipitate was eluted from the beads by washing the beads with 50 mM glycine (pH 2.8). The washes were collected and neutralized with 1M Tris-HCl (pH 8.0). The neutralized washes were pooled and incubated with beads that had rabbit serum IgG antibodies crosslinked to them. The purpose of this step was to remove the proteins in the pooled washes which had been immunoprecipitated from the retina extract by the non-specific IgG antibodies in the syntaxin 3 antiserum. After the incubation, the cleared washes were collected, and pooled together. The pooled washes were then concentrated several times and run on SDS-PAGE gels. The gels were either stained with silver or Coomassie Blue. Protein bands visible on the coomassie gel (refer to Figure 15 on next page) were cut out and sent to the proteonomic core facility at UT Houston for mass spectrometric analysis.

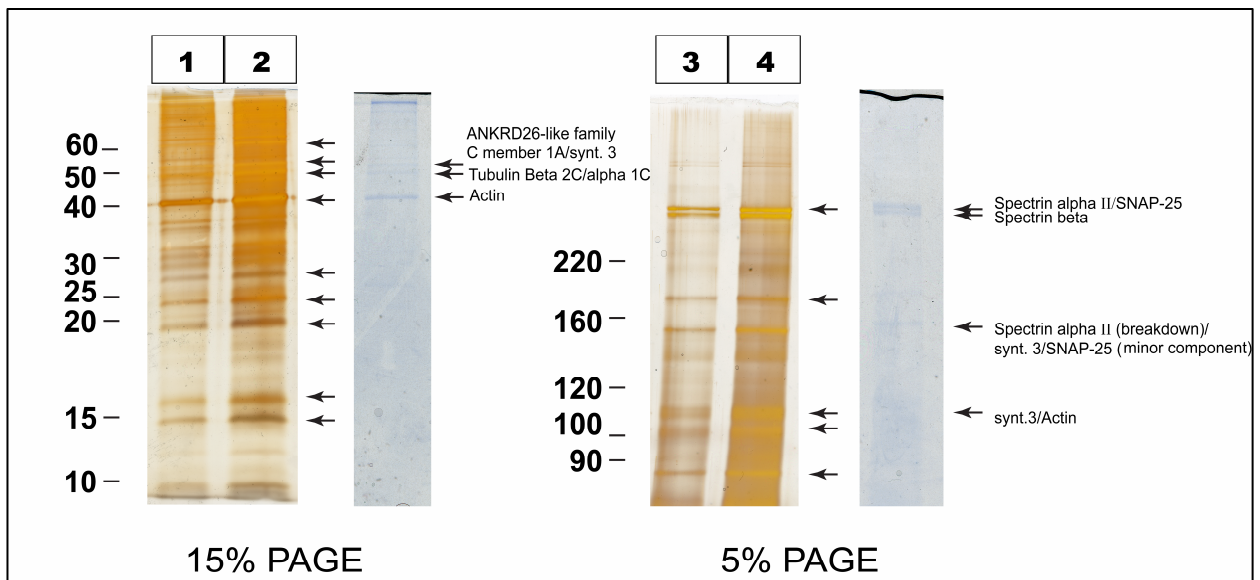


**Figure 15 . Cytoskeletal Proteins are in a Complex with Syntaxin 3B**

Syntaxin 3B and interacting proteins were immunoprecipitated (IP) from bovine retina extract with a syntaxin 3 antibody. The immunoprecipitate was concentrated several times and separated on a 5% or 15% SDS-PAGE gel. Gels were stained with either silver or Coomassie Blue. Lanes 1&3: first concentration. Lanes 2&4: second concentration. Sample shown on the coomassie gel was concentrated twice. Major protein bands visible on the coomassie stained gels were cut out and analyzed by mass spectrometry. Proteins that were clearly identified by MS are labeled. IP and mass spectrometric analysis was repeated twice.

Surprisingly, the mass spectrometer did not detect the  $\text{Ca}_v1.4$  channel in the immunoprecipitate. Instead, a variety of cytoskeletal proteins were identified as syntaxin 3B interacting proteins. The interacting proteins were neuronal spectrin, actin, ankyrin repeat domain 26 (ANKRD26)-like family C member 1A, and tubulin. In addition to the cytoskeletal proteins, syntaxin 3 (presumably syntaxin 3B based on the findings in Curtis et al., 2008) and SNAP-25 were detected in the immunoprecipitate.

Because western blotting is more sensitive than mass spectrometry, the immunoprecipitate was probed on a Western blot for  $\alpha_{1F}$  to verify the  $\text{Ca}_v1.4$  channel does co-immunoprecipitate with syntaxin 3B from bovine retina. The precipitate was also probed for neuronal spectrin alpha II to confirm the results of the mass spectrometric analysis (Figure 16).

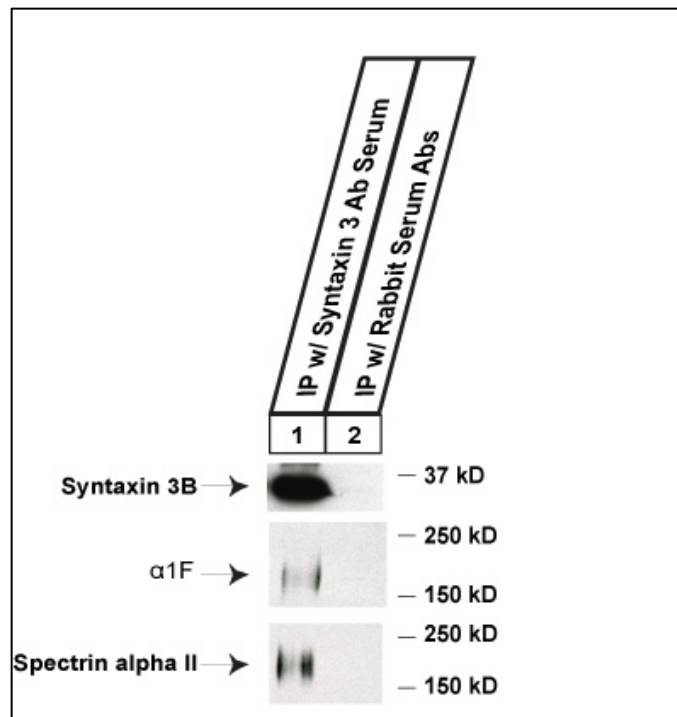


**Figure 16. Neuronal Spectrin Alpha II and the Ca<sub>v</sub>1.4 Channel Interact With Syntaxin 3B.**

Western blotting of immunoprecipitate from IP with bovine retina extract. Although the Ca<sub>v</sub>1.4 channel was not detected by mass spectrometry analysis, western blotting revealed that both the α<sub>1F</sub> subunit and syntaxin 3B were present in the immunoprecipitate. This is similar to the results from the IP with mouse retina extract. Western blotting also confirmed the interaction between spectrin alpha II and syntaxin 3B. Blot shown is representative of three experiments.

As shown in Figure 16, the α<sub>1F</sub> subunit was detected in the immunoprecipitate from bovine retina extract. Neuronal spectrin alpha II was also detected in the immunoprecipitate. Given that the Ca<sub>v</sub>1.4 channel was detected in the immunoprecipitate by western blotting and not mass spectrometry suggests that the amount of Ca<sub>v</sub>1.4 in the immunoprecipitate is very low. The low abundance of Ca<sub>v</sub>1.4 could make it difficult to see Ca<sub>v</sub>1.4 on a Coomassie gel. Given that the only bands sent for analysis were those that were fairly easy to see on the Coomassie gel, it is possible Ca<sub>v</sub>1.4 was not detected by the mass spectrophotometer because it was never cut out from the Coomassie gel. Alternatively, Ca<sub>v</sub>1.4 may have been present in one of the protein bands that were sent for analysis but it was present at a level that was too low to be detected by the mass spectrometer.

## **Discussion**

### **Syntaxin 3B and SNAP-25**

Previous work by my lab has shown that syntaxin 3B can interact with SNAP-25 and form a functional t-SNARE complex. However, data from *in vitro* binding experiments suggest that SNAP-25 has a lower affinity for syntaxin 3B than for syntaxin 1A (Curtis et al., 2008; Liu and Janz, unpublished data). To elucidate why SNAP-25 had a lower affinity for syntaxin 3B, we referred to a study by Dulubova and colleagues which showed that syntaxin 1A can exist both in an open and a closed state. In the closed state, the N-terminus of syntaxin 1A folds over onto the SNARE binding domain blocking its interaction with SNAP-25 (1999). Based on this information, we hypothesized that due to differing N-terminal regions, syntaxin 3B resides more in the closed state than syntaxin 1A.

In line with our hypothesis, removal of syntaxin 3B's N-terminus does increase binding between syntaxin and SNAP-25 (Figure 12). Admittedly, the GST Pulldown data do not provide a definitive answer as to whether syntaxin 3B resides more in the closed conformation than syntaxin 1A. X-ray crystallography or Nuclear Magnetic Resonance (NMR) analysis will have to be performed in the future to compare the structures of the two syntaxins in order to assess whether syntaxin 3B is more closed than syntaxin 1A. Nevertheless, the GST Pulldown data show the N-terminal domain of syntaxin 3B plays a role in the regulation of t-SNARE complex formation in retinal ribbon synapses. Perhaps modification of the N-terminal domain acts as a conformational switch that shifts syntaxin 3B from the closed to the open state.

How might the N-terminal domain be modified to induce a conformational change? Because protein phosphorylation is a common mechanism for regulating protein function, it was hypothesized that formation of the syntaxin 3B/SNAP-25 complex might be regulated via phosphorylation of syntaxin 3B's N-terminus. It has been demonstrated that  $\text{Ca}^{2+}$ /calmodulin dependent kinase II (CaMKII) can phosphorylate the N-terminal domain of syntaxin 3A (Risinger and Bennett, 1999). As noted in the Introduction, syntaxin 3A and 3B have identical N-terminal domains (refer to Figure 8). Given this information, Xiaoquin Liu, the post-doctoral

fellow in my lab, performed phosphorylation experiments to analyze whether syntaxin 3B is a substrate of CAMKII. The results of the experiments are shown in Figure 17.

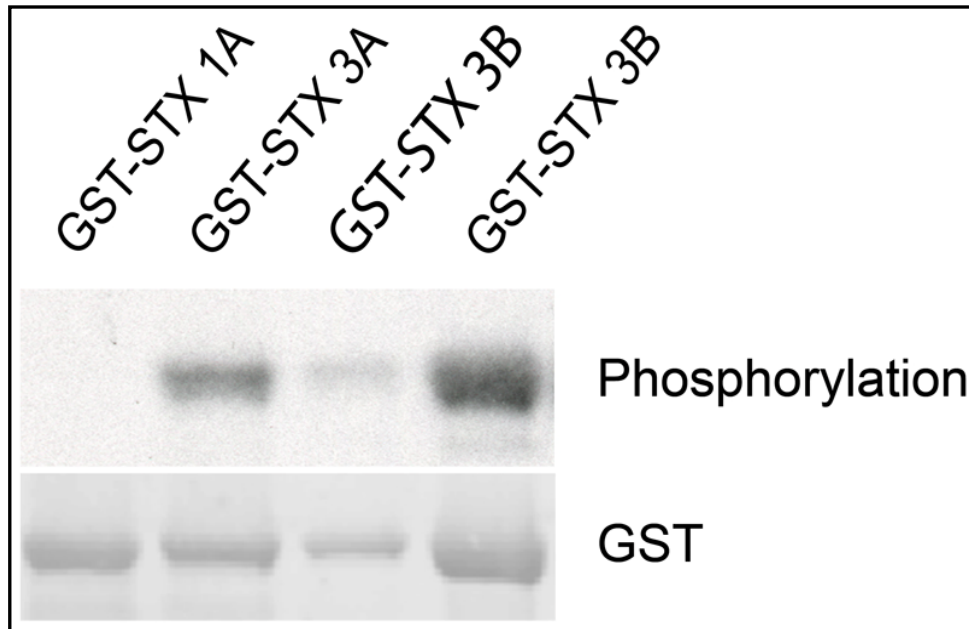


**Figure 17. Phosphorylation of Mouse Syntaxin 3B by CaMKII**

Phosphorylated GST-fusion proteins were separated by 12% SDS-PAGE, transferred to nitrocellulose membrane, exposed to x-ray film (upper panel), and analyzed by immunoblotting with GST monoclonal antibodies (lower panel). Syntaxin 1A was used as negative control, syntaxin 3A as positive control. Two concentrations of syntaxin 3B were used for this experiment. (Courtesy of Xiaquin Liu and Roger Janz)



As demonstrated in Figure 18, CaMKII can phosphorylate syntaxin 3B. To identify potential CaMKII phosphorylation sites within syntaxin 3B, the amino acid sequence of syntaxin 3B was analyzed using the METAPREDPS program (<http://metapred.umn.edu>). Four potential phosphorylation sites were identified: Thr<sup>14</sup>, Thr<sup>81</sup>, Ser<sup>145</sup>, and Ser<sup>187</sup> (Figure 18). To determine which of the amino acid residues are phosphorylated by CaMKII, site-directed mutagenesis was used to generate syntaxin 3B mutants in which threonine at position 14 and 81 and serine at position 145 and 187 were replaced by alanine respectively (T14A, T81A, S145A, and S187A). As shown in Figure 18, the syntaxin 3B T14A mutant was the only mutant that was not phosphorylated by CaMKII.

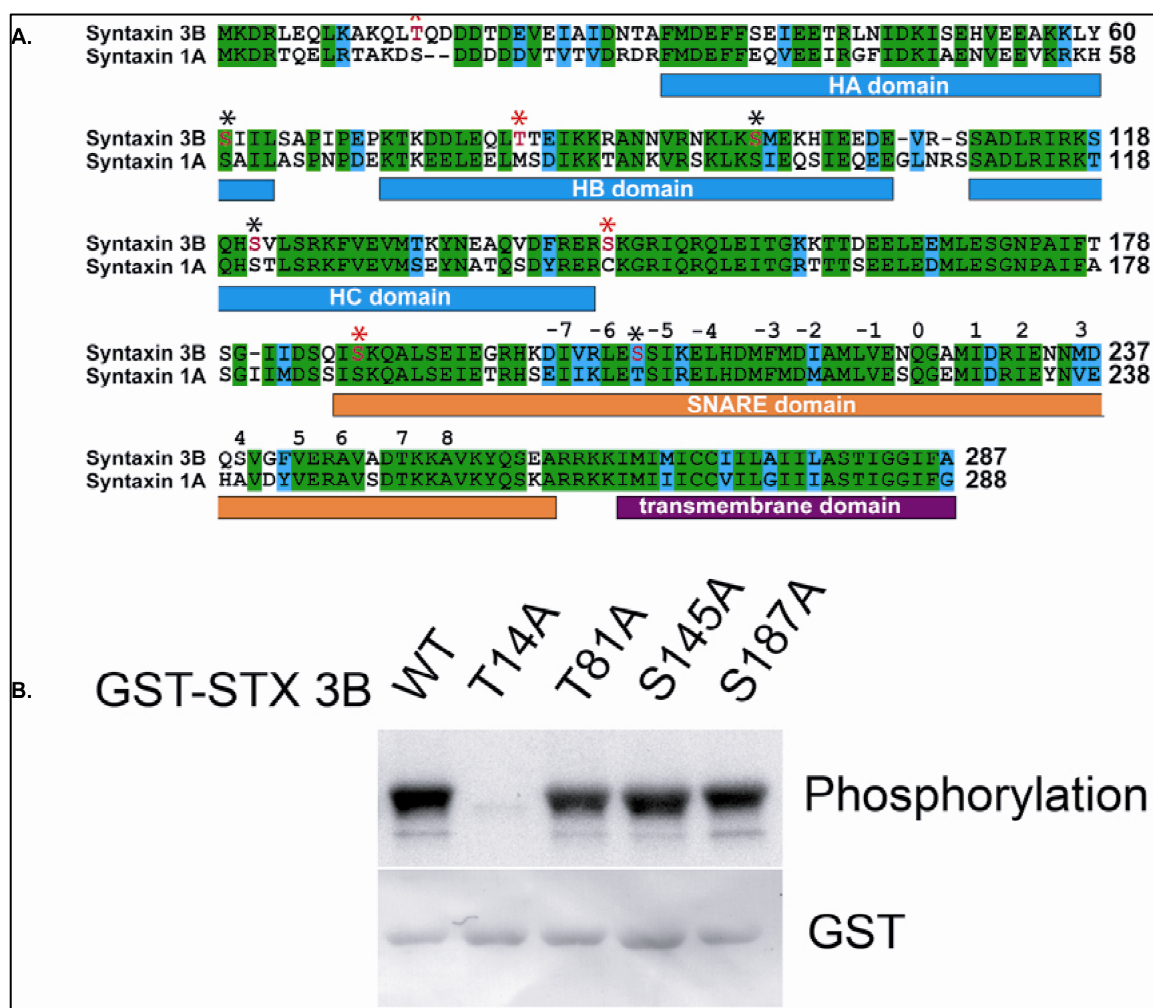


**Figure 18. Identification of Syntaxin 3B Phosphorylation Site.**

**A:** Potential phosphorylation sites within mouse syntaxin 3B as predicted by the METAPREDPS program. Red asterisks indicate the potential phosphorylation sites. **B:** Phosphorylation of wild type syntaxin 3B and T14A, T81A, S145A, and S187A syntaxin 3B mutants by CaMKII. (Courtesy of Xiaoquin Liu and Roger Janz)

To analyze how CaMKII-mediated phosphorylation of syntaxin 3B might affect binding between syntaxin 3B and SNAP-25, Xiaquin Liu performed a GST pulldown experiment with mouse retina extract and a syntaxin 3B phosphomimic in which threonine at position 14 was replaced by glutamate (T14E). A syntaxin 3B phosphomimic had to be used for the *in vitro* binding experiments because it was shown in preliminary experiments that CAMKII does not phosphorylate GST-tagged wild-type syntaxin 3B to a level that is sufficient for *in vitro* binding experiments (data not shown). As shown in Figure 19A, when threonine is replaced with glutamate at position 14, more SNAP-25 binds to syntaxin 3B (compare binding with GST-wild-type syntaxin 3B to binding with GST-syntaxin 3B phosphomimic). This affect appears to be due to the addition of a negative charge at position 14 as binding between SNAP-25 and GST-syntaxin 3B T14A is comparable to binding between SNAP-25 and GST-wild-type syntaxin 3B. Binding between recombinant SNAP-25 and GST-syntaxin 3B phosphomimic or wild-type syntaxin 3B was analyzed by incubating different amounts of recombinant SNAP-25 with the recombinant syntaxin 3B proteins. The GST-syntaxin 3B phosphomimic bound more SNAP-25 than GST-wild-type syntaxin 3B at each corresponding concentrations of SNAP-25 (Figure 19B). To quantitatively analyze the change in the binding properties of the recombinant syntaxin 3B proteins with recombinant SNAP25, 1 ml of 2 µg/ml of recombinant SNAP-25 was incubated with GST-wild-type syntaxin 3B and the GST-syntaxin 3B phosphomimic. The pulldown samples were analyzed by immunoblotting with SNAP-25 monoclonal antibodies. For quantitative analysis, the blots were probed with fluorescence-labeled secondary antibodies. The membrane was stained with Ponceau S to monitor the amounts of the recombinant proteins in each pulldown (Figure 19C, lower panel). The fluorescent signal was analyzed quantitatively with ImageJ program. Recombinant SNAP-25 showed a showed a significantly stronger affinity for GST-syntaxin 3B phosphomimic than GST-wild-type syntaxin 3B (Figure 19D).

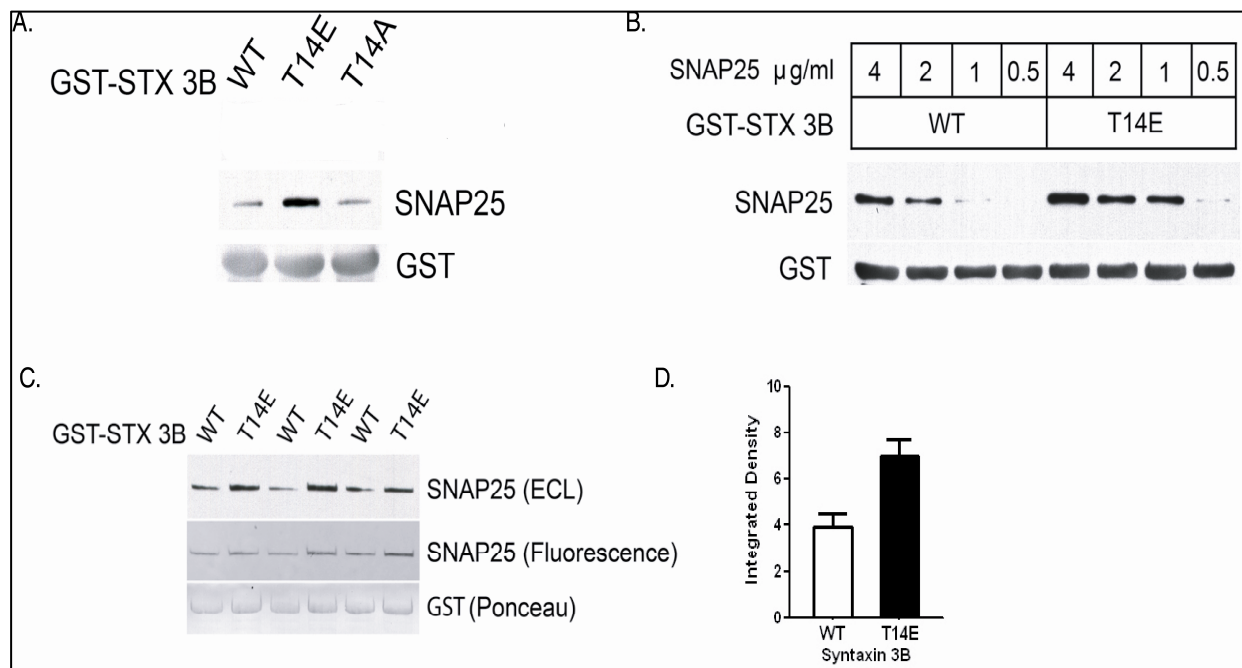


**Figure 19. CAMKII-mediated Phosphorylation of Syntaxin 3B Increases Binding Between Syntaxin 3B and SNAP-25**

A syntaxin 3B phosphomimic (T14E) was used in GST Pulldowns to test the effect of phosphorylation of syntaxin 3B on binding between syntaxin 3B and SNAP-25. The pulldown samples were analyzed by immunoblotting with SNAP-25 monoclonal antibodies. The membrane was probed with an antibody to GST or stained with Ponceau S to ensure that the amount of the recombinant proteins in each pulldown was comparable. **A.** Retina extract was incubated with GST-syntaxin 3B WT, T14E, and T14A. The syntaxin 3B phosphomimic bound more SNAP-25 than the other recombinant syntaxin 3B proteins. **B.** Different amounts of recombinant SNAP-25 were incubated with GST-syntaxin 3B WT and T14E. The phosphomimic bound more recombinant SNAP-25 than GST-syntaxin 3B WT. **C.** 1 ml of 2  $\mu\text{g/ml}$  of recombinant SNAP-25 was incubated with GST-syntaxin 3B WT and T14E. **D.** Quantitative analysis of binding between syntaxin 3B and SNAP-25. (Courtesy of Xiaoquin Liu and Roger Janz)

Overall, the *in vitro* binding experiments with the syntaxin 3B phosphomimetic (T14E) protein indicate phosphorylation of syntaxin 3B by CAMKII increases binding between syntaxin 3B and SNAP-25 (Liu and Janz, unpublished data). Taken together, these results show that CAMKII-mediated phosphorylation of syntaxin 3B likely regulates the formation of the syntaxin 3B/SNAP-25 complex. For illustrative purposes, a proposed model of how CAMKII regulates the formation of syntaxin 3B/SNAP-25 complex is shown below (Figure 20).

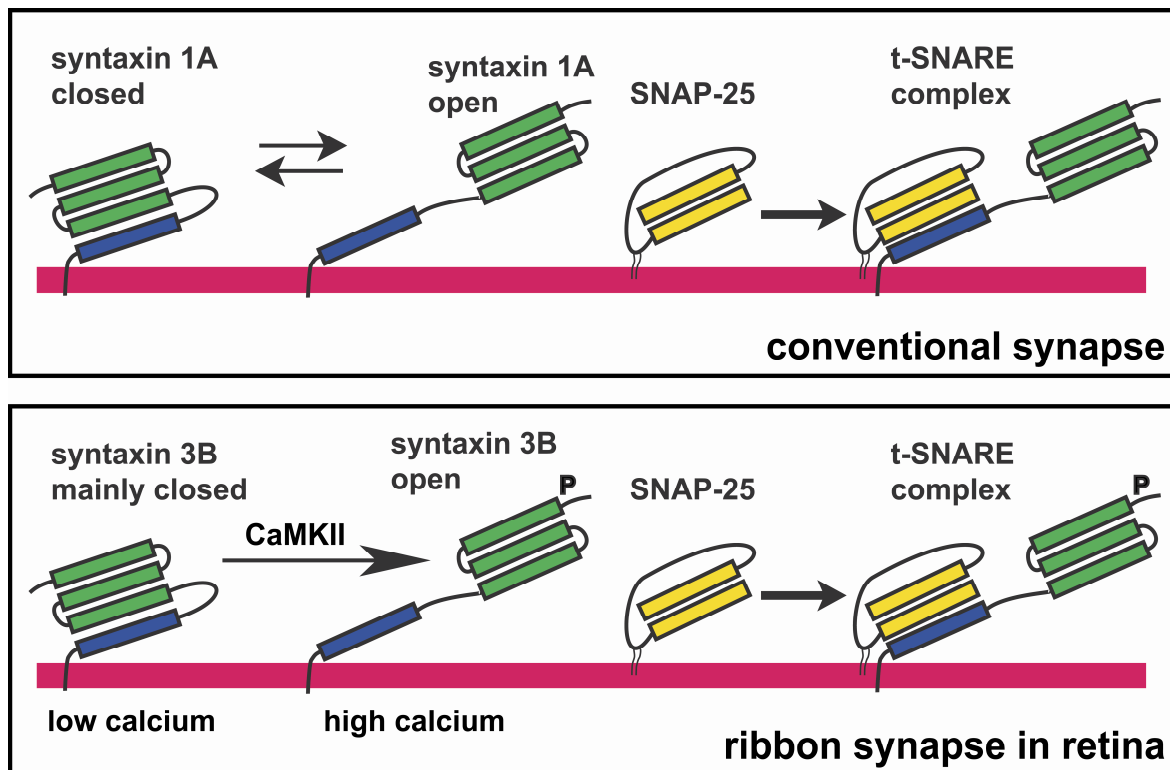


**Figure 20. Regulation of t-SNARE Complex Formation in Ribbon Synapses of the Retina: A Proposed Model**

**A.** In conventional synapses, syntaxin 1A exists in a closed and an open conformation that are in equilibrium. In the closed conformation, the N-terminus of syntaxin 1A (green) folds over onto the SNARE binding domain (blue). When syntaxin 1A is in the closed conformation it cannot interact with SNAP-25. Only the “open” conformation of syntaxin 1A can bind to SNAP-25 and form a functional t-SNARE complex. **B.** In ribbon synapses of the retina, syntaxin 3B exists mainly in the closed conformation. To open syntaxin 3B, the N-terminal domain of syntaxin 3B must be phosphorylated by CAMKII (phosphorylation of syntaxin 3B by CAMKII is presumed to occur when intraterminal calcium is high). Once open, syntaxin 3B forms a complex with SNAP-25.

Is the CAMKII regulatory mechanism present in all retinal ribbon synapses or a subset of retinal ribbon synapses? Two observations suggest the CAMKII regulatory mechanism is common to all retinal ribbon synapses. First, CAMKII $\alpha$  has been shown to be present in both the inner and outer plexiform layers of the retina (Ullrich and Südhof, 1994). Second, synapsin 1, the main substrate of CAMKII in conventional synapses, is absent from both photoreceptors and bipolar cells (Mandell et al., 1990; Benfenati et al., 1992; Ullrich and Südhof, 1994; von Kriegstein et al., 1999; Chi et al., 2003). In view of this, it is possible syntaxin 3B acts as one of the main targets of CAMKII in retinal ribbon synapses. Collectively, these observations lend support to the idea that CAMKII-mediated phosphorylation of syntaxin 3B regulates the formation of the syntaxin 3B/SNAP-25 complex in all retinal ribbon synapses. However, much work is still required in order to determine if the CAMKII regulatory mechanism is utilized by all retinal ribbon synapses or specific types of retinal ribbon synapses.

What is the purpose of CAMKII-mediated phosphorylation of syntaxin 3B? CAMKII is activated by calmodulin (CaM), a Ca<sup>2+</sup> binding protein that has been shown to play a role in Ca<sup>2+</sup> signaling (Gaertner et al., 2004). As such, one could speculate phosphorylation of syntaxin 3B by CAMKII acts to coordinate syntaxin 3B/SNAP-25 complex formation with changes in intraterminal calcium levels. This regulatory mechanism might ensure that the rate of vesicle release from a photoreceptor or bipolar cell is proportional to its level of depolarization.

#### **Regulation of SNARE Complex Formation through CAMKII-mediated Phosphorylation of Syntaxin 3B**

In Curtis et al., 2008, a reconstituted liposome fusion was performed in collaboration with Blair Doneske from Dr. James McNew Lab at Rice University to determine if syntaxin 3B can form a complex with SNAP-25 and synaptobrevin/VAMP2 and mediate fusion of lipid bilayers. The reconstituted liposome assay was performed as follows: 1. v-SNARE synaptobrevin/VAMP2 was reconstituted into liposomes composed of fluorescent and non-fluorescent lipids. The fluorescent lipids had either the fluorophore rhodamine or the

fluorophore NBD (7-nitro-2-1,3-benzoxadiazol-4-yl) attached to their head groups. Close proximity of rhodamine to NBD due to the small surface area of liposomes results in NBD fluorescence quenching. 2. The t-SNAREs SNAP-25 and syntaxin 3B were reconstituted together as preformed t-SNARE complexes into liposomes containing nonfluorescent lipids. 3. After reconstitution, the v- and t-SNARE liposomes were mixed together. Dilution of lipids occurred when a v-SNARE liposome fused with a t-SNARE liposome, resulting in dequenching of the fluorophore NBD (refer to Figure 21). This increase in NBD fluorescence (excitation = 460 nm, emission = 538 nm) was monitored at 2 minute intervals for 120 minutes. Detergent was then added to determine the maximum NBD fluorescence. The kinetic data was normalized as a percent of maximum fluorescence as previously described (Parlati et al., 1999; Scott et al., 2003).

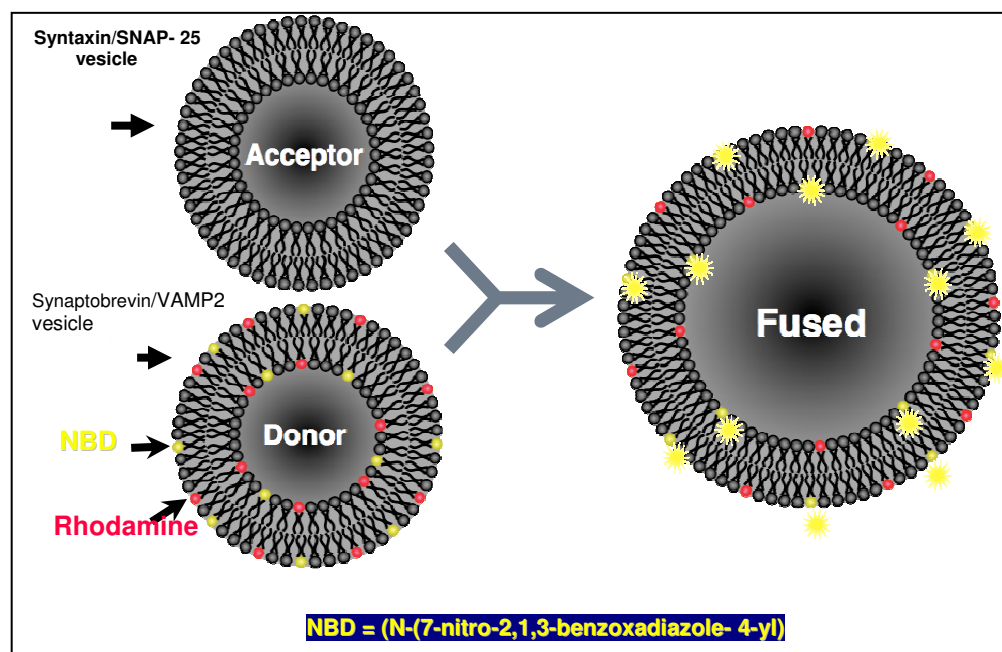


**Figure 21. Illustration of Reconstituted Liposome Fusion Assay**

Fluorophore rhodamine is shown in red. Fluorophore NBD (7-nitro-2-13- benzoxadiazol-4-yl) is shown in yellow.

The data from the assay showed that syntaxin 3B can interact with SNAP-25 and synaptobrevin/VAMP2 and mediate the fusion of membrane bilayers. The rate of fusion from 4 to 14 minutes was slower than with syntaxin 1A (Figure 22A & C). This slower rate of fusion

was not due to fewer SNAP-25/syntaxin 3B complexes, since the amount of SNAP-25/syntaxin 3B was similar to the amount of SNAP-25/syntaxin 1A (Figure 22B). The fusion rate from 100 to 110 minutes was similar between the t-SNARE vesicles (Figure 22C). For a negative control, soluble synaptobrevin/VAMP2 minus the transmembrane domain was included in the reaction. Insignificant fusion was seen when this blocking peptide was included.

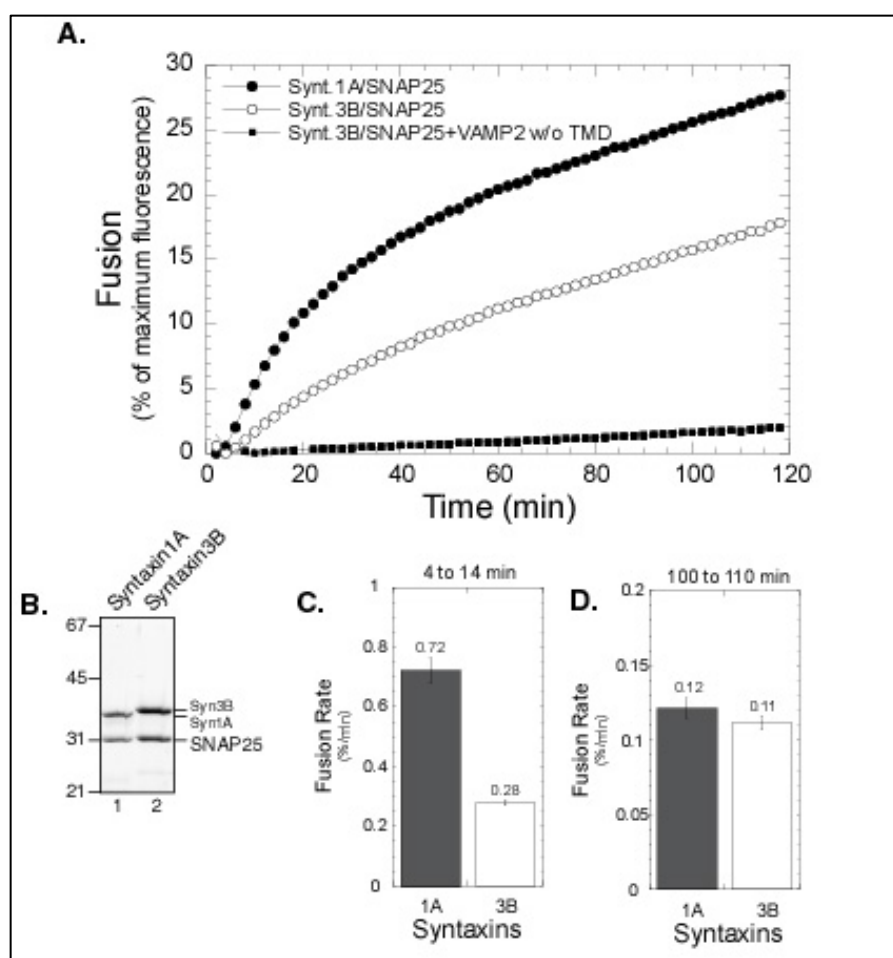


**Figure 22. Syntaxin 3B Can Interact with SNAP-25 and Synaptobrevin/VAMP2 and Form a Functional SNARE Complex**

A. Liposomes containing either syntaxin 1A/SNAP-25 (filled circles) or syntaxin 3B/SNAP-25 (open circles) t-SNARE complexes were mixed with v-SNARE liposomes containing Synaptobrevin/VAMP2. Background levels of fusion were determined by including soluble Synaptobrevin/VAMP2 (Synaptobrevin/VAMP2 w/o TMD, no symbol) to reactions containing syntaxin 3B/SNAP-25. Lipid mixing was monitored as an increase in NBD fluorescence for 120 minutes. Fusion is represented as percent maximum fluorescence obtained following detergent solubilization of liposomes. B. Five microliters of liposomes containing either syntaxin 1A/SNAP-25 or syntaxin 3B/SNAP-25 t-SNARE complexes were run on a SDS-PAGE gel and stained with Coomassie. C. Histogram showing the fusion rate from 4 to 14 minutes. D. Histogram showing fusion rate from 100 to 110 minutes. Reprinted from reference 10 with kind permission from Elsevier.



Although the reconstituted liposome fusion assay demonstrated that syntaxin 3B can form a functional complex with the neuronal SNAREs SNAP-25 and synaptobrevin/VAMP2, the results of the assay raised the question why is the initial rate of fusion slower with syntaxin 3B? As noted in my Master's thesis, two processes determine the overall rate of fusion with the reconstituted liposome fusion assay: the rate of docking and the rate of fusion of the liposomes (Parlati et. al., 1999). In order for the rate of docking not to be limiting at the start of the reaction, the v- and t-liposomes are preincubated overnight at 4°C. This allows interbilayer complexes to form without significant fusion. These complexes are assumed to be partially assembled. After incubation, the temperature is switched to 37 °C and the interbilayer complexes completely assemble allowing the predocked vesicles to fuse. After the predocked vesicles fuse, both the rate of docking and the rate of fusion contribute to the fusion rate (Figure 23).

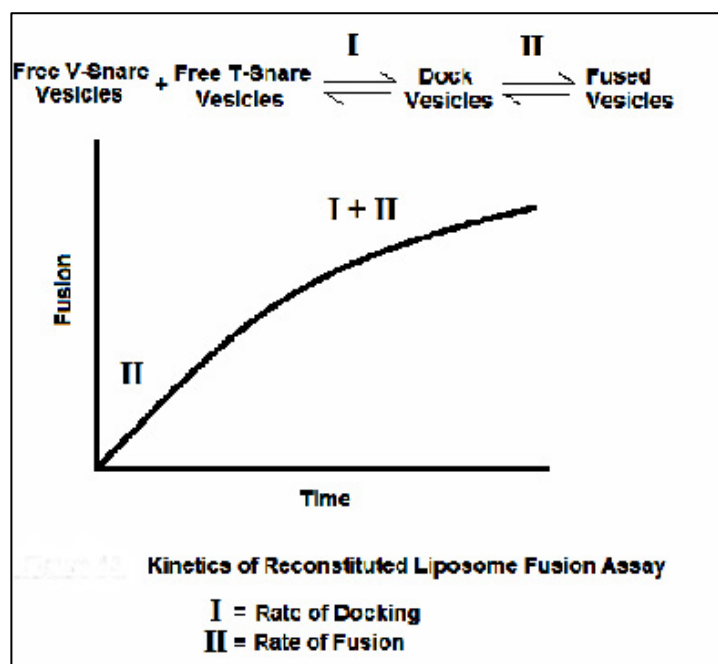


**Figure 23. Model of Kinetics of Reconstituted Liposome Fusion Assay**

In my Master's thesis, I proposed the reason why the initial fusion rate is slower with syntaxin 3B is the transition from partial to complete complex assembly during the preincubation step is slower when the SNARE complex contains syntaxin 3B. Thus, the



predocked vesicles fuse at a slower rate. Although this may be accurate, in light of the data from phosphorylation experiments performed by Xiaquin Liu, I would like to propose an alternative explanation here. In a paper by Parlati and colleagues, it was shown that removal of syntaxin 1A's N-terminal domain increases the rate of fusion between v and t-SNARE liposomes (1999). This observation suggested that the N-terminal domain of syntaxin 1A regulates the docking of synaptobrevin/VAMP2 with the syntaxin 1A/SNAP-25 complex presumably by folding over onto the t-SNARE complex (Parlati et al., 1999; Melia et al., 2002; Blair Doneske, personal communication). In this study, we proposed that syntaxin 3B resides more in a closed state than syntaxin 1A. If syntaxin 3B favors a closed conformation, it is possible the number of interbilayer complexes that form between synaptobrevin/VAMP2-and syntaxin 3B/SNAP-25 liposomes during the preincubation step is low due to syntaxin 3B's N-terminal domain folding over onto the t-SNARE complex. As a result, with syntaxin 3B both the rate of docking and the rate of fusion are rate-limiting at the start of the reaction. Interestingly, throughout the duration of the reaction the fusion rate with syntaxin 3B is slower than the fusion rate with syntaxin 1A. This implies that the N-terminal domain of syntaxin 3B may interfere with the docking and assembly of SNARE complexes more than the N-terminal domain of syntaxin 1A does. The N-terminal domain of syntaxin 3B may need to be modified in order for efficient docking and assembly of SNARE complexes to occur. Phosphorylation of syntaxin 3B's N-terminus by CAMKII may be one mechanism the retinal ribbon synapses utilize to ensure synaptobrevin/VAMP2 can interact with t-SNARE complexes in an efficient manner (refer to Figure 24).

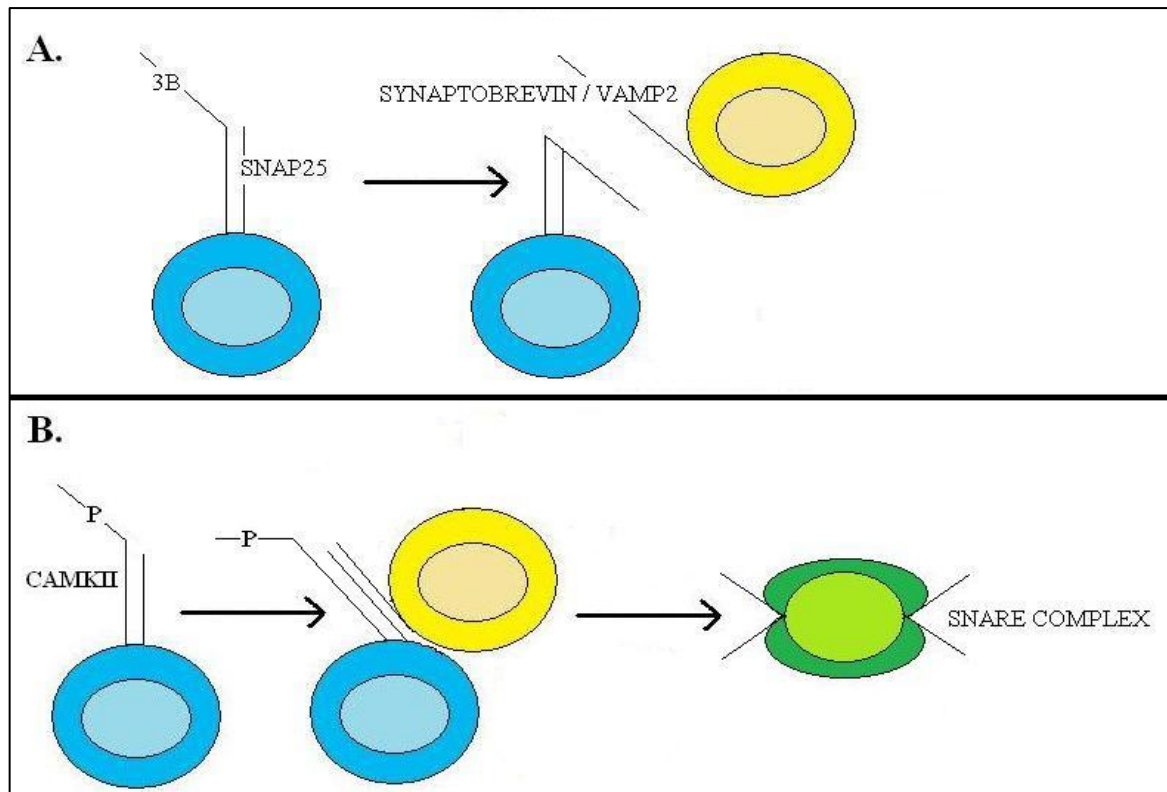


**Figure 24. Model of How CAMKII-mediated Phosphorylation of Syntaxin 3B May Regulate the Interaction of Synaptobrevin/VAMP2 with the Syntaxin 3B/SNAP-25 Complex**

A. Without CAMKII-mediated phosphorylation of syntaxin 3B, formation of interbilayer complexes is hindered by the N-terminal domain of syntaxin 3B folding over onto syntaxin 3B/SNAP-25 complex.

B. Phosphorylation of syntaxin 3B by CAMKII reduces the likelihood that the N-terminal domain of syntaxin 3B will fold over onto the syntaxin 3B/SNAP-25 complex. Thus, synaptobrevin/VAMP2 can interact with the syntaxin 3B/SNAP-25 complex. This leads to the fusion of v and t-SNARE liposomes.

Of course, as proposed in my Master's thesis, regulatory proteins such as complexins 3 or 4 may also play a role in facilitating the interaction between SNARE proteins in the ribbon synapses of the retina. In the future, syntaxin 3B minus its N-terminal domain, CAMKII phosphorylated syntaxin 3B and/or complexins 3 and 4 will have to be included in the reconstituted liposome fusion assay to test these possibilities.

### **Syntaxin 3B and Ca<sub>v</sub>1.4 channel**

Syntaxin 1A/B has been shown to interact with and modulate several of the presynaptic calcium channels which support neurotransmitter release from conventional synapses (Sheng et al., 1994; Wiser et al., 1996). One calcium channel modulated by syntaxin 1A is the Lc-type calcium channel (Ca<sub>v</sub>1.2). Because modulation of Ca<sub>v</sub>1.2 by syntaxin 1A involves two transmembranal cysteine residues (C271, C272) which are conserved in syntaxin 3B, we hypothesized syntaxin 3B may be capable of interacting with and regulating Ca<sub>v</sub>1.2 and/or other types of L-type calcium channels such as the Ca<sub>v</sub>1.3 and Ca<sub>v</sub>1.4 channels which support neurotransmitter release from retinal ribbon synapses (Heidelberger and Matthews, 1992; Morgans, 2001; Arien et al., 2003; LoGiudice et al., 2005; Cohen et al., 2007; Xiao et al., 2007; Tippens et al., 2008).

Consistent with our hypothesis, Ca<sub>v</sub>1.4, the predominate calcium channel in mammalian rods, co-immunoprecipitates with syntaxin 3B from mouse retina extract. In regard to the model presented in the introduction, this data supports the idea that the L-type calcium channels are kept in proximity of the t-SNARE complex by binding to syntaxin 3B (refer to Figure 25).

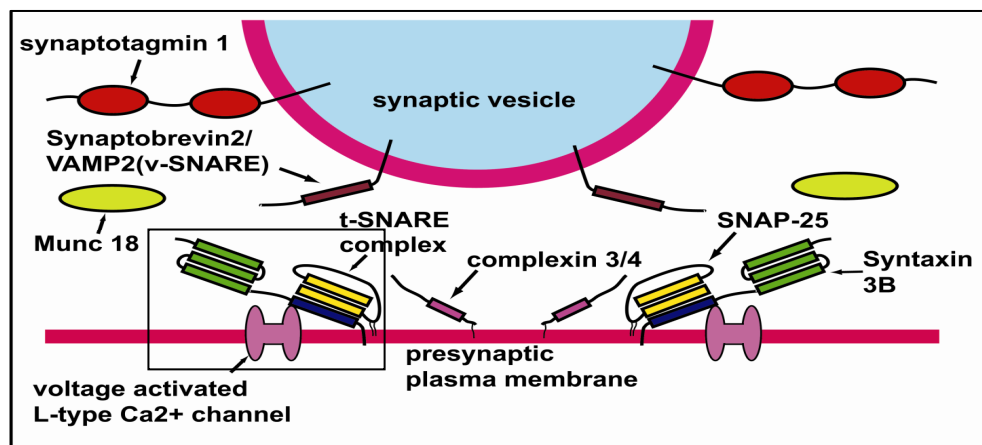


**Figure 25. Model of Synaptic Vesicle Exocytosis in Retinal Ribbon Synapses**

What is the function of the interaction between syntaxin 3B and Ca<sub>v</sub>1.4? Given that mammalian rods express the low-affinity calcium sensor, Synaptotagmin I/II and the unitary conductance of the Ca<sub>v</sub>1.4 channel is very small compared to other voltage-gated calcium

channels, it is likely the main function of the syntaxin 3B-Ca<sub>v</sub>1.4 interaction is to position the synaptic vesicle release machinery near the Ca<sub>v</sub>1.4 channel(s) (von Kriegstein et al., 1999; Heidelberger et al., 2003; Bernston and Morgans, 2003; Doering et al., 2005).

Cohen and colleagues have proposed a model whereby one syntaxin 1A molecule is connected to two Ca<sub>v</sub>1.2 channels via the cysteine residues in the transmembrane domain of syntaxin 1A (C271, C272). In this model, one transmembranal cysteine residue interacts with one calcium channel and the other transmembranal cysteine residue interacts with a second channel. Through this type of interaction, multiple syntaxin 1A molecules can cluster calcium channels together to generate a releasing complex (2007). As noted earlier, C271 and C272 are conserved in syntaxin 3B. If these two residues are involved in the interaction between syntaxin 3B and Ca<sub>v</sub>1.4, it is possible another function of the syntaxin 3B-Ca<sub>v</sub>1.4 interaction is to cluster Ca<sub>v</sub>1.4 channels together. Clustering of Ca<sub>v</sub>1.4 channels would ensure that the synaptic vesicles are exposed to a high concentration of calcium in spite of the low single-channel conductance of Ca<sub>v</sub>1.4 channels.

The data from the immunoprecipitation experiment do not answer the question of whether or not syntaxin 3B alters the kinetic properties of the Ca<sub>v</sub>1.4 channel. In the future, whole-cell patch clamp recordings of HEK 293 cells transfected with syntaxin 3B and the Ca<sub>v</sub>1.4 channel could be used to determine if syntaxin 3B can alter the activity of Ca<sub>v</sub>1.4. In addition, immunoprecipitation experiments could test the hypothesis that syntaxin 3B is a binding partner of the Ca<sub>v</sub>1.3 channel. If syntaxin 3B does interact with the Ca<sub>v</sub>1.3 channel, HEK 293 cells could be transfected with syntaxin 3B and the Ca<sub>v</sub>1.3 channel and whole-cell patch clamp recordings could be used to determine if syntaxin 3B can alter the activity of Ca<sub>v</sub>1.3. Overall, much work is still required in order to determine if syntaxin 3B modulates the kinetic properties of the Ca<sub>v</sub>1.3 and Ca<sub>v</sub>1.4 channels.

### **Proteomics to Identify Syntaxin 3B Interacting Proteins**

To confirm Ca<sub>v</sub>1.4 is a binding partner of syntaxin 3B and identify other proteins that interact with syntaxin 3B, syntaxin 3B and interacting proteins were immunoprecipitated from

bovine retina extract with a syntaxin 3 antibody. The immunoprecipitated proteins were then analyzed by mass spectrometry. Interestingly, although Ca<sub>v</sub>1.4 co-immunoprecipitates with syntaxin 3B from mouse retina extract, the mass spectrometer did not detect Ca<sub>v</sub>1.4 in the immunoprecipitate from bovine retina. The proteins detected in the immunoprecipitate were neuronal spectrin, actin, ankyrin repeat domain 26 (ANKRD26)-like family C member 1A, tubulin, syntaxin 3B and SNAP-25.

One reason why the Ca<sub>v</sub>1.4 channel was not detected in the sample is the amount of Ca<sub>v</sub>1.4 in the immunoprecipitate might have been so low that it was not visible on the Coomassie gel and thus it was not detectable in the gel. Another reason why the channel was not detected is it may have been present in one of the weaker bands that were sent for analysis but it was below the detection limit of the mass spectrometer. Why would the amount of Ca<sub>v</sub>1.4 in the immunoprecipitate be so low? The answer to this question may be that not all of the syntaxin 3B in the retina extract can be immunoprecipitated due to epitope availability and/or binding conditions. Of the syntaxin 3B that can be immunoprecipitated, the majority might be in a complex with other proteins such as SNAP-25 or cytoskeletal proteins. The percentage of immunoprecipitated syntaxin 3B that is in a complex with Ca<sub>v</sub>1.4 might be very low. This assumption is reasonable given that Ca<sub>v</sub>1.4 is expressed only in photoreceptors, whereas SNAP-25 and cytoskeletal proteins are expressed in both bipolar and photoreceptor cells. In support of this idea, western blotting showed that both syntaxin 3B and the  $\alpha 1F$  subunit of Ca<sub>v</sub>1.4 were present in the immunoprecipitate that was sent for mass spectrometric analysis (Figure 16).

The results of the mass spectrometric analysis suggest that neuronal spectrin, actin, ankyrin repeat domain 26 (ANKRD26)-like family C member 1A, and tubulin are syntaxin 3B interacting proteins. In line with the mass spectrometric data, western blotting showed that syntaxin 3B and neuronal spectrin, a plasma membrane-associated cytoskeletal protein composed of two alpha subunits and two beta subunits, immunoprecipitate as a complex (Figure 15). At the time the western blotting was performed, antibodies to actin, ankyrin repeat

domain 26 (ANKRD26)-like family C member 1A, and tubulin were not available. Thus, it is not certain at this point if the data from mass spectrometric analysis is accurate in regard to these proteins being binding partners of syntaxin 3B.

What could be the biological function of the interaction between syntaxin 3B and spectrin? Based on the observation that synaptic proteins including syntaxin 1A are mislocalized in *Drosophila*  $\alpha$ - and  $\beta$ -spectrin protein null mutants, it is reasonable to propose that the main function of the syntaxin 3B-spectrin interaction is to position syntaxin 3B at active zones (Featherstone et al., 2001). However, given that spectrin can interact with actin filaments which play a role in intracellular vesicle trafficking and actin is one of the proteins that was co-immunoprecipitated with syntaxin 3B, it is possible the function of the syntaxin 3B-spectrin interaction is to traffic synaptic vesicles to release sites. In the future, experiments will be designed to test the two hypotheses presented here.

### **Chapter 3: Molecular Characterization of Presynaptic Proteins from Goldfish Retina**

3.1 Cloning Syntaxin 3B and Other Presynaptic Proteins from Goldfish Retina.

3.2 Analysis of the Expression and Distribution of Presynaptic Proteins in the Goldfish Retina.

## **Material and Methods**

### **Animals**

Goldfish (*Carassius auratus*, 4-5" in length) were maintained on a 12 hour light/dark cyclic lighting. Goldfish were killed by decapitation and pithing. Tissue for frozen sections for immunohistochemical studies were obtained from light adapted goldfish at the time of euthanasia. For all other experiments tissue was obtained from goldfish that were dark adapted for 20 minutes before euthanasia. All animal procedures conformed to National Institutes of Health (NIH) guidelines and were approved by the Animal Welfare Committee of the University of Texas Health Science Center at Houston.

### **Bioinformatics**

EST database searches were performed with the BLAST program suite at the NCBI website. The protein sequences were aligned in the ClustalW and Boxshade programs with default settings at the Biology Workbench (<http://workbench.sdsc.edu/>).

### **Reverse-Transcription PCR**

Total RNA was isolated from goldfish tissue with TRI Reagent (Ambion) using the manufacturer's protocol. cDNA was generated using the Transcriptor First Strand cDNA Synthesis Kit (Roche). Five micrograms of total RNA from each tissue was used in this reaction. The synthesized cDNA was then used for PCR. PCR products were separated on a 2.0% agarose gel and, after visualization, isolated from the gel, purified, and sequenced by Seqwright (Houston, TX). Primer sequences were as follows: Syntaxin 3A:

AAAGACATTGTGCGTCTGGAG and CACCTCAATGTTATCAACCATGT, Syntaxin

3B:GATTCAGGGATTTCCTCAACAAG and GACTGGTCCATGTTGTTCTCAA, and Beta-actin:

AAGATCTGGCATCACACCTTCTA and ATCACCAGAGTCCATCACGATAC.

### **Absolute Real-Time PCR**

The cDNA used for this PCR was the cDNA used in the Reverse-Transcription PCR.

Expression of syntaxin 3A and 3B in goldfish retina was analyzed with a Smartcycler II (Cepheid) by the SYBR Green method. For the analytical samples, each reaction was



composed of 24 µl of master mix (SYBR Green Jumpstart Taq Ready Mix (Sigma), 1.0 µM primers, and deionized water) and 1 ul of retina cDNA (1.0 g/l). To generate the syntaxin 3A and 3B standard, cDNA fragments were generated by RT-PCR from retina mRNA using primers derived from the zebrafish sequence (Syntaxin 3B Primers CAGAAATATGAAGGACCGACTGGAACAACTAAA and AAACACAACAATCCCCAGAATCGCACAGCAAAACAT; Syntaxin 3A Primers GATTCAGGGATTTCCTAAACAAG and ACTGCTTTACCCACATTACCT ). The syntaxin 3A and B fragments were cloned into the pCR2.1-TOPO vector and the sequences verified by sequencing. For the standards, each reaction consisted of 24 µl of master mix (SYBR Green Jumpstart Taq Ready Mix (Sigma), 1.0 µM primers, and deionized water) and a defined amount of syntaxin 3A or 3B plasmid and 1µg of genomic *E.coli* DNA as carrier in a volume of 1 ul. The cycling parameters for the reaction with syntaxin 3B were as follows: 94°C 2 min., 94°C 45 sec., 58 °C 1 min., 72 °C 1 min. 35 cycles. The cycling parameters for the reaction with syntaxin 3A were as follows: 94°C 2 min., 94°C 45 sec., 56 °C 1 min., 72 °C 1 min. 35 cycles. Primers used for PCR were the same as those used for the RT-PCR.

### **Cloning**

RNA was isolated from goldfish retina; cDNA was generated by reverse transcription as described (Curtis et al., 2008). Using primers designed on the basis of zebrafish syntaxin 3A, syntaxin 3B, complexin III, and syntaptotagmin I cDNA, the corresponding goldfish cDNAs were amplified, subcloned, and sequenced by Seqwright (Houston, TX). This procedure was performed twice in order to clone syntaxin 3A, syntaxin 3B, complexin III, and syntaptotagmin I cDNA from goldfish tissue. Primer sequences were as follows: Syntaxin 3A (Primers GATTCAGGGATTTCCTAAACAAG and ACTGCTTTACCCACATTACCT), Syntaxin 3B (Primers CAGAAATATGAAGGACCGACTGGAACAACTAAA and AAACACAACAATCCCCAGAATCGCACAGCAAAACAT), complexin III (Primers 331 and 332), syntaptotagmin I (Primers 344 and 334).

### **Complexin III Riboprobe**

Goldfish Complexin III cDNA cloned into the pCR2.1-TOPO vector was used to generate a digoxigenin-labeled antisense RNA probe with the DIG RNA Labeling kit (SP6/T7) from Roche. For *in vitro* transcription, complexin III-pCR2.1-TOPO vector was linearized with BamHI and T7 RNA polymerase was used to transcribe complexin III cDNA. Agarose gel electrophoresis (1.0%) was used to assess the quality of riboprobe.

### **Single-Cell Reverse Transcription PCR**

Goldfish retina was dissociated as described in Heidelberger and Matthews, 1992. Single cells with the morphological characteristics of Mb1 bipolar neurons were picked up with a pipette by applying gentle suction by either opening the pressure valve to atmospheric pressure or by gentle suction by mouth. The individual cells were then deposited into a PCR tube containing deionized water and frozen by dipping the tube into liquid nitrogen. The cell was stored at -80 °C until needed. To generate cDNA, the cell was thawed and four microliters of the cell lysate was used for the reverse transcription reaction. The Transcriptor First Strand cDNA Synthesis Kit (Roche) was used to generate cDNA for PCR. Two rounds of PCR were performed. At the end of the first PCR, aliquots of the reactions were transferred to new tubes. Fresh PCR reagents were added to the tubes and a second PCR was performed. The following cycling parameters were used with each round of PCR: 94°C 2 min., 94°C 45 sec., 58 °C 1 min., 72 °C 1 min., 72 °C 10 min. 40 cycles.

### **Antibodies**

The goldfish syntaxin 3B polyclonal antibody was raised in rabbits by Cocalico Biologicals Inc. (Reamstown, PA) against a bacterially-expressed GST fusion protein containing amino acids 2-178 of recombinant goldfish syntaxin 3B. For immunohistochemistry, the syntaxin 3 antiserum was used at dilution of 1:400. Secondary antibody was goat anti-rabbit Alexa Fluor 488 (Molecular Probes, Eugene, OR). Secondary fluorescent antibodies were used at a dilution of 1:200. Antibodies for immunostaining were diluted in 1% goat serum, 0.3% Triton X-100 in TBS (pH 7.4).

### **Immunofluorescent labeling of frozen sections**

Eyecups were fixed in 4% formaldehyde in phosphate-buffered saline (PBS; pH 7.4). After fixation, eyecups were rinsed several times in PBS (pH 7.4), cryoprotected in 20% sucrose in PBS, embedded in OCT embedding medium, and fast frozen. Tissue was sectioned on a cryostat at a thickness of 30  $\mu\text{m}$ . Immunolabeling was performed on frozen sections as previously described (Heidelberger et al., 2003).

### **Microscopy**

Immunolabeled specimens were scanned with a 0.2- $\mu\text{m}$  step size on a Zeiss Laser Scanning Microscope 510 Meta (Carl Zeiss, Inc., Thornwood, NY) with a Zeiss 40x 1.3 NA Plan-NEOFLUAR oil objective. Image scale was calibrated and image brightness and contrast were adjusted as necessary to highlight specific immunolabeling. Single optical sections (0.45  $\mu\text{m}$  thickness) were acquired with one fluorescence channel. Specific band pass filters for single labeling were used to achieve proper separation of signals (543/560 LP).

### **3.1 Cloning Syntaxin 3B and Other Synaptic Proteins from Goldfish Retina.**

“The Mb1 bipolar neuron in the goldfish has been used extensively to study the physiological properties of ribbon synapses. The large diameter of the Mb1 bipolar neuron synaptic terminal (8-12  $\mu\text{m}$ ) enables one to measure presynaptic calcium currents, intracellular presynaptic calcium concentration, and synaptic vesicle exo-and endocytosis simultaneously (Heidelberger and Matthews, 1992; Heidelberger, 1998). Given these technical advantages this neuron has served as a model system for ribbon synapses in general (Heidelberger and Matthews, 1991; Heidelberger and Matthews, 1992; Heidelberger and Matthews, 1994; Lagnado et al., 1996; von Gersdorff H. and Matthews, 1994; Zenisek et al., 2000). Although the Mb1 bipolar neuron is considered an ideal model cell in which to study neurotransmitter release from ribbon synapses, little is known about the presynaptic proteins that mediate synaptic vesicle exocytosis from this cell. Most of the studies analyzing the expression of presynaptic proteins in retinal ribbon synapses have been performed in mammals, specifically mice and rats (Curtis et al., 2008; Reim et al., 2005; Sherry et al., 2006; Sherry et al., 2003; von Kriegstein and Schmitz, 2003; von Kriegstein et al., 1999; Wang et al., 2003). The few studies that have analyzed presynaptic proteins in goldfish retinal ribbon synapses have used antibodies that were originally developed for mammalian presynaptic proteins (Berntson and Morgans, 2003; Heidelberger et al., 2003).” (excerpt from Curtis et al., 2010 with kind permission from Elsevier). Because the goldfish homologues of these mammalian presynaptic proteins have not been cloned, it is unknown whether the epitopes recognized by the mammalian antibodies are conserved in goldfish presynaptic proteins. As such, the data from these above mentioned studies may or may not be accurate.

To fill in the gaps regarding what proteins mediate synaptic vesicle exocytosis from goldfish retinal ribbon synapses, I used a variety of molecular biological approaches to assess whether the proteins which play a role in synaptic vesicle exocytosis in mammalian retinal ribbon synapses are present in the goldfish retina. Of note, some of the results from the experiments shown in the next section are published in Curtis et al., 2010.

## **Results**

### **Syntaxin 3B in the Goldfish**

As a first step towards elucidating the composition of the synaptic vesicle fusion exocytotic machinery in goldfish retinal ribbon synapses, syntaxin 3B was cloned from goldfish retina. To do this, the EST (Expressed Sequence Tags) database from zebrafish was screened using the program tblastn (NCBI) with the mouse syntaxin 3B sequence. The zebrafish database was screened because zebrafish and goldfish are in the same family and the zebrafish homologues of many mammalian presynaptic proteins have been cloned.

One EST clone derived from a zebrafish retina cDNA library which contained a sequence homologous to syntaxin 3B (IMAGE clone:4786252) was identified and completely sequenced. This clone contained a reading frame for the majority of the protein, but was lacking part of the N-terminus. In order to complement the sequence, the genomic zebrafish database was screened and the sequence of the partial clone was compared with the corresponding syntaxin 3 gene (Ensembl gene ID: ENSDARG00000001880 (WWW.ENSEMBL.ORG)). Interestingly, a comparison of the syntaxin 3 gene in zebrafish and in mouse showed the exon/intron structure of the zebrafish syntaxin 3 gene is very similar to the exon/intron structure of the mouse syntaxin 3 gene (Curtis et al., 2008). As such, both zebrafish and mouse syntaxin 3A and 3B are generated by differential splicing of exons 8, 9 and 10. Given that the structure of the syntaxin 3 gene did not appear to differ much across species, it was predicted the amino acid sequence of goldfish syntaxin 3B would be very similar to the amino acid sequences of zebrafish and mouse syntaxin 3B.

The sequence of the zebrafish syntaxin 3 gene was used to complement the region coding for the N-terminus of the predicted zebrafish syntaxin 3B protein. Reverse transcription (RT)-PCR using primers derived from the syntaxin 3B zebrafish sequence was then used to amplify goldfish syntaxin 3B cDNA from mRNA isolated from goldfish retina. The obtained PCR fragments were sequenced and used to predict the goldfish syntaxin 3B protein sequence. The amino acid sequence of the predicted goldfish syntaxin 3B was aligned with

the amino acid sequences of mouse syntaxin 1A (the syntaxin isoform found in conventional synapses), mouse syntaxin 3B, and zebrafish syntaxin 3B (Figure 26).

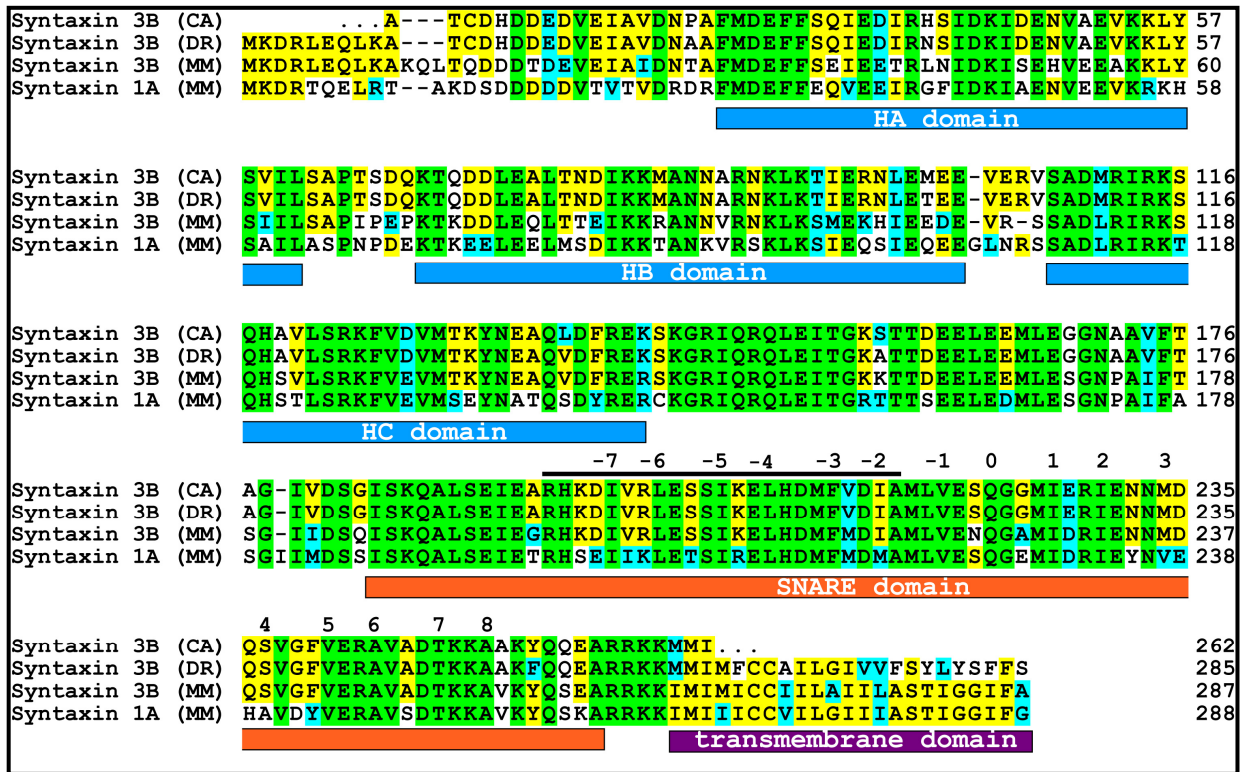


### Figure 26. Sequence Alignment of Syntaxin Isoforms

The protein sequences of the goldfish (CA) syntaxin 3B, zebrafish (DR) syntaxin 3B and the mouse (MM) syntaxin 3B and syntaxin 1A have been aligned for maximal homology using CLUSTALW. Sequences are identified on the left and residues numbered on the right. Residues that are conserved in all four proteins are labeled with green background. Residues conserved between three of the syntaxin isoforms are labeled with yellow background. Conservative exchanged residues are labeled with blue background. The positions of the conserved domains are marked below the sequence. The positions of the hydrophobic interacting layers are numbered in relation to the glutamine (Q) of the central 0 layer. Reprinted from reference 11 with kind permission from Elsevier.

The sequence of the goldfish syntaxin 3B protein is highly homologous to the zebrafish syntaxin 3B sequence (98 % identity). Goldfish syntaxin 3B is 75% identical at the amino acid level to mouse syntaxin 3B. The SNARE domains of goldfish and mouse syntaxin 3B were 89% identical. Thus, syntaxin 3B is strongly conserved between mammals and fish. To evaluate the expression pattern of the syntaxin 3 gene in fish, the zebrafish EST database was searched using the zebrafish syntaxin 3B sequence. Twenty EST-clones that could clearly be

identified as syntaxin 3 mRNA transcripts were found. Most EST sequences corresponded to the 5'-end of the syntaxin 3B transcript which is identical to the 5'-end of the syntaxin 3A transcript. As such, these clones could correspond to clones of syntaxin 3A or 3B. No clones corresponding to the syntaxin 3 isoforms, syntaxin 3C or 3D, were found in the search. This result indicates that these isoforms are either expressed at very low levels or not at all in zebrafish. The majority of the 20 identified EST clones were derived from mRNA isolated from embryonic or adult whole animals (9 clones). Among the clones generated from mRNA of defined tissues 4 clones were from eye/retina, 3 from kidney, and the rest were from a variety of other tissues (brain, gut, olfactory epithelium and ovary (one clone each)). This distribution pattern mirrors the expression pattern of the mouse syntaxin 3 gene with the highest level of expression in the retina and the kidney. The tissue distribution of syntaxin 3A and 3B in the goldfish was investigated using Reverse Transcription-PCR with mRNA isolated from retina, brain and kidney (Figure 27).

As shown in Figure 27A, the PCR reactions with the syntaxin 3B primers produced a strong signal in the retina sample and a weak signal in the brain sample. No syntaxin 3B could be detected in the kidney samples. In contrast, the PCR reactions with the syntaxin 3A primers generated strong signals in the kidney and brain, and a weak signal in the retina sample. To compare the expression level of syntaxin 3A to syntaxin 3B in the retina, we used quantitative real-time PCR to measure the copy number of each of the two different syntaxin 3 transcripts (Figure 27B). The results of the experiment demonstrate that syntaxin 3B mRNA is about 7 times more abundant than syntaxin 3A mRNA. This demonstrates that syntaxin 3B is the major syntaxin 3 isoform expressed in the goldfish retina.

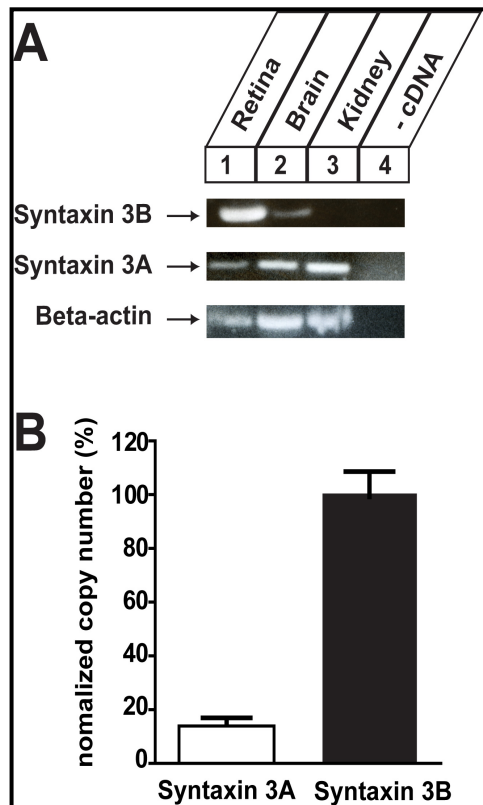


**Figure 27. Expression of Syntaxin 3B in the Goldfish**

A. Reverse-transcription PCR (RT-PCR) was performed to analyze the expression of Syntaxin 3A and 3B and beta actin in retina, brain and kidney. B. Real time PCR analysis of expression of syntaxin 3A and 3B in goldfish retina. Data have been normalized to the value of ssyntaxin 3B cDNA. Syntaxin 3A:  $896.1 \pm 139.3$  N=6 Syntaxin 3B:  $6419 \pm 608.4$  N=6. Reprinted from reference 11 with kind permission from Elsevier.

**Complexin 3 in the Goldfish**

Complexins are a family of small proteins (14-18 kDa) that play a role in neurotransmitter release through interactions with SNARE proteins. Four complexin isoforms have been identified in the mouse: complexin 1, 2, 3, and 4 (McMahon et al., 1995; Reim et al., 2005). Complexins 1 and 2 are expressed in conventional synapses. Complexin 3 (CPX 3) is expressed in both conventional and retinal ribbon synapses, whereas complexin 4 (CPX 4) is expressed only in retinal ribbon synapses (Reim et al., 2005).

Using immunohistochemistry, Reim and colleagues showed complexin 3 and 4 are differentially expressed in ribbon synapses of the mouse retina. CPX 3 is expressed in rod



photoreceptors, cone photoreceptors, and rod bipolar cells. CPX 4 is expressed in rod photoreceptors and cone bipolar cells (2005).

The goldfish Mb1 bipolar cell receives the majority of its inputs from rod photoreceptors; thus, it is considered a rod-dominate bipolar cell (Sherry et al., 1993). Because CPX 3 is a constituent of the synaptic vesicle exocytotic fusion machinery in mouse rod bipolar cells, it was of interest to clone CPX 3 from the goldfish retina to obtain a goldfish CPX 3 cDNA clone that could be used to analyze the expression and function of CPX 3 in the Mb1 bipolar cell.

To clone CPX 3 from the goldfish retina, RT-PCR with primers derived from zebrafish complexin 3 cDNA was used to amplify goldfish complexin 3 cDNA from mRNA isolated from goldfish retina. The PCR fragment shown in Figure 28 was purified and sequenced to predict the goldfish complexin 3 protein sequence. As shown in Figure 29, goldfish complexin 3 is very similar to mouse and zebrafish complexin 3. The SNARE binding domains (site that interacts with the SNARE complex) of goldfish and zebrafish complexin 3 are 96% identical at the amino acid level. The SNARE binding domains of goldfish and mouse complexin 3 are 83% identical. The N-termini of goldfish and zebrafish complexin 3 are 96% identical and the N-termini of goldfish and mouse complexin 3 are 77% identical. The accessory alpha helices of goldfish and zebrafish complexin 3 are 94% identical. The accessory alpha helices of goldfish and mouse complexin 3 are 61% identical. The C-termini of goldfish and zebrafish complexin 3 are 94% identical and the C-termini of goldfish and mouse complexin 3 are 75 % identical. Overall, the sequencing data shows that complexin 3 is conserved between mammals and fish.

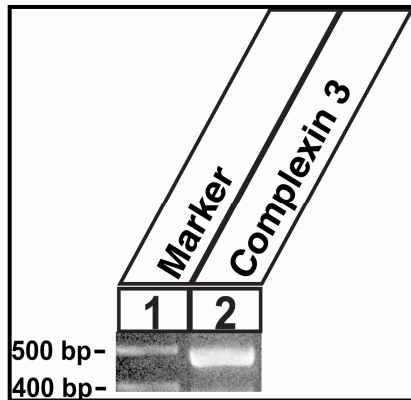


**Figure 28. Cloning of Complexin 3 from Goldfish**

Lane 1: Marker. Lane 2: Goldfish complexin 3 was cloned from goldfish retina using primers derived from zebrafish complexin 3.

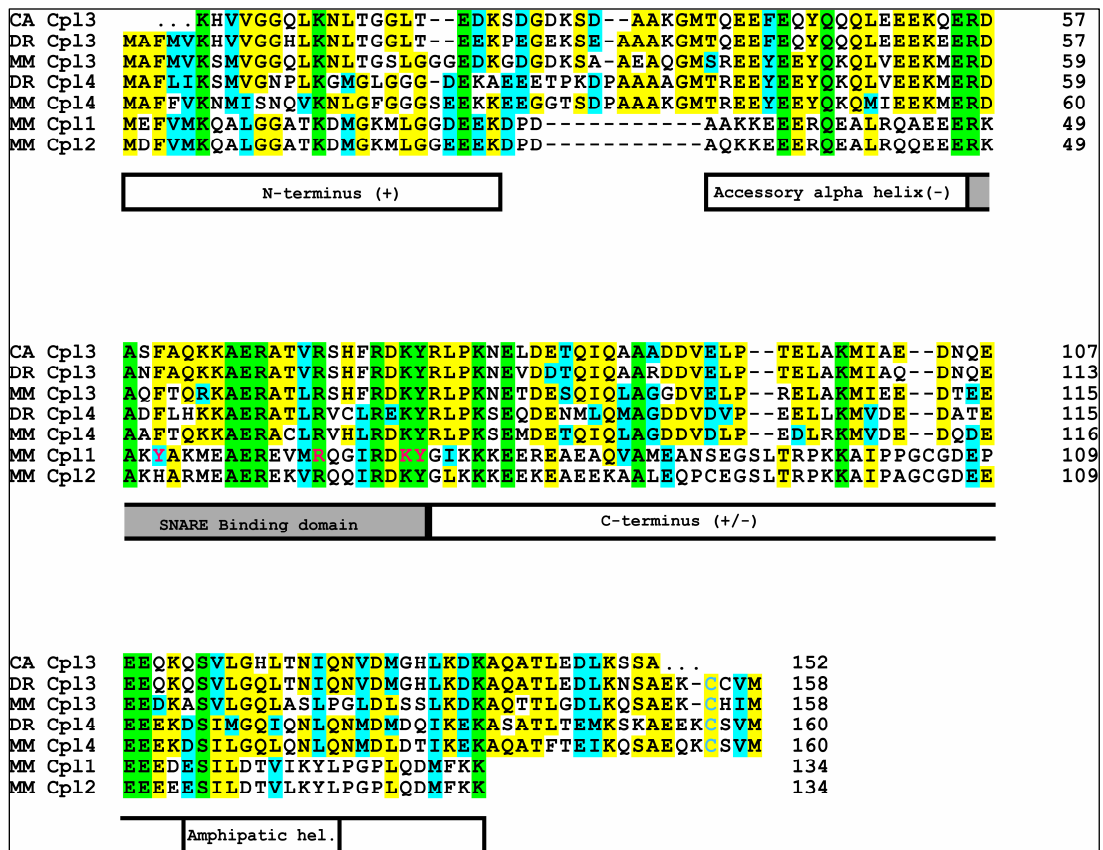


**Figure 29. Sequence Alignment of Different Complexin (Cpl) Isoforms**

The protein sequences of goldfish (CA) complexin 3, zebrafish (DR) complexin 3 and 4, and all mouse (MM) complexin isoforms have been aligned for maximal homology using CLUSTALW. Sequences are identified on the left and residues numbered on the right. Residues that are conserved in all complexins listed above are labeled with green background. Residues conserved between two or more complexin isoforms regardless of species are labeled with yellow background. Conservative exchanged residues are labeled with blue background. The positions of the conserved domains are marked below the sequence.

*In situ* hybridization is a technique that is used to determine the cellular localization of a specific gene within a specific tissue. In view of this, we decided to use *in situ* hybridization to analyze the expression pattern of complexin 3 in the goldfish retina . First, the CPX 3 cDNA clone was used to generate a riboprobe. The quality of the probe was then checked by running the riboprobe on an agarose gel. The lack of smearing on the gel indicated the riboprobe was not degraded and could be used for *in situ* hybridization (Figure 30)

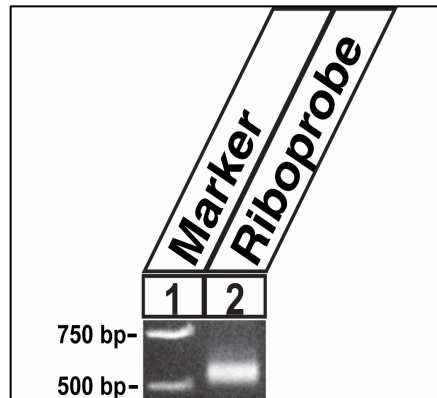


**Figure 30. Complexin 3 Riboprobe for *In Situ* Hybridization in Goldfish Retina.**

Lane 1: Marker. Lane 2: Digoxigenin-labeled Complexin 3 antisense riboprobe. The DNA template for the labeling reaction was Goldfish Complexin 3 cDNA cloned into the pCR2.1-TOPO vector.

Although the riboprobe appeared to be of good quality, the results of the *in situ* hybridization experiment were inconclusive. One major reason why the results could not be interpreted is the quality of the tissue was very poor. The bipolar cell bodies were difficult to identify because the inner nuclear layer of the retina was tattered. In addition, there was a lot of background from the detection reagent. Although signal was seen in a few photoreceptor cell bodies, a significant proportion of the signal was in the ganglion cell layer and outer plexiform layer. Overall, *in situ* hybridization may not be the best approach for analyzing the expression of CPX 3 in the Mb1 bipolar cell.

## **Synaptotagmin 1 in the Goldfish**

The Mb1 bipolar cell releases synaptic vesicles both phasically and tonically. These two modes of release have divergent calcium requirements. Phasic release is triggered when intraterminal calcium is 20-200  $\mu\text{M}$ . In contrast, tonic release is induced when intraterminal calcium is 1-2  $\mu\text{M}$  (Heidelberger et al., 1994; Lagnado et al., 1996). Since phasic vesicle release from the Mb1 bipolar neuron occurs when intraterminal calcium is high, it has been proposed this mode of release is mediated by a low-affinity  $\text{Ca}^{2+}$  sensor. Following this line of thought, tonic vesicle release from this cell is thought to be mediated by a high-affinity  $\text{Ca}^{2+}$  sensor as this mode of release can be triggered by low calcium levels.

What are the  $\text{Ca}^{2+}$  sensors for phasic and tonic release? Considering synaptotagmins are thought to function as  $\text{Ca}^{2+}$  sensors in cellular exocytosis, it is likely the  $\text{Ca}^{2+}$  sensors for phasic and tonic release from the Mb1 bipolar neuron are members of the synaptotagmin family of proteins (Südhof, 2002). In mouse conventional synapses the highly homologous vesicular synaptotagmins, synaptotagmin 1 and 2 (aka synaptotagmin 1/2), mediate fast, synchronous synaptic vesicle exocytosis (Geppert et al., 1994). It is thought synaptotagmin 1/2 plays a role in vesicle fusion by interacting with the SNARE complex and plasma membrane phospholipids in a  $\text{Ca}^{2+}$ -dependent manner through its two C2 domains (known as C2A and C2B) (reviewed in Rizo and Rosenmund, 2008).

Synaptotagmins 1/2 bind phospholipids as a function of  $\text{Ca}^{2+}$  ( $\text{EC}_{50} \approx 10\text{-}20 \mu\text{M Ca}^{2+}$ ) (Sugita et al., 2002). As indicated by the half-maximal binding value, binding of synaptotagmins 1/2 to phospholipids is not optimal at the calcium concentrations which support phasic and tonic release from the Mb1 bipolar cell. In view of this, there is speculation that other members of the synaptotagmin family may function as  $\text{Ca}^{2+}$  sensors for these two modes of release. Several groups have analyzed which synaptotagmin isoforms are expressed in the Mb1 bipolar cell using mammalian antibodies (Berntson and Morgans, 2003; Heidelberger et al., 2003). In the study by Heidelberger and colleagues, a commercial antibody (Synaptic Systems (SYSY)) directed against amino acids 120-130 of mouse

synaptotagmin 1 strongly labeled the IPL of goldfish retina with very weak staining of the OPL. Interestingly, double-labeling of the goldfish retina with the synaptotagmin 1/2/ antibody and the Mb1 bipolar cell marker protein kinase C (PKC) showed that the synaptotagmin 1/2 staining the goldfish IPL was localized to conventional synapses but not to Mb1 bipolar cell terminals. In line with this finding, no signal was seen in the terminals of freshly isolated Mb1 bipolar cells. Two other antibodies used in this study, a commercial antibody (Chemicon) directed against amino acids 1-23 of mouse synaptotagmin 1 and a commercial antibody (Stressgen) directed against an unknown mouse synaptotagmin 1 epitope, also did not label the Mb1 bipolar cell. In agreement with the study by Heidelberger and colleagues, Berntson and Morgans reported no labeling of the Mb1 bipolar cell with a synaptotagmin 1/2 antibody called ID12. Instead of synaptotagmin 1/2, Berntson and Morgans reported seeing labeling of the Mb1 bipolar cell with an antibody directed against synaptotagmin 3.

Although the data from these studies suggest that synaptotagmin isoform(s) besides synaptotagmin 1/2 may act as the calcium sensor(s) for neurotransmitter release in the Mb1 bipolar cell, it is unknown whether the epitopes recognized by the mouse synaptotagmin 1/2 antibodies are conserved in goldfish synaptotagmin 1/2. In regard to the study by Heidelberger and colleagues, the lack of signal in the Mb1 bipolar cell with the Synaptic Systems antibody may be the result of the inability of the antibody to recognize goldfish synaptotagmin 1/2, not the lack of synaptotagmin 1/2 in this cell type. Following this line of thought, if the epitope recognized by the Synaptic Systems antibody is not conserved between mouse and goldfish synaptotagmin 1/2, it is possible the labeling of conventional synapses in the goldfish IPL by the Synaptic Systems antibody may be due to the antibody recognizing a protein other than goldfish synaptotagmin 1/2. The synaptotagmin antibodies used in the Berntson and Morgans study to immunolabel the Mb1 bipolar cell may not have given accurate results as the Materials and Methods section of the study did not list the epitope recognized by ID12 nor was it mentioned in the Materials and Methods section whether or not the synaptotagmin 3 antibody used in the study was raised against mammalian or goldfish synaptotagmin 3. Taken

together, these studies illustrate more work must be done in order to definitively identify the  $\text{Ca}^{2+}$  sensors for phasic and tonic release from the goldfish Mb1 bipolar cell.

As a first step towards determining what synaptotagmin isoforms are expressed in the goldfish Mb1 bipolar cell, synaptotagmin 1 was cloned from the goldfish retina. To clone synaptotagmin 1 from the goldfish retina, RT-PCR with primers derived from the synaptotagmin 1 zebrafish sequence was used to amplify the goldfish synaptotagmin 1 cDNA from mRNA isolated from goldfish retina. The PCR fragment shown in Figure 31 was purified and sequenced to predict the goldfish synaptotagmin 1 protein sequence (refer to Figure 32).

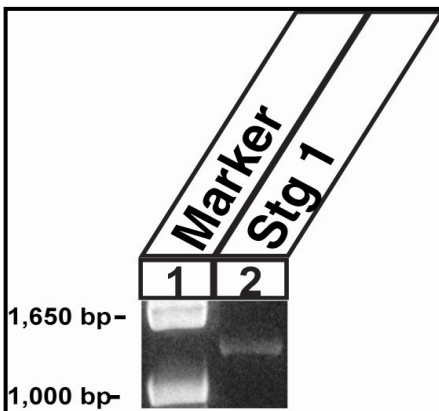


**Figure 31. Cloning of Synaptotagmin 1 from Goldfish**

Lane 1: Marker. Lane 2: Primers derived from zebrafish Synaptotagmin 1 were used to amplify Synaptotagmin 1 cDNA from goldfish retina.

DR Sytg 1	MSRREARVGNPAPTAAPFVPG-----NSTEAAGPGPRETKDEMFSKVKNKFMNEL	50
GF Sytg 1	..MSRREALVGNPAPSAAPGVSG-----NSTEAAGPGPRDTKDEMFSKVKDKFMNEL	50
MM Sytg 1	MVSASRPEALAAPVTTVATLVPH-----NATEPASPG-EGKEDAFSKLKQKFMNEL	50
MM Sytg 2	MRNIFKRNQEPNVAPATTTATMPLAPVAPADNSTESTGPG-ESQEDMFAKLKEKEFNEI	58
TM domain		
DR Sytg 1	HKIPLPSWAIVAIAFVAVVLVVSCCFCICKKWIFKKKNKKKGKDKG-KNAINMKDVKDG-	108
GF Sytg 1	HKIPLPSWAIVAIAFVAVVLVVSCCFCICKKWIFKKKNKKKGKDKG-KNAINMKDVTDG-	108
MM Sytg 1	HKIPLPPWALIAIAIVAVLLVVTCCFCVCKKCLFKKKNKKKGKKEGKKNAINMKDVKDLG	110
MM Sytg 2	NKIPLPPWALIAMAVVAGLLLLTCCFCICKKCCCKKKKNKKEKGKGMKNAMNMKDMKGG-	117
C2A domain		
DR Sytg 1	--IKTEALKDEDDAETGLTDETEKE-VEPKKEEKLGLQYSMDYNFTENTLIVGIIQAAEL	165
GF Sytg 1	--IKTEALKDEDDAETGLTDETEKE-VEPKKEEKLGLQYSLDYNFTENTLIVGIIQAAEL	165
MM Sytg 1	KTMKDQALKD-DDAETGLTDGEEK-EPEKKEEKLGLQYSLDYDFQNNQLLVGIIQAAEL	168
MM Sytg 2	-----QDDDAETGLTEGEGEGEKEPEPNLGLKQFSLDYDFQANQLTVGVLAQAAEL	169
SYSY		
C2A domain		
DR Sytg 1	PAMDMDGGTSDPYVKVYLLPDKKKKFETKVHRKTLNPFVNEQFTFKVPYTELGGKTLVMTV	225
GF Sytg 1	PAMDMDGGTSDPYVKVYLLPDKKKKFETKVHRKTLNPFVNEQFTFKVPYTELGGKTLVMTV	225
MM Sytg 1	PALDMDGGTSDPYVKVYLLPDKKKKFETKVHRKTLNPFVNEQFTFKVPYSELGGKTLVMAV	228
MM Sytg 2	PALDMDGGTSDPYVKVYLLPDKKKKYETKVHRKTLNPAFNETFTFKVPYQELGGKTLVMAI	229
C2A domain		
DR Sytg 1	YDFDRFSKHDALGDVKVPMNKVDFSHVTEEWRDLQSAEKEEQEKLGDICFSLRYVPTAGK	285
GF Sytg 1	YDFDRFSKHDALGDVKVPMNKVDFSHVTEEWRDLQSAEKEEQEKLGDICFSLRYVPTAGK	285
MM Sytg 1	YDFDRFSKHDIIIGEFKVPMMNTVDFGHVTEEWRDLQSAEKEEQEKLGDICFSLRYVPTAGK	288
MM Sytg 2	YDFDRFSKHDIIIGEVKVPMMNTVDLGQPIEEWRDLQGGEEKEPEKLGDICTSLRYVPTAGK	289
C2B domain		
DR Sytg 1	LTVVVLEAKNLKKMDVGGLSDPYVKIHLMQNGKRLKKKKTTIKKNTLNPYYNESFSFEVP	345
GF Sytg 1	LTVVVLEAKNLKKMDVGGLSDPYVKIHLMQNGKRLKKKKTTIKKNTLNPYYNESFSFEVP	345
MM Sytg 1	LTVVVLEAKNLKKMDVGGLSDPYVKIHLMQNGKRLKKKKTTIKKNTLNPYYNESFSFEVP	348
MM Sytg 2	LTVCIILEAKNLKKMDVGGLSDPYVKIHLMQNGKRLKKKKTTVKKKTLNPYFNESFSFEIP	349
C2B domain		
DR Sytg 1	FEQIQKVQVVITVLDYDKIGKNDALGKVFVGLNSTGTSLRHWSMDLANPRRPIAQWHVLK	405
GF Sytg 1	FEQIQKVQVVITVLDYDKIGKNDALGKVFVGLNSSGTSLRHWSMDLANPRRPIAQWHVLK	405
MM Sytg 1	FEQIQKVQVVITVLDYDKIGKNDALGKVFVGYNSTGAELRHWSMDLANPRRPIAQWHTLQ	408
MM Sytg 2	FEQIQKVQVVITVLDYDKLGKNEALGKIFVGSNATGTSLRHWSMDLANPRRPIAQWHSK	409
DR Sytg 1	PEEEVDALLAQKK	419
GF Sytg 1	PEEEVDAQL...	
MM Sytg 1	VEEEVDAMLA VKK	421
MM Sytg 2	PEEEVDALLGKNK	42

**Figure 32. Sequence Alignment of Synaptotagmin Isoforms**

The protein sequences of goldfish (CA) synaptotagmin 1, zebrafish (DR) synaptotagmin 1, and mouse (MM) synaptotagmin 1 and 2 have been aligned for maximal homology using CLUSTALW. Sequences are identified on the left and residues numbered on the right. Residues that are conserved in all synaptotagmin isoforms are labeled with green background. Conservative exchanged residues are labeled with yellow background. Unconserved residues are labeled with white background. The positions of the conserved domains are marked above the protein sequence. Epitope recognized by Synaptic Systems Ab is underlined and denoted by the letters SYSY.

As shown in Figure 32, goldfish synaptotagmin 1 is 97% identical at the amino acid level to zebrafish synaptotagmin 1. Goldfish synaptotagmin 1 is 84% identical at the amino acid level to mouse synaptotagmin 1. As mentioned previously, mouse synaptotagmin-1/2 binds calcium, SNAREs, and phospholipids through its tandem C2 domains, C2A and C2B (reviewed in Rizo and Rosenmund, 2008). Interestingly, several of the residues that are not conserved between mouse and goldfish synaptotagmin 1 reside in the C2A domain (refer to Figure 32). Given the C2A domain in mouse synaptotagmin 1 plays a role in the overall calcium sensitivity of synaptotagmin 1, it is possible the lower degree of conservation in this region might result in goldfish and mouse synaptotagmin 1 having different calcium sensitivities (Fernandez-Chacon et al., 2001; Rizo et al., 2006).

**3.2 Analysis of the Expression and Distribution of Presynaptic Proteins in the Goldfish****Retina.**

As a first step towards identifying which cell types in the goldfish retina express syntaxin 3B, RT-PCR analysis was performed using mRNA from single cells isolated from dissociated retina. Cells were classified as Mb1 goldfish bipolar neurons or as non-bipolar cells based on morphological criteria (Heidelberger and Matthews, 1992).



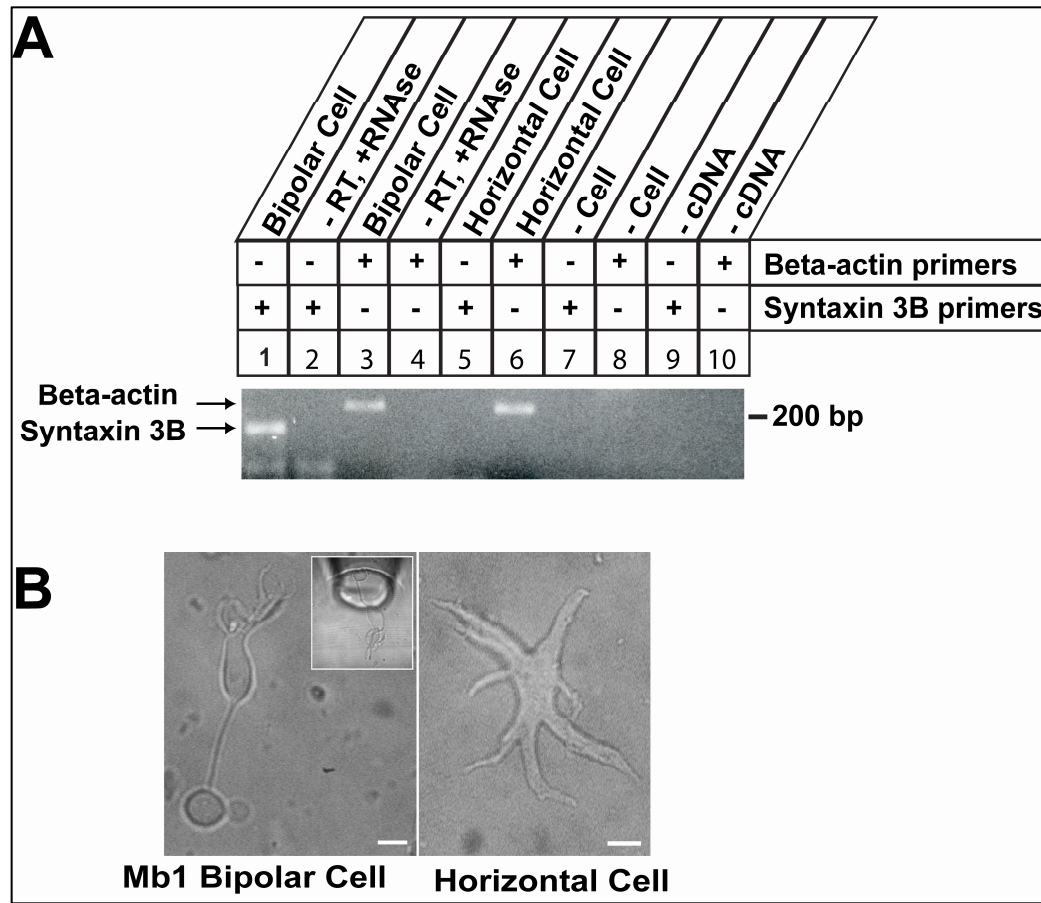


**Figure 33 . Expression of Syntaxin 3B in Isolated Bipolar Cells from Goldfish Retina**

A. Single-cell Reverse-Transcription PCR was performed to confirm the presence of Syntaxin 3B in the Mb1 bipolar cell. Primers used for RT-PCR are marked on the right. Arrows mark the position of the specific PCR products. Input is labeled on top. Controls lane 2 and 4 show PCR reactions performed on mRNA from bipolar cells without reverse transcriptase and with added RNase A. Controls lanes 7 and 8 show PCR reactions performed on bath solution without cells. B. Representative pictures of a Mb 1 bipolar cell and a horizontal cell collected for single cell PCR. Reprinted from reference 11 with kind permission from Elsevier.

As shown in Figure 33, syntaxin 3B is expressed in the Mb1 bipolar cell (Lane 1). Because genomic DNA and Total RNA were not separated after cell lysis, RNase A was added to some of the cell lysate to ensure the primers used in the PCR amplified cDNA and not genomic DNA. In case RNase A did not degrade all of the mRNA present, Reverse Transcriptase (RT) was also excluded from these samples. The absence of a signal in this negative control indicates that only cDNA was amplified (Lanes 2 and 4). Beta-actin was used as a positive control to confirm there were no procedural errors in the extraction of Total RNA

from the bipolar cells (Lane 3). Morphology was used to guide the collection of the bipolar cells from the dish; therefore, cells that were morphologically different from the bipolar cell (horizontal cell) were collected as negative controls. As expected, these cells expressed Beta-actin, but not syntaxin 3B (Lanes 5 & 6). Because a small amount of bathing solution was collected during the acquisition of the bipolar cells, the bathing solution alone was included as a negative control. The lack of signal in this sample indicates the syntaxin 3B mRNA and the Beta-actin mRNA were from the cells and not the bathing solution (Lanes 7 & 8). As a negative control, cDNA was omitted from the PCR reaction to ensure the PCR reagents were not contaminated (Lanes 9 & 10). The analysis showed that the Mb1 bipolar neurons express syntaxin 3B mRNA (Figure 33, Lane 1). In contrast, syntaxin 3B mRNA could not be detected in the horizontal cells under the same conditions.

In order to investigate the distribution of syntaxin 3B protein in the goldfish retina, an antibody was raised against a recombinant protein that consisted of the N-terminus of syntaxin 3B fused to GST. The N-termini of syntaxin 3A and 3B are identical; therefore, the antibody is predicted to recognize both isoforms of syntaxin 3. However, the real time PCR results indicate that syntaxin 3B is the major form of syntaxin 3 expressed in the goldfish retina. Thus, the majority of the protein recognized by the antibody should correspond to syntaxin 3B.

The antibody was affinity purified and tested by western blot analysis of goldfish retina extract. The purified antibody strongly reacted with a protein of about 32 kD, the predicted size of syntaxin 3B (data not shown). The purified antibody was then used to investigate the distribution of syntaxin 3B in the goldfish retina. The Syntaxin 3 antibody strongly labeled the inner and outer plexiform layers in the goldfish retina (Fig. 34). Strongly labeled puncta were visible throughout the inner plexiform layer (IPL). In the innermost IPL, terminals with the distinctive size, morphology, and location of Mb1 bipolar cell terminals were strongly labeled. Labeling in the OPL, which houses the ribbon synapses of the photoreceptors, was also strong. The staining pattern indicates that syntaxin 3B in the goldfish retina is found in ribbon synapse-containing synaptic layers. This is similar to distribution that has been observed in the

mouse (Curtis et al., 2008). Taken together, data from single-cell RT-PCR, quantitative real time RT-PCR, and immunostaining indicates syntaxin 3B is a component of the Mb1 bipolar cell synaptic vesicle exocytotic fusion machinery.

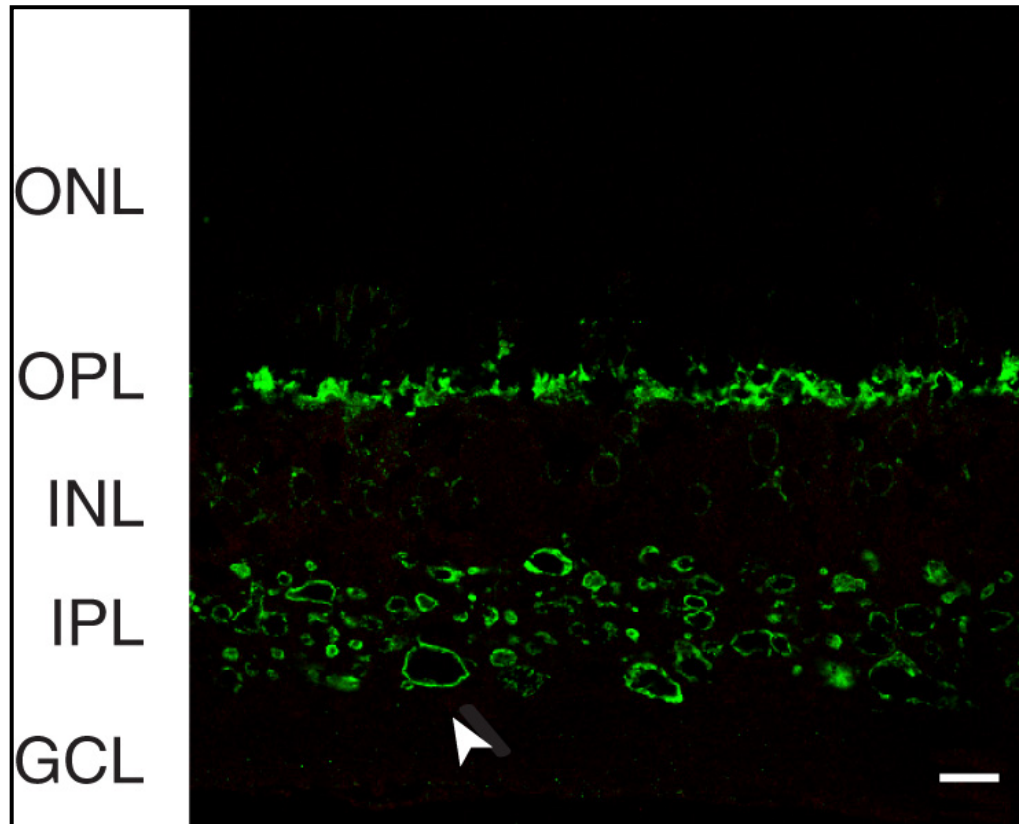


**Figure 34. Localization of Syntaxin 3B in Goldfish Retina**

A goldfish retina section was immunolabeled with a syntaxin 3 antibody. Staining was present in the synaptic layers of the retina (inner and outer plexiform layers (IPL, OPL). Arrowhead denotes potential Mb1 bipolar cell terminal. (ONL= outer nuclear layer; INL= inner nuclear layer; GCL= ganglion cell layer). Scale bar= 10  $\mu$ m.

## Discussion

### Syntaxin 3B in the Goldfish Retina

The Mb1 bipolar neuron in the goldfish has been used extensively to study the physiological properties of ribbon synapses; however, little is known about the presynaptic proteins that mediate synaptic vesicle exocytosis from this cell. To elucidate whether syntaxin 3B is a component of the synaptic vesicle fusion exocytotic machinery in goldfish retinal ribbon synapses, reverse transcription (RT)-PCR using primers derived from syntaxin 3B zebrafish cDNA was used to amplify goldfish syntaxin 3B cDNA from mRNA isolated from goldfish retina. The results of this experiment revealed that goldfish syntaxin 3B is 98% identical at the amino acid level to zebrafish syntaxin 3B and 75% identical at the amino acid level to mouse syntaxin 3B (Figure 16). In view of this information, it can be concluded that syntaxin 3B is an evolutionarily conserved protein.

In Curtis et al., 2008, we showed that syntaxin 3B is the only syntaxin 3 isoform in mouse retinal ribbon synapses (Figure 35, shown below). In contrast, both syntaxin 3A and 3B are expressed in the goldfish retina. However, data from quantitative real-time PCR indicate that syntaxin 3B is the major syntaxin 3 isoform expressed in the goldfish retina (Figure 27).

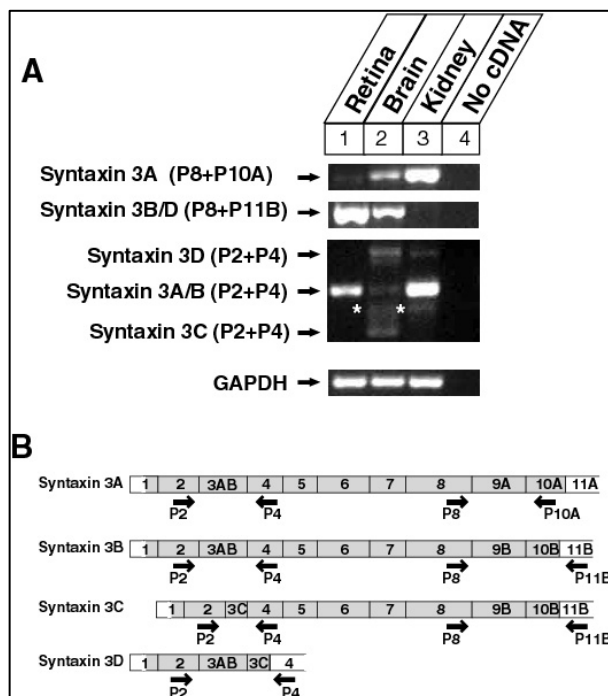


### **Figure 35. Syntaxin 3B is the Syntaxin 3 Isoform in the Mouse Retina.**

A. Results of ReverseTranscription PCR. Asterisks mark non-specific PCR products. B. mRNA transcripts of syntaxin 3 isoforms. Schematic showing how the RT-PCR primers were designed. Reprinted from reference 10 with kind permission from Elsevier.

Single-cell RT-PCR and immunohistochemistry were used to confirm the presence of syntaxin 3B in the Mb1 bipolar cell (Figures 33 & 34). After it was determined that syntaxin 3B is a constituent of synaptic vesicle exocytotic fusion machinery in the Mb1 bipolar cell, electrophysiological experiments were performed in collaboration with Dr. Ruth Heidelberger's lab to analyze the role of syntaxin 3B in neurotransmitter release in a vertebrate retinal bipolar cell. For these experiments, a peptide derived from the N-terminal half of the SNARE domain of goldfish syntaxin 3B was generated. The syntaxin 3B SNARE peptide was dialyzed into the synaptic terminal of the Mb1 bipolar neuron and exocytosis was monitored via membrane capacitance measurements (Curtis et al., 2010). The results of the electrophysiological experiments showed that the syntaxin 3B SNARE peptide inhibits functional refilling of the releasable pool of synaptic vesicles in synaptic terminals of retinal bipolar neurons (Figure 36).

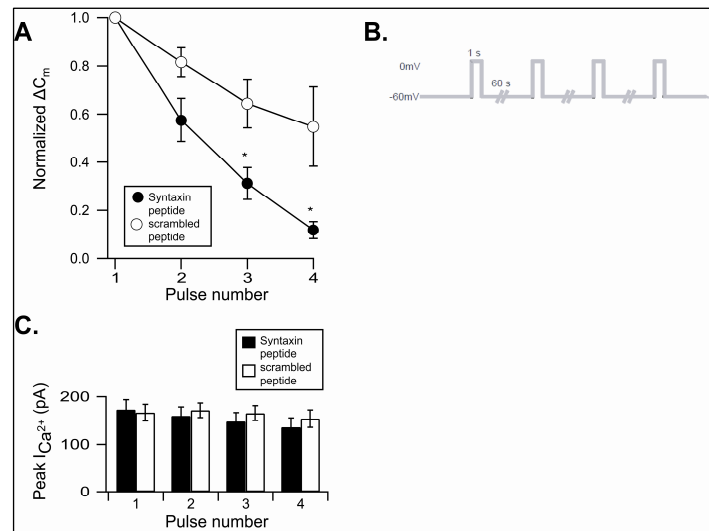


### **Figure 36. Syntaxin 3B Peptide Inhibits Functional Refilling of Releasable Pool**

A. Isolated Mb1 bipolar cells terminals were dialyzed with internal solution containing either the Syntaxin 3B SNARE peptide (black circles,  $n = 5$ ) or a scrambled control peptide (white circles,  $n = 5$ ). Four 1 s depolarizing pulses (-60 to 0 mV) were given with an interpulse interval of 60 seconds (Figure 36B). The change in membrane capacitance ( $\Delta C_m$ ) measured for each pulse was normalized to the magnitude of the response to the first pulse.  $\Delta C_m$  evoked by the first pulse was not significantly different between the two groups. Normalized  $\Delta C_m$  shows decrease in functional pool refilling by the 3rd and 4th pulse compared to the magnitude of the response to pulse 1 (compare cells dialyzed with syntaxin 3B peptide (black circles) to cells dialyzed with scrambled control (white circles). Data are expressed in mean  $\pm$  s.e.m. p-values  $< 0.05$  are marked with asterisks. C. There was no significant difference in the mean peak amplitudes of the calcium current between cells dialyzed with the SNARE binding domain of Syntaxin 3B (black bars,  $n = 5$ ) and those dialyzed with the scrambled control (white bars,  $n = 5$ ). (Courtesy of Proleta Datta) Reprinted from reference 11 with kind permission of Elsevier.

Functional refilling of the releasable pool can be impaired if there is a decrease in the number of vesicles physically present at the active zone or if there is a decrease in the number of vesicles at the active zone that are in a fusion-competent state. Given that *in vitro* binding data from my lab indicates the syntaxin 3B SNARE peptide can interfere with the formation of native SNARE complexes (Figure 37, shown below ,Bogdanova and Janz, unpublished data), it is likely the syntaxin 3B SNARE peptide blocks exocytosis by interfering with SNARE complex-mediated docking and fusion of synaptic vesicles with the presynaptic plasma membrane. Overall, the electrophysiological data supports the hypothesis that syntaxin 3B plays an important role in neurotransmitter release from vertebrate retinal ribbon synapses.

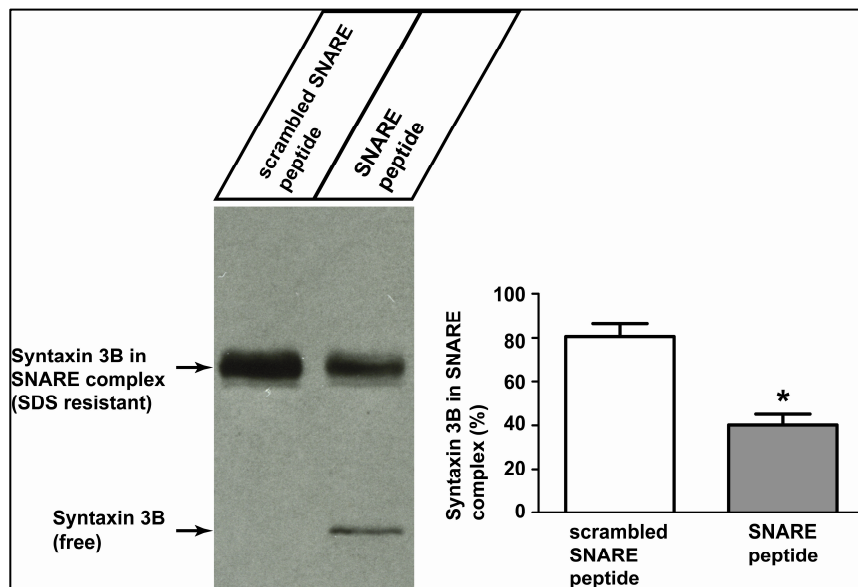


**Figure 37. Syntaxin 3B Peptide Interferes with the Formation of New SNARE Complexes**

Goldfish retina was homogenized in a buffer containing 1% Triton-X-100 and centrifuged. The supernatant was mixed with a peptide derived from the first half of the goldfish syntaxin 3B SNARE domain (see figure 3) or a scrambled control peptide (final peptide concentration 0.5  $\mu$ M) and incubated for 2 hrs. at room temperature. The samples were then mixed with SDS-sample buffer, separated by SDS-PAGE without boiling of the samples and analyzed by western blot with the syntaxin 3 antibody. Under these conditions the majority of syntaxin 3B is found in high molecular SDS-resistant SNARE complexes (top arrow). The SNARE peptide inhibits the formation of new SNARE complexes as apparent by the presence of the free syntaxin 3B (bottom arrow). The remaining SNARE complexes (top arrow) were likely already assembled in the tissue and are not affected by the SNARE peptide (Right figure). Percentage of syntaxin 3B in SNARE complexes when homogenate was mixed with either scrambled SNARE peptide or syntaxin 3B peptide (Left figure). (Courtesy of Nataliia Bogdanova and Roger Janz)

### **Complexin 3 in the Goldfish Retina**

Complexins are a family of small proteins (14-18 kDa) that play a role in neurotransmitter release through interactions with SNARE proteins. Four complexin isoforms have been identified in the mouse: complexin 1, 2, 3, and 4 (McMahon et al., 1995; Reim et al., 2005). As noted earlier, complexins 3 and 4 are the complexin isoforms expressed in mouse retinal ribbon synapses. Using electroretinographic recordings (ERG) from *Cplx3* and *Cplx4* single- and double-knockout mice, Reim and colleagues have shown that loss of complexins 3 and/or 4 leads to the altered timing of signal transmission from photoreceptors to bipolar cells in OPL, alterations in transmitter release at bipolar cell terminals, changes in the timing of synaptic processing in the inner retina, and mild visual deficits (2009). Taken together, the ERG data from Reim and colleagues indicate that complexins 3 and 4 are essential regulators of release at retinal ribbon synapses. However, the ERG data does not provide the information required to determine the exact role of complexins 3 and 4 at retinal ribbon synapses. For this level of analysis, patch-clamp experiments of membrane capacitance changes at individual ribbon synaptic terminals are needed. Mammalian retinal neurons have nerve terminals that are too small for patch clamping. As mentioned previously, the goldfish rod-dominate Mb1 bipolar cell has a large terminal which is ideal for measuring changes in membrane capacitance that occur during neurotransmitter release (Heidelberger and Matthews, 1992; Heidelberger, 1998). If complexins 3 and/or 4 are expressed in the goldfish Mb1 bipolar cell, it may be possible to use the goldfish Mb1 bipolar cell to elucidate the role of complexins 3 and 4 in neurotransmitter release at retinal ribbon-style synapses.

In this present study, complexin 3 was the focus because it is the complexin isoform that is expressed in mouse rod bipolar cells (Reim et al., 2005). To clone complexin 3 from goldfish retina, reverse transcription (RT)-PCR using primers derived from zebrafish complexin 3 cDNA was used to amplify goldfish complexin 3 cDNA from mRNA isolated from goldfish (Figure 28). The amplified cDNA was sequenced to predict the goldfish complexin 3 protein sequence. Interestingly, complexin 3 is very similar to mouse complexin 3 (Figure 29). Thus, it

is likely goldfish and mouse complexin 3 do not differ much in how they regulate neurotransmitter release.

It has been shown that three distinct domains in mouse complexin 1 differentially regulate synaptic vesicle exocytosis (refer to Figure 29 for mouse complexin 1 protein sequence). The N-terminal domain of complexin 1 has a positive effect on vesicle fusion. The accessory alpha helix of complexin 1 restricts spontaneous vesicle fusion. The C-terminal domain stimulates vesicle fusion in an *in vitro* fusion system (Xue et al., 2007; Giraudo et al., 2008; Malsam et al., 2009; Maximov et al., 2009). The N-terminal domain, accessory alpha helix, and C-terminal domain is where complexin 1 and 3 differ the most from one another. This implies the complexin 3 domains might differ from the complexin 1 domains in how they regulate synaptic vesicle release. As noted previously, goldfish complexin 3 is highly homologous to mouse complexin 3. If complexin 3 is expressed in the Mb1 bipolar cell, it may be possible to elucidate what role the different domains of complexin 3 play in neurotransmitter release by dialyzing the different domains of goldfish complexin 3 into the Mb1 bipolar cell (the exogenous complexin 3 domains should disrupt interactions between the endogenous complexin 3 domains and their binding partners) and monitoring exocytosis via membrane capacitance measurements.

To analyze the expression of CPX 3 in the goldfish retina, the CPX 3 cDNA clone mentioned above was used to generate a riboprobe for *in situ* hybridization (Figure 20). The riboprobe was generated without difficulty and appeared to be of good quality; however, the results of the *in situ* hybridization experiment were inconclusive. *In situ* hybridization may not be the best method to use to assess whether or not CPX 3 is expressed in the Mb1 bipolar cell due to the disadvantages of this technique. One disadvantage of *in situ* hybridization is it can be difficult to determine what fixation method should be used to fix the tissue. The "best" fixation method is one that allows access of the probe to the target sequence, retains maximal levels of cellular target RNA, and maintains the morphology of the tissue. The fixative used for the CPX 3 *in situ* was 4% paraformaldehyde which provides good RNA retention and probe



penetration. In spite of these advantages, tissue morphology can be altered with 4% paraformaldehyde. Given that poor tissue quality contributed to the inability to interpret the results of the CPX 3 *in situ*, it is possible 4% paraformaldehyde may not be the best fixative to use for this experiment. This must be taken into consideration if the CPX 3 *in situ* experiment is repeated in the future.

A second disadvantage is the riboprobe and the RNA in the tissue can be degraded by RNases. This can occur rather easily because RNases are very stable and abundant. One way to avoid this problem is to be very careful when handling the tissue and use a DNA probe. However, while a DNA probe is not subject to degradation by RNases, DNA-RNA hybrids are less stable than RNA-RNA hybrids. For this reason, a riboprobe was used for the CPX 3 *in situ* in spite of the risk of degradation by RNases.

Another disadvantage of *in situ* hybridization is the hybridization and washing conditions must be optimal in order for the probe to bind to its target sequence. The affinity of the probe for its target sequence can be altered by the temperature, pH, formamide, and salt concentration of the hybridization buffer. Determining what temperature, pH, formamide, and salt concentration the hybridization buffer should have is sometimes a matter of trial and error. For the CPX 3 *in situ*, only one temperature, pH, formamide, and salt concentration was tried. This may have been one reason why the *in situ* experiment was unsuccessful. In regard to washing conditions; if too stringent, a loss of sensitivity can occur and if not stringent enough, high background can be a problem. The washing conditions used for the CPX 3 *in situ* may or may not have been optimal as the washing conditions were never varied in order to determine the best way to wash the tissue.

Because of the disadvantages mentioned above, instead of *in situ* hybridization, immunohistochemistry will be used in the future to elucidate whether or not CPX 3 is expressed in the Mb1 bipolar cell. To do this, the goldfish CPX 3 cDNA will be subcloned into an expression vector to generate a recombinant protein that can be used to produce an antibody which specifically recognizes goldfish CPX 3. The CPX 3 antibody could then be

used to immunolabel an isolated Mb1 bipolar cell to determine if CPX 3 is a constituent of the Mb1 bipolar cell synaptic vesicle exocytotic fusion machinery.

### **Synaptotagmin 1 in the Goldfish Retina**

Synaptotagmins are a family of proteins that act as calcium sensors for cellular exocytosis. One member of the synaptotagmin family, synaptotagmin 1/2, is thought to be the calcium sensor for fast, synchronous neurotransmitter release in mouse conventional synapses (Südhof, 2002; Geppert et al., 1994). Due to a lack of antibodies specific for goldfish synaptotagmins, it is currently unknown whether the Mb1 bipolar cell calcium sensor is synaptotagmin 1 and/or another member of the synaptotagmin family member. As a first step towards elucidating which synaptotagmin isoforms are expressed in the Mb1 bipolar cell, synaptotagmin 1 was cloned from the goldfish retina using reverse transcription (RT)-PCR with primers derived from zebrafish synaptotagmin 1 cDNA (Figure 31). The amplified cDNA was sequenced to predict the goldfish synaptotagmin 1 protein sequence (Figure 32). The results of the sequencing reaction revealed that goldfish synaptotagmin 1 is 97% identical at the amino acid level to zebrafish synaptotagmin 1 and 84% identical at the amino acid level to mouse synaptotagmin 1. Thus, synaptotagmin 1 is a protein that is conserved among vertebrates. Although goldfish and mouse synaptotagmin 1 are very similar at the amino acid level, there are several amino acid residues that are not conserved between the two proteins. Many of the unconserved residues are located in region referred to as the C2A domain. This is an interesting finding because the C2A domain in mouse synaptotagmin 1 is believed to play a role in the overall affinity of synaptotagmin 1 for calcium. In light of the results shown here in this study, it is possible goldfish and mouse synaptotagmin 1 have different calcium affinities. Binding experiments with goldfish synaptotagmin 1 will have to be performed in the future to assess the affinity of this protein for calcium.

As noted earlier, the inability to determine whether synaptotagmin 1 is present in the Mb1 bipolar cell has been largely due to questions regarding whether or not antibodies raised against mouse synaptotagmin 1 can reliably detect goldfish synaptotagmin 1 (Berntson and

Morgans, 2003; Heidelberger et al., 2003). A comparison of the goldfish and mouse synaptotagmin 1 protein sequences reveals that one of the antibodies used in the study by Heidelberger and colleagues should be able to recognize goldfish synaptotagmin 1. This particular antibody was raised against amino acids 120-130 of mouse synaptotagmin 1 (Synaptic Systems) which are conserved in goldfish synaptotagmin 1 (refer to Figure 32). Interestingly, when Heidelberger and colleagues used the Synaptic Systems antibody to immunolabel the Mb1 bipolar cell and other types of goldfish bipolar cells, no signal was detected. In view of this, it is likely labeling of the goldfish IPL with the Synaptic Systems antibody is localized to conventional synapses as suggested by Heidelberger and colleagues. The Chemicon antibody that was used in the study should not recognize goldfish synaptotagmin 1 because the epitope it is directed against is not conserved between goldfish and mouse synaptotagmin 1. Thus, it is not surprising that the Chemicon antibody did not label the IPL of the goldfish. It is surprising, however, that the Chemicon antibody labeled the OPL of the goldfish retina. This labeling is most likely cross-reactivity of the antibody with a protein similar to mouse synaptotagmin 1 given that the antibody is not predicted to recognize goldfish synaptotagmin 1. In regard to the ID12 antibody used in the Bernston and Morgans study, it is difficult to interpret their results without knowing what epitope the ID12 antibody recognizes. In addition, more information about the synaptotagmin 3 antibody used in the study is needed. Overall, in view of the sequence data obtained in this study and the results of Heidelberger and colleagues it is likely that synaptotagmin 1 is expressed in the conventional not the ribbon-style synapses of the goldfish retina. An alternative to this interpretation, as proposed by Heidelberger and colleagues, is that the epitope recognized by the Synaptic Systems antibody is unavailable in the ribbon-style synapses due to interactions with synaptic proteins or phospholipids, or post-translational modification. To examine these possibilities, single cell RT-PCR and/or immunolabeling of the Mb1 bipolar cell with a goldfish synaptotagmin 1 specific antibody will have to be performed in the future to confirm whether or not synaptotagmin 1 is expressed in the Mb1 bipolar cell. In addition, future experiments will have to address whether

the Mb1 bipolar neuron utilizes another synaptotagmin isoform such as synaptotagmin 3 for calcium sensing.

### **Final Discussion**

A central finding of this present study is that t-SNARE complex formation in retinal ribbon synapses may be regulated via CAMKII-mediated phosphorylation of syntaxin 3B. To date, there is no evidence to suggest that t-SNARE complex formation in conventional synapses is regulated by a similar mechanism (Snyder et al., 2006). Although it is currently unknown why t-SNARE complex formation differs between the two synapse types, the answer may lie with the ability of calmodulin to alter its calcium binding properties. In a paper by Gaertner and colleagues, it was shown that in the presence of a protein called RC3/Neurogranin, the affinity of calmodulin for calcium decreases, whereas in the presence of CAMKII the affinity of calmodulin for calcium increases (2004). To date, it is unknown whether RC3/Neurogranin is expressed in photoreceptors and/or bipolar cells. If RC3/Neurogranin or other proteins that can alter the calcium binding properties of calmodulin are present in photoreceptors and/or bipolar cells, calmodulin in retinal ribbon synapses may have a dynamic range of calcium binding kinetics that would allow it to signal changes in intracellular calcium concentration that follow changing light levels. Calmodulin could then transfer this information to the synaptic vesicle exocytotic machinery through CAMKII-mediated phosphorylation of syntaxin 3B. Thus, the calcium sensitivity of the synaptic vesicle exocytotic machinery in retinal ribbon synapses might have a level of flexibility that the synaptic exocytotic machinery in conventional synapses might not possess. This flexibility might be one reason retinal ribbon synapses are able to release neurotransmitter both tonically and phasically.

Another important finding of this study is most of the synaptic proteins in mammalian retinal ribbon synapses are conserved in the Mb1 bipolar cell. This supports the use of the Mb1 bipolar cell as a model for neurotransmitter release from vertebrate retinal bipolar cells. In regard to vertebrate photoreceptors, the salamander rod and cone have been used frequently as model cells for photoreceptor neurotransmitter release due to their large terminals which

allow for membrane capacitance and presynaptic calcium measurements. One interesting finding from several studies with salamander rods and cones is that synaptic transmission appears to be faster in cones than rods (Cadetti et al., 2005; Rabl et al., 2005; reviewed in Thoreson 2007) Although the mechanisms which give rise to this difference between rods and cones have not been elucidated, one possible mechanism may be formation of the t-SNARE complex is regulated differently in cones than rods. As noted in the Results section, binding between syntaxin 3B and SNAP-25 is very weak in the absence of CAMKII-mediated phosphorylation of syntaxin 3B. If the CAMKII regulatory mechanism is present in cones but not rods, it is possible the syntaxin 3B/SNAP-25 complex forms more quickly and efficiently in cones than rods. This could potentially lead to a faster rate of vesicle release from cones compared to rods. However, without knowing whether syntaxin 3B is conserved in salamander rods and cones or if CAMKII-mediated phosphorylation of syntaxin 3B occurs in cones as opposed to rods, the ideas proposed here remain speculative. In addition, more experiments are needed to confirm CAMKII-mediated phosphorylation of syntaxin 3B is physiologically relevant and the ability of other kinases to regulate binding between syntaxin 3B and SNAP-25 must also be tested. In sum, the findings in this study provide a starting point for future experiments to elucidate how differences in the composition of the synaptic vesicle exocytotic machinery can give rise to distinct neurotransmitter release characteristics between synapse types.

## **Bibliography**

1. Arien H, Wiser O, Arkin IT, Atlas D. Syntaxin 1A modulates the voltage-gated L-type calcium channel (Ca<sub>v</sub>1.2) in a cooperative manner. *J. Biol. Chem.* 278(31): 29231-29239. 2003.
2. Atlas, D. Functional and physical coupling of voltage-sensitive calcium channels with exocytotic proteins: ramifications for the secretion mechanism. *J. Neurochem* 77(4):972-85.2001.
3. Brändstatter JH, Wässle H, Betz H, Morgans CW. The plasma membrane protein SNAP-25, but not syntaxin, is present at photoreceptor and bipolar cell synapses in the rat retina. *Eur J Neurosci* 8:823-828. 1996.
4. Bech-Hansen NT, Naylor MT, Maybaum TA, Pearce WG, Koop B, Fishman GA, Mets M, Musarella MA, Boycott KM. Loss-of-function mutations in a calcium-channel  $\alpha$ 1-subunit gene in Xp11.23 cause incomplete X-linked congenital stationary night blindness. *Nature Genetics* 19:260-3. 1998.
5. Benfenati F, Valtorta F, Rubenstein JL, Gorelick FS, Greengard P, and Czernik AJ. Synaptic vesicle-associated Ca<sup>2+</sup>/calmodulin-dependent protein kinase II is a binding protein for synapsin I. *Nature* 359: 417-420. 1992.
6. Berntson AK, Morgans CW. Distribution of the presynaptic calcium sensors, synaptotagmin I/II and synaptotagmin III, in the goldfish and rodent retinas. *J Vis* 3: 274-280.2003.
7. Cadetti L, Tranchina D, Thoreson WB. A comparison of release kinetics and glutamate receptor properties in shaping rod-cone differences in EPSC kinetics in the salamander retina. *J Physiol.* 569:773-788. 2005.
8. Chi, P., Greengard, P., and Ryan, T.A. Synaptic vesicle mobilization is regulated by distinct synapsin I phosphorylation pathways at different frequencies. *Neuron* 38, 69-78. 2003.

9. Cohen R, Marom M, Atlas D. Depolarization-evoked secretion requires two vicinal transmembrane cysteines of syntaxin 1A. *PLoS One* 2(12): e1273. 2007.
10. Curtis LB, Doneske B, Liu X, Thaller C, McNew JA, and Janz R. Syntaxin 3B is t-SNARE specific for ribbon synapses of the retina. *J. Comp. Neurol.* 510(5): 550-559. 2008.
11. Curtis LB, Datta P, Liu X, Bogdanova N, Heidelberger R, and Janz R. Syntaxin 3B is Essential for the Exocytosis of Synaptic Vesicles in Ribbon Synapses of the Retina. *Neurosci* 166(3): 832-841. 2010.
12. Doering CJ, Hamid J, Simms B, McRory JE and Zamponi GW.  $Ca_v1.4$  encodes a calcium channel with low open probability and unitary conductance. *Biophys J.* 89(5):3042-3048. 2005.
13. Dulubova I, Sugita S, Hill S, Hosaka M, Fernandez I, Südhof TC, Rizo J. A conformational switch in syntaxin during exocytosis: role of munc18. *EMBO J.* Aug 16;18(16):4372-82. 1999.
14. Featherstone DE, Davis WS, Dubreuil RR, and Broadie K. *Drosophila*  $\alpha$ - and  $\beta$ -mutations disrupt presynaptic neurotransmitter release. *J. Neurosci* 21(12): 4215-4224. 2001.
15. Fernandez-Chacon R, Königstorfer A, Gerber SH, Garcia J, Matos MF, Steven CF, Brose N, Rizo J, Rosenmund C, and Südhof TC. Synaptotagmin I functions as a calcium regulator of release probability. *Nature* 410:41-49. 2001.
16. Fox MA, Sanes JR. Synaptotagmin I and II are present in distinct subsets of central synapses. *J Comp Neurol.* Jul 10;503(2):280-96. 2007.
17. Gaertner TR, Putkey JA, Waxham MN. RC3/ Neurogranin and  $Ca^{2+}$ / Calmodulin-dependent Protein Kinase II Produce Opposing Effects on the Affinity of Calmodulin for Calcium. *J. Biol. Chem.* 279(38): 39374-39382. 2004.

18. Geppert M, Goda Y, Hammer RE, Li C, Rosahl TW, Stevens CF, and Sudhof TC. Synaptotagmin I: a major  $\text{Ca}^{2+}$  sensor for transmitter release at a central synapse. *Cell*. 79:717-727. 1994.
19. Gil-Loyzaga P, Pujol R. Synaptophysin in developing cochlea. *Int. J. Devl. Neurosci*. 6: 155-160. 1988.
20. Giraudo CG, Garcia-Diaz A, Eng WS, Yamamoto A, Melia TJ, Rothman JE. Distinct domains of complexins bind SNARE complexes and clamp fusion in vitro. *J Biol Chem*. Jul 25;283(30):21211-9. 2008.
21. Heidelberger R, Matthews G. Inhibition of calcium influx and calcium current by gamma-aminobutyric acid in single synaptic terminals. *Proc Natl Acad Sci U S A*. Aug 15;88(16):7135-9. 1991.
22. Heidelberger R, Matthews G. Calcium influx and calcium current in single synaptic terminals of goldfish retinal bipolar neurons. *J Physiology* 447:235-256. 1992.
23. Heidelberger R, Heinemann C, Neher E and Matthews G. Calcium dependence of the rate of exocytosis in a synaptic terminal. *Nature* 371:513-515. 1994.
24. Heidelberger R Adenosine triphosphate and the late steps in calcium-dependent exocytosis at a ribbon synapse. *J Gen Physiol* 111:225-241. 1998.
25. Heidelberger R, Wang MM, Sherry DM. Differential distribution of synaptotagmin immunoreactivity among synapses in the goldfish, salamander, and mouse retina. *Vis Neurosci* 20:37-49. 2003.
26. Heidelberger R, Thoreson WB, Witkovsky P. Synaptic transmission at retinal ribbon synapses. *Prog Retin Eye Res*. Nov;24(6):682-720. 2005.
27. Hoda JC, Zaghetto F, Koschak A, Striessnig J. Congenital stationary night blindness type 2 mutations S229P, G369D, L1068P, and W1440X alter channel gating or functional expression of  $\text{Ca}_v1.4$  L-type  $\text{Ca}^{2+}$  channels. *Journal of Neuroscience* 25(1):252-9. 2005.



28. Hogan MJ, Alvarado JA, Weddell JE. *Histology of the Human Eye: An atlas and textbook*. Philadelphia: Saunders, 1971.
29. Ibaraki K, Horikawa HP, Morita T, Mori H, Sakimura K, Mishina M, Saisu H, Abe T. Identification of four different forms of syntaxin 3. *Biochem Biophys Res Commun* 211:997-1005. 1995.
30. Jackman SL, Choi SY, Thoreson WB, Rabl K, Bartoletti TM, Kramer RH. Role of the synaptic ribbon in transmitting the cone light response. *Nat. Neuroscience*. 12(13):303-10. 2009.
31. Janz R, Südhof TC. SV2C is a synaptic vesicle protein with an unusually restricted localization: anatomy of a synaptic vesicle protein family. *Neuroscience*. 94(4):1279-90. 1999.
32. Lagnado L, Gomis A, Job C. Continuous vesicle cycling in the synaptic terminal of retinal bipolar cells. *Neuron* 17:957-967. 1996.
33. Lenzi D, von Gersdorff H. Structure suggests function: the case for synaptic ribbons as exocytotic nanomachines. *Bioessays*. Sep;23(9):831-40. 2001.
34. LoGiudice L, Henry D, Matthews G. Identification of calcium channel  $\alpha 1$  subunit mRNA expressed in retinal bipolar cells. *Molecular Vision* 12:184-9. 2006.
35. Malsam J, Seiler F, Schollmeier Y, Rusu P, Krause JM, Söllner TH. The carboxy-terminal domain of complexin I stimulates liposome fusion. *Proc Natl Acad Sci U S A*. Feb 10;106(6):2001-6. 2009.
36. Mandell, J.W., Townes-Anderson, E., Czernik, A.J., Cameron, R., Greengard, P., and De Camilli, P. Synapsins in the vertebrate retina: absence from ribbon synapses and heterogeneous distribution among conventional synapses. *Neuron* 5, 19-33. 1990.
37. Mansergh F, Orton NC, Vessey JP, Lalonde MR, Stell WK, Tremblay F, Barnes S, Rancourt DE, Bech-Hansen NT. Mutation of the calcium channel gene *Cacna1f*

- disrupts calcium signaling, synaptic transmission and cellular organization in mouse retina. *Hum Mol Genet.* Oct 15;14(20):3035-46. 2005.
38. Maximov A, Tang J, Yang X, Pang ZP, Südhof TC. Complexin controls the force transfer from SNARE complexes to membranes in fusion. *Science.* Jan 23;323(5913):516-21. 2009.
  39. McMahon HT, Missler M, Li C, Südhof TC. Complexins: cytosolic proteins that regulate SNAP receptor function. *Cell* 83:111-119.1995.
  40. Melia TJ, Weber T, McNew JA, Fisher LE, Johnston RJ, Parlati F, Mahal LK, Sollner TH, and Rothman JE. Regulation of membrane fusion by the membrane –proximal coil of the t-SNARE during zippering of SNAREpins. *J Cell Biology* 158: 929-940. 2002.
  41. Morgans CW, Brändstätter JH, Kellerman J, Betz H, Wässle H. A SNARE complex containing syntaxin 3 is present in ribbon synapses of the retina. *J Neurosci* 16:6713-6721. 1996.
  42. Morgans CW. Localization of the  $\alpha_{1F}$  calcium channel subunit in the rat retina. *Invest. Ophthalmol. Vis. Sci.* 42:2414-2418. 2001.
  43. Parlati F, Weber T, McNew JA, Westermann B, Söllner TH, Rothman JE. Rapid and efficient fusion of phospholipid vesicles by the alpha-helical core of a SNARE complex in the absence of an N-terminal regulatory domain. *Proc Natl Acad Sci USA* 96:12565-12570.1999.
  44. Parsons TD, Sterling P. Synaptic ribbon. Conveyor belt or safety belt? *Neuron.* Feb 6;37(3):379-82. 2003.
  45. Pevsner J, Hsu SC, Braun JE, Calakos N, Ting AE, Bennett MK, Scheller RH. Specificity and regulation of a synaptic vesicle docking complex. *Neuron* 13:353-361.1994a

46. Prescott E, Zenisek D. Recent progress towards understanding the synaptic ribbon. *Current Opinion in Neurobiology* 15:431-436. 2005.
47. Rabl K, Cadetti L, Thoreson WB. Kinetics of exocytosis is faster in cones than rods. *J Neurosci.* 25:4633-4640. 2005.
48. Reim K, Mansour M, Varoqueaux F, McMahon HT, Sudhof TC, Brose N, Rosenmund C. Complexins regulate a late step in Ca<sup>2+</sup>-dependent neurotransmitter release. *Cell* 104:71-81.2001.
49. Reim K, Wegmeyer H, Brandstätter JH, Xue M, Rosenmund C, Dresbach T, Hofmann K, Brose N. Structurally and functionally unique complexins at retinal ribbon synapses. *J Cell Biol* 169:669-680.2005.
50. Reim K, Regus-Leidig H, Ammermüller J, El-Kordi A, Radyushkin K, Ehrenreich H, Brandstätter JH, and Brose N. Aberrant function and structure of retinal ribbon synapses in the absence of complexin 3 and complexin 4. *J Cell Science* 122:1352-1361. 2009.
51. Risinger C, Bennett MK. Differential phosphorylation of syntaxin and synaptosome-associated protein of 25 kDa (SNAP-25) isoforms. *J Neurochem* 72(2):614-24.1999.
52. Rizo J, Chen X, Arac D. Unraveling the mechanisms of synaptotagmin and SNARE function in neurotransmitter release. *Trends in Cell Biology* 16(7):340-350.2006.
53. Rizo J, Rosenmund C. Synaptic vesicle fusion. *Nat Struct Mol Biol* 15(7): 665–674. 2008.
54. Rodieck, RW. The First Steps in Seeing. Sunderland, MA: Sinauer Associates. January 15,1998.
55. Roux I, Safieddine S, Nouvian R, Grati M, Simmler MC, Bahloul A, Perfettini I, Le Gall M, Rostaing P, Hamard G, Triller A, Avan P, Moser T, Petit C. Otoferlin, defective in a human deafness form, is essential for exocytosis at the auditory ribbon synapse. *Cell* 127: 277-289. 2006.

56. Safieddine S, Wenthold RJ. The glutamate receptor subunit delta1 is highly expressed in hair cells of the auditory and vestibular systems. *J. Neuroscience* 17:7523-7531. 1997.
57. Safieddine S, Wenthold RJ. SNARE complex at the ribbon synapse of cochlear hair cells: analysis of synaptic vesicle-and synaptic membrane-associated proteins. *Eur J Neurosci* 11:803-812.1999.
58. Schaeffer SF, Raviola E. Membrane recycling in the cone cell endings of the turtle retina. *J. Cell Biol* 79: 802-825. 1978.
59. Schmitz F, Augustin I, Brose N. The synaptic vesicle priming protein Munc13-1 is absent from tonically active ribbon synapses of the rat retina. *Brain Res. Mar* 23;895(1-2):258-63. 2001.
60. Scott BL, Van Komen JS, Liu S, Weber T, Melia TJ, McNew JA. Liposome fusion assay to monitor intracellular membrane fusion machines. *Methods Enzymol* 372:274-300. 2003.
61. Sheng ZH, Rettig J, Takahashi M, Catterall WA. Identification of a syntaxin-binding site on N-type calcium channels. *Neuron* 13(6):1303-13. 1994.
62. Sherry DM, Mitchell R, Standifer KM, du PB. Distribution of plasma membrane-associated syntaxins 1 through 4 indicates distinct trafficking functions in the synaptic layers of the mouse retina. *BMC Neurosci* 7:54. 2006.
63. Sherry DM, Wang MM, Frishman LJ. Differential distribution of vesicle associated membrane protein isoforms in the mouse retina. *Mol Vis* 9: 673-688.2003.
64. Sherry DM, Yazulla S. Goldfish bipolar cells and axon terminal patterns: a Golgi study. *J.Comp. Neurol.* 329(2):188-200.1993.
65. Snyder DA, Kelly ML, Woodbury DJ. SNARE complex regulation by phosphorylation. *Cell Biochem. Biophys.* 45: 111-123. 2006.

66. Sollner T, Bennett MK, Whiteheart SW, Scheller RH, Rothman JE. A protein assembly-disassembly pathway in vitro that may correspond to sequential steps of synaptic vesicle docking, activation, and fusion. *Cell* 75:409-418.1993.
67. Sterling P, Matthews G. Structure and function of ribbon synapses. *Trends Neurosci.* Jan;28(1):20-9. 2005.
68. Südhof TC. Synaptotagmins: why so many? *J Biol Chem.* Mar 8;277(10):7629-32. 2002.
69. Sugita S, Shin OH, Weiping H, Lao Y, Sudhof TC. Synaptotagmins form a hierarchy of exocytotic  $\text{Ca}^{2+}$  sensors with distinct  $\text{Ca}^{2+}$  affinities. *EMBO* 21(3): 270-280.2002.
70. Sutton RB, Fasshauer D, Jahn R, Brunger AT. Crystal structure of a SNARE complex involved in synaptic exocytosis at 2.4 Å resolution. *Nature* 395 (6700): 328-9. 1998.
71. Tippens AL, Pare JF, Langwieser N, Moosmang S, Milner TA, Smith Y, Lee A. Ultrastructural evidence for pre-and postsynaptic localization of Cav1.2 L-type  $\text{Ca}^{2+}$  channels in the rat hippocampus. *J. Comp. Neurol.* 506(4):569-83. 2008.
72. Thoreson WB. Kinetics of synaptic transmission at ribbon synapses of rods and cones. *Mol Neurobiol* 36(3): 205-223.2007.
73. Toonan RF and Verhage M. Vesicle trafficking pleasure and pain from SM genes. *Trends in Cell Biology* 13(4):177-86. 2003.
74. Ullrich B, Sudhof T.C. Distribution of synaptic markers in the retina: implications for synaptic vesicle traffic in ribbon synapses. *J. Physiol Paris* 88, 249-257. 1994.
75. Von Gersdoff H and Matthews G. Dynamics of synaptic vesicle fusion and membrane retrieval in synaptic terminals. *Nature* 367: 735–739, 1994a.
76. Von Kriegstein K, Schmitz F, Link E, Südhof TC. Distribution of synaptic vesicle proteins in the mammalian retina identifies obligatory and facultative components of ribbon synapses. *Eur. J. Neurosci.* 11(4):1335-48. 1999.

77. Von Kriegstein K, Schmitz F. The expression pattern and assembly profile of synaptic membrane proteins in ribbon synapses of the developing mouse retina. *Cell Tissue Res* 311:159-173. 2003.
78. Wang MM, Janz R, Belizaire R, Frishman LJ, Sherry DM. Differential distribution and developmental expression of synaptic vesicle protein 2 isoforms in the mouse retina. *J Comp Neurol* 460:106-122. 2003.
79. Weber T, Zemelman BV, McNew JA, Westermann B, Gmachl M, Parlati F, Sollner TH, Rothman JE. SNAREpins: minimal machinery for membrane fusion. *Cell* 92:759-772.1998.
80. Wiser O, Bennett MK, Atlas D. Functional interaction of syntaxin and SNAP-25 with voltage-sensitive L- and N-type  $Ca^{2+}$  channels. *EMBO* 15(16): 4100-4110. 1996.
81. Xue M, Reim K, Chen X, Chao HT, Deng H, Rizo J, Brose N, and Rosenmund C. Distinct domains of complexin I differentially regulate neurotransmitter release. *Nat. Struct. Mol. Biol.* 14, 949-958. 2007.
82. Xiao H, Chen X, and Steele EC, Jr. Abundant L-type calcium channel  $Ca(v)1.3$  ( $\alpha 1D$ ) subunit mRNA is detected in rod photoreceptors of the mouse retina via in situ hybridization. *Mol. Vis.* 13, 764-771. 2007.
83. Zanazzi G, Matthews G. The molecular architecture of ribbon presynaptic terminals. *Mol. Neurobiol* 39:130-148. 2009.
84. Zenisek D, Steyer JA, Almers W Transport, capture and exocytosis of single synaptic vesicles at active zones. *Nature* 406:849-854. 2000.
85. Kolb H, Fernandez E, Nelson R, Jones BW. (Last updated 2010). Webvisions: The Organization of the Retina and Visual System. Retrieved 1 December 2009 from <http://www.webvision.med.utah.edu>.

